

**Titre:** Catalytic Upgrading of Softwood Kraft Lignin to Value Added

Title: Chemicals

**Auteur:** Samira Lotfi

Author:

**Date:** 2015

**Type:** Mémoire ou thèse / Dissertation or Thesis

**Référence:** Lotfi, S. (2015). Catalytic Upgrading of Softwood Kraft Lignin to Value Added Chemicals [Thèse de doctorat, École Polytechnique de Montréal]. PolyPublie.

Citation: <https://publications.polymtl.ca/1964/>

 **Document en libre accès dans PolyPublie**

Open Access document in PolyPublie

**URL de PolyPublie:** <https://publications.polymtl.ca/1964/>

PolyPublie URL:

**Directeurs de  
recherche:** Gregory Patience

Advisors:

**Programme:** Génie chimique

Program:

UNIVERSITÉ DE MONTRÉAL

CATALYTIC UPGRADING OF SOFTWOOD KRAFT LIGNIN TO VALUE ADDED  
CHEMICALS

SAMIRA LOTFI  
DÉPARTEMENT DE GÉNIE CHIMIQUE  
ÉCOLE POLYTECHNIQUE DE MONTRÉAL

THÈSE PRÉSENTÉE EN VUE DE L'OBTENTION  
DU DIPLÔME DE PHILOSOPHIÆ DOCTOR  
(GÉNIE CHIMIQUE)  
NOVEMBRE 2015

UNIVERSITÉ DE MONTRÉAL

ÉCOLE POLYTECHNIQUE DE MONTRÉAL

Cette thèse intitulée :

CATALYTIC UPGRADING OF SOFTWOOD KRAFT LIGNIN TO VALUE ADDED  
CHEMICALS

présentée par : LOTFI Samira

en vue de l'obtention du diplôme de : Philosophiæ Doctor

a été dûment acceptée par le jury d'examen constitué de :

M. STUART Paul, Ph.D., président

M. PATIENCE Gregory S., Ph. D., membre et directeur de recherche

M. PERRIER Michel, Ph. D., membre

Mme STEVANOVIC Tatjana, Ph. D., membre

**DEDICATION**

*Dedicated to  
My beloved parents, my lovely sister,  
My guardian angel forever, my lovely husband  
Thank you for your endless love,  
sacrifices, and support . . .*

## ACKNOWLEDGMENTS

I would like to acknowledge all who in one way or another contributed to the completion of this thesis. First and foremost, I wish to express my deep and sincere gratitude to my supervisor Prof. Gregory S. Patience for his solid support, motivation, caring and patience, as well as for providing me with an excellent atmosphere in which to conduct my research. His vast knowledge and logical way of thinking helped me throughout this process. It was a pleasure to work with him ; the lessons he taught me go beyond what is written in this thesis and will help me in all aspects of my life.

I would like to acknowledge the members of my committee, Prof. Tatjana Stevanovic, Prof. Michele Perrier, Prof. Paul Stuart for taking interest in my work, examining my thesis and providing insightful comments.

I also wish to gratefully acknowledge the financial support from NSERC (the Natural Sciences and Engineering Research Council of Canada), which made this research work possible.

I thank the unforgettable kindness of all members of the Lignowork and FIBER networks. Their knowledgeable and warmth made the collaboration highly beneficial for me. I made a number of friends all around Canada and my best memories are the times I have spent with them. I would like to offer my special thanks to Dr. John Schmidt from FPIInnovation, Dr. Cedric Briens from Western university, Dr. Tom Baker from the university of Ottawa, Dr. Theo van de Ven from the McGill university and Dr. Lamfeddal Kouisni at FPIInnovation for many valuable discussion that we had during the annual meeting and their collaborations on my data analysis. I am so thankful to Dr. Glenn A. Facey at the university of Ottawa for NMR analysis, and Mr. Alain Gagné at FPIInnovation for GC-MS analysis and Ms. Alexandra Matei, Ms. Louiza Mahrouche and Ms. Venne Karine at université de Montréal for LC-MS analysis.

I would like to acknowledge the other professors and technical staff at the Chemical Engineering department at École polytechnique de Montréal, especially the  $CM^2$  laboratory for providing the best possible assistance with my project.

I would also like to extend my thanks to all my colleagues in Prof. Patience's group for sharing their knowledge and ideas, and to all my colleagues who helped me at various points during the Ph.D. thesis process.

My deepest appreciation goes to the technicians in the Department of Chemical Engineering, particularly Robert Delisle, Jean Haurd, Martine Lamarche and Gino Robin, for their

excellent technical assistance.

I am also thankful to Mr. Charles Bruel for translating abstract to French.

I genuinely express my profound gratefulness to my beloved husband, Roozbeh Mollaabasi, as I owe my success to his love, patience, heartfelt sympathy, and support. Thank you Roozbeh, you have always been there for me in every situation.

And last but not least, from the bottom of my heart, I would like to express my endless gratitude to my mother, father, lovely sister and her family for the absolute support they have provided me throughout my entire life, and without whose love, spiritual encouragement and altruism I would not be where I am now. Words are powerless to express what I feel in my heart for them.

## RÉSUMÉ

Les forêts constituent la première des ressources naturelles du Canada et le développement d'une industrie forestière compétitive l'une des pierres angulaires de son économie. Cette dernière fait toutefois face à de sérieux défis depuis quelques années. L'augmentation des émissions de gaz à effet de serre révèle la nécessité de développer des bio-raffineries plus durables dont la rentabilité économique dépend grandement de l'usage qui peut être fait de la lignine, qui représente jusqu'à 40 % de la masse totale des plantes. La lignine est un bio-polymère aromatique tridimensionnel constitué de blocs phénylpropéniques connectés par différents types de liaisons :  $\beta$ -O-4, 5-5,  $\beta$ - $\beta$  0 et 4-O-5. L'industrie des pâtes et papiers rejette, comme déchets, de larges quantités de cette lignine qui pourraient être valorisés en produits chimiques ou en hydrocarbures. La structure complexe et l'hétérogénéité de la lignine sont les principaux obstacles à son utilisation industrielle. Un débouché prometteur serait la production de biomatériaux tels que les composites en fibres de carbones, les fibres, les polyuréthanes, etc. Toute la lignine rejetée par les bio-raffineries ou l'industrie des pâtes et papiers n'est toutefois pas adaptée pour la synthèse de biomatériaux, sa conversion en hydrocarbures ou en produit chimiques est donc un sujet d'actualité. L'hydrogénolyse, l'hydrodésoxygénation, l'oxydation et la pyrolyse sont les principales méthodes de valorisation de la lignine. Compte tenu du faible prix des hydrocarbures et des composés aromatiques, la synthèse d'acides utiles pour l'industrie constitue notre principal objectif. La coupure oxydante des cycles aromatiques de la lignine produit des acides dicarboxyliques qui ont des applications dans les polymères ainsi que dans les industries pharmaceutiques et alimentaires et représentent donc un marché important mais peu abordé dans la littérature. Notre approche consiste dans l'emploi, pour la première fois, d'un système gaz-solide pour l'oxydation partielle de la lignine en acides carboxyliques sur un catalyseur hétérogène. Nous nous sommes concentrés sur l'introduction du catalyseur dans un microréacteur à lit fluidisé, sur l'optimisation du procédé et sa modélisation cinétique pour déboucher sur une nouvelle méthode prometteuse pour l'oxydation partielle de lignine en produits chimiques. Dans la première partie de cette thèse, nous identifions un nouveau système hétérogène gaz-solide-liquide pour la conversion de lignine en acides carboxyliques. Un sujet qui est abordé dans le troisième chapitre consacré à l'oxydation partielle de lignine en acides carboxyliques sur du vanadium pyrophosphate et de l'Al-V-Mo en phase gaz ("Gas phase partial oxidation of lignin to carboxylic acids over vanadium pyrophosphate and Al-V-Mo "). Une pompe seringue atomise une solution alcaline de lignine dans un micro-lit-fluidisé catalytique opérant au-dessus de 300 °C. Les catalyseurs hétérogènes à base de vanadium sont les plus actifs pour casser les liaisons de la lignine,

ouvrir les cycles aromatiques et oxyder sélectivement la lignine en aromatiques et en acides carboxyliques dont le rendement est principalement affecté par la température et le ratio  $C : O_2$ . Le système souffre d'un faible rendement et d'un taux de désactivation du catalyseur important mais notre séquence d'injection de la lignine a permis de maintenir la conduite propre de façon ininterrompue pendant plusieurs heures, de réduire la formation de coke et la désactivation du catalyseur tout en améliorant le rendement en composés organiques à hauteur de 25 %. Un contact direct entre les, grandes, molécules de lignines et le catalyseur accélère la désactivation de ce dernier. Une désactivation qui peut aussi être causée par la solution alcaline, par les impuretés présentes dans la lignine ou par l'eau. Les dégradations thermiques et oxydatives sont deux des méthodes pour convertir la lignine en produits chimiques dont une grande part est condensable et dont la séparation est donc coûteuse. Ces inconvénients nous ont conduits à introduire un nouveau système qui fait l'objet de la seconde partie de cette thèse consacrée à la conversion directe et sélective de ces vapeurs en produits chimiques. Nous y caractérisons les conversions et les sélectivités des produits de la lignine dans un microréacteur à lit-fluidisé opérant jusqu'à 600 °C et y modélisons les mécanismes de sa dégradation à l'aide d'analyses thermogravimétriques avec des taux de chauffages de  $5 \text{ K min}^{-1}$  à  $30 \text{ K min}^{-1}$  (Chapitre 4). C'est un domaine où les données expérimentales sont rares, en particulier en ce qui concerne l'oxydation de la lignine. Le rendement en produits liquides (majoritairement des aromatiques) est d'environ 20 % dans les deux cas. Dans l'air, l'oxygène réagit avec la lignine pour former du CO, du CO<sub>2</sub> et du CH<sub>4</sub> alors que le noir de carbone est majoritaire dans le nitrogène. Un modèle à deux étapes décrit correctement le taux de dégradation. Il y a, durant l'oxydation, une compétition entre la formation de gaz et de liquides et la conversion du liquide en gaz via une nouvelle oxydation. Dans la pyrolyse, le noir de carbone provient de la repolymérisation des produits phénoliques formés. L'oxydation catalysée et sélective de ces monomères en produits chimiques est le sujet de notre cinquième chapitre. Pour cela, nous avons introduit un système semi-discontinu en deux étapes incluant le craquage thermo-oxydant de lignine suivi par une régénération du catalyseur avec l'oxydation des résidus carbonés. La lignine se dégrade graduellement avec l'augmentation de la température. Les aromatiques produits passent au travers du lit catalytique où ils s'oxydent partiellement de façon sélective. Dans un premier temps, nous avons considéré quatre configurations de réacteurs pour étudier l'effet de l'oxygène et de la vapeur d'eau sur la dégradation de la lignine et par conséquent sur le rendement final. La conversion de la lignine en composés liquides, sur la base d'un bilan carbone, est plus importante en présence d'eau et d'oxygène, les conditions oxydantes améliorent donc le rendement avec un catalyseur VPO. Toute la lignine se convertit en liquide ou en gaz. La formation de coke est considérablement réduite. Nous avons ensuite synthétisés et testés différents catalyseurs pour identifier des matériaux



actifs pour la conversion de lignine en acides carboxyliques. Le catalyseur de vanadium favorise principalement la transformation de lignine en acide maléique. Le choix du support affecte le rendement et la distribution des produits. Les catalyseurs basiques sont moins actifs que ceux acides pour la dégradation de la lignine. Nous avons aussi testé la transformation de lignine non purifiée, celle qui est directement produite par les industries de pâtes et papiers et les bio-raffineries. Le résultat est comparable à celui obtenu à partir de lignine pure. Il est intéressant que les impuretés n'affectent pas la méthode et qu'elles accroissent même parfois la sélectivité en acides. Finalement nous avons analysé les effets de la concentration initiale en  $O_2$  et en eau et ceux du temps de résidence  $\tau$  sur le rendement en produits liquides et gazeux ainsi que sur la sélectivité des produits dans le cas du catalyseur  $TiO_2-WO_3$ , un catalyseur qui a une bonne sélectivité pour l'acide butyrique (Section 6). Nous avons développé un modèle cinétique pour décrire le procédé d'oxydation catalytique et évaluer l'influence des conditions opératoires initiales sur l'oxydation catalytique de lignine dont les paramètres sont déterminés à l'aide d'une analyse locale. L'effet des paramètres considérés sur le rendement de la réaction a lui aussi été étudié. Une plus grande concentration en oxygène augmente le ratio de liquide sur gaz (de  $> 10\%$ ) et favorise les composés aromatiques de petite taille. Pour convertir ce liquide en acide butyrique, moins de  $5\%$  d'oxygène est requis lorsque  $\tau$  est supérieur à  $0.5s$ . Une augmentation du temps de résidence améliore la sélectivité en acide butyrique. À l'aune des connaissances acquises lors de cette étude, nous pouvons introduire l'oxydation partielle de lignine dans un réacteur gaz-solide à lit fluidisé comme une nouvelle approche pour la transformation de la lignine en composés valorisés et en particuliers en acides carboxyliques. Dans les systèmes gaz-solide-liquide, la lignine est introduite lentement dans le lit où elle est directement en contact avec le catalyseur, elle s'évapore et s'oxyde, à la surface du catalyseur ou dans le lit, en composés aromatiques et en acides carboxyliques. Dans les systèmes gaz-solides, la dégradation thermo-oxydative de la lignine génère des vapeurs qui sont oxydées sélectivement en acides carboxyliques. Le catalyseur acide à base de vanadium, molybdène et tungstène supportés sur  $Al_2O_3$ , HZSM-5,  $TiO_2$  a démontré des performances prometteuses pour la conversion de lignine en produits chimiques fins et en acides dicarboxyliques, spécialement ceux en  $C_4$ . Cependant, l'activité et la sélectivité du catalyseur affecte le rendement et la distribution en produits liquides. Il en va de même pour la température, la concentration d' $O_2$  et celle d'eau/vapeur. Le modèle cinétique local proposé est simple mais prédit correctement la conversion de lignine, sa sélectivité et les effets des différents paramètres. En plus de la lignine purifiée, celle impure directement produite par l'industrie peut être utilisée pour ce procédé, particulièrement dans le cas du réacteur gaz-solide. Le sous-produit de la méthode est du gaz de synthèse qui peut être converti en hydrocarbures ou en produits chimiques par des procédés déjà connus et employés.

## ABSTRACT

Forests are the most significant of Canada's resources. Establishing the forest industry is one of the cornerstones of the Canadian economy. However, it has been facing unexpected challenges for the past few years. The increase in the emission of greenhouse gases demonstrate the need for developing sustainable bio-refineries. The use of lignin, which constitutes up to 40 % of total plant mass, has a crucial effect on viability of bio-refineries. Lignin is a three-dimensional aromatic bio-polymer consisting of phenylpropene units that are connected together with various linkages such as  $\beta$ -O-4, 5-5,  $\beta$ - $\beta'$  and 4-O-5. The pulp and paper industry produces a huge amount of lignin as waste. Hence it can serve as a potential feedstock to produce materials, fuel and chemicals. The complex structure of lignin and its heterogeneity are the barriers to the industrial scale usage of lignin. The production of bio-material such as carbon fiber composite materials, fibers, polyurethane etc. are promising lignin products. However, all remaining lignin from bio-refineries or pulp and paper industries are not suitable for bio-material application. Hence the utilization of this abundant lignin is valuable for conversion to fuels and chemicals. Hydrogenolysis, hydrodeoxygenation, oxidation and pyrolysis are the most common used ways to upgrade lignin. Due to the cheaper price of fuels and aromatic chemicals, our main aim is to focus on industrially important acids. The oxidative cleavage of lignin aromatic rings leads to dicarboxylic acids that could be used in polymer, pharmaceutical and food industries, and it may constitute a large market. However, there is little work on this in the literature.

We approach this subject by employing a gas-solid heterogeneous system for the partial oxidation of lignin to carboxylic-acids in the presence of heterogeneous catalyst for the first time. We targeted the catalyst used, a micro fluidized-bed reactor, the optimization of the process, and kinetic modelling to pave a new avenue in the partial oxidation of lignin into fine chemicals.

In the first step of this thesis, we identify a new gas-solid-liquid heterogeneous system for the conversion of lignin into carboxylic acids. In this regard, the third chapter of this thesis is devoted to the "Gas phase partial oxidation of lignin to carboxylic acids over vanadium pyrophosphate and Al-V-Mo ". A syringe pump atomized an alkaline lignin solution into a catalytic micro fluidized-bed operating above 300 °C. Among the synthesized heterogeneous catalysts, vanadium based catalysts were active to cleave lignin bonds, open aromatic rings and selectively oxidize lignin to carboxylic acids and aromatics. Both, temperature and the C:O<sub>2</sub> ratio affect the yield of carboxylic acids. The system suffers from a low yield and a

high catalyst deactivation rate. To reduce the catalyst agglomeration, we modified the system with forced cycling catalyst regeneration. The sequence lignin injection helped to keep the line clear for several hours uninterrupted, reduced coke formation and catalyst deactivation rate, and increase the yield of organic compounds up to 25 %.

The direct contact of huge lignin molecules with the catalyst accelerates, catalyst deactivation rate. Alkaline solution, lignin impurities and water can also deactivate catalysts. These disadvantages lead us to introduce a new system. Thermal and oxidative degradation are two methods for the conversion of lignin into chemicals. The condensable products constitute a wide range of chemicals, so their separation is costly. The direct conversion of these evaporates into selective chemicals is investigated in the second part of this thesis. We characterized the lignin product yield and selectivity in a micro-fluidized bed reactor operating up to 600 °C and modelled the degradation mechanism with use of thermogravimetric analysis at a heating rate of 5 K min<sup>-1</sup> to 30 K min<sup>-1</sup> (Chapter 4). There is little data concerning these processes, particularly in lignin oxidation. The liquid product yield (predominantly aromatics) was  $\sim 20\%$  for both cases. In air, oxygen reacted with lignin and mainly form CO, CO<sub>2</sub> and CH<sub>4</sub> while in nitrogen char was the principal product. A two-step model accurately described the degradation rate. During oxidation there is a competition between liquid and gas formation, and liquid converts to gas with further oxidation. In pyrolysis, char comes from the repolymerization of the formed phenolic. The selective catalytic oxidation of these monomers into chemicals is the topic of our fifth chapter.

To do so, we introduced a two-step semi-batch system featuring the thermo-oxidative cracking of lignin, followed by a catalyst oxidation of volatiles. The lignin degraded gradually with an increase of temperature, and the produced aromatics were passed through the bed of the catalyst for selective partial oxidation. First, we considered four reactor configurations to study the effect of oxygen and water vapour in lignin degradation and consequently the final product yield. More carbon converted to liquid when lignin degrades in the presence of water and oxygen and consequently passed through VPO as an oxidative catalyst. All the lignin converted to liquid and gas, and coke formation was reduced considerably. Then we synthesized and tested various catalysts to identify the active material in the conversion of lignin to carboxylic acids. Vanadium catalysts mainly convert lignin to maleic acid, and catalyst supports change product distribution and yield. Basic catalysts were not as active as acidic catalysts in terms of the degradation of lignin. We also tested unwashed lignin, which is the direct product of the pulp and paper and bio-refinery industries. The result was comparable with pure lignin. Impurities did not affect this method, and were even found to increase acid selectivity to some extent.

Finally, we screened the effect of initial  $O_2$  and water concentration and  $\tau$  on the yield of liquid, gas and product selectivity for a  $TiO_2$ - $WO_3$  catalyst, which has a good selectivity to butyric acid (Section 6). We then developed a kinetic model to describe the catalytic oxidation process and evaluate the influences of operating conditions on the catalytic oxidation of lignin under initial reaction conditions. Last, we derive the kinetic parameters by using a lumped kinetic model. Higher oxygen concentration was found to increase the liquid to gas ratio ( $>10\%$ ) and oxygen degrades lignin to smaller aromatic compounds. To convert this liquid to butyric acid,  $<5\%$  oxygen is required when  $\tau$  is higher than 0.5 s. In addition, an increase of residence time improves butyric acid selectivity.

With the help of the insight gained in this study we can say that the partial oxidation of lignin in the gas-solid fluidized-bed reactor is a novel approach for upgrading lignin to value-added chemicals and in particularly carboxylic acids as an open chain product from lignin. In the gas-solid-liquid system, lignin was introduced to the bed slowly, directly contacted with the catalyst, evaporates, and oxidized on the surface of the catalyst or in the bed and converted to aromatic compounds and carboxylic acids. In the gas-solid system, thermo-oxidative degradation of lignin lead to vapours that are selectively oxidized to carboxylic acids. Acidic catalyst based on vanadium, molybdenum and tungsten on the  $Al_2O_3$ , HZSM-5,  $TiO_2$  demonstrated promising performance in the conversion of lignin to fine chemicals and dicarboxylic acids, especially  $C_4$  ones. However, catalyst activity and selectivity changes the liquid product yield and selectivity but reaction condition such as temperature,  $O_2$  concentration, and water/steam concentration have a considerable effect, as well. The proposed lumped kinetic model, however, was simple but accurately predicts lignin conversion, product selectivity and the effect of various parameters. Beside pure lignin, unwashed lignin can act as the feed for these processes, especially in gas-solid reactors. The by-product of the introduced method was syngas, which can be converted into fuel and chemicals.

## TABLE OF CONTENTS

DEDICATION . . . . .	iii
ACKNOWLEDGMENTS . . . . .	iv
RÉSUMÉ . . . . .	vi
ABSTRACT . . . . .	ix
TABLE OF CONTENTS . . . . .	xii
LIST OF TABLES . . . . .	xvi
LIST OF FIGURES . . . . .	xvii
CHAPTER 1 INTRODUCTION . . . . .	1
CHAPTER 2 COHERENCE OF THE ARTICLES . . . . .	5
CHAPTER 3 LITERATURE REVIEW . . . . .	8
3.1 Lignin . . . . .	8
3.2 Lignin valorization . . . . .	8
3.2.1 Pyrolysis . . . . .	10
3.2.2 Hydrogenation reduction . . . . .	11
3.2.3 Biochemical degradation . . . . .	13
3.2.4 Gasification . . . . .	14
3.2.5 Oxidation . . . . .	15
3.3 Heterogeneous catalyst systems . . . . .	17
3.4 Catalytic degradation of lignin . . . . .	18
3.5 Carboxylic acids from lignin . . . . .	19
3.6 Carboxylic acid production . . . . .	21
3.7 Fluidized-bed reactor . . . . .	22
3.7.1 Micro-fluidized-bed reactor . . . . .	23
3.8 Injection . . . . .	24
3.8.1 Liquid injection . . . . .	24
3.8.2 Solid injection . . . . .	25
3.9 Analytical method . . . . .	26

3.10 Kinetic modeling . . . . .	27
CHAPTER 4 ARTICLE 1 - GAS PHASE PARTIAL OXIDATION OF LIGNIN TO CARBOXYLIC ACIDS OVER VANADIUM PYROPHOSPHATE AND ALUMINUM- VANADIUM-MOLYBDENUM . . . . .	
4.1 Abstract . . . . .	29
4.2 Introduction . . . . .	29
4.3 Results and Discussion . . . . .	32
4.3.1 Catalyst characterization . . . . .	32
4.3.2 Spray atomization . . . . .	34
4.3.3 VPP partial oxidation of lignin . . . . .	35
4.3.4 Al-V-Mo partial oxidation of lignin . . . . .	37
4.3.5 Oxidation-reduction system . . . . .	41
4.3.6 Lignin degradation pathways . . . . .	43
4.4 Conclusions . . . . .	46
4.5 Experimental Section . . . . .	47
4.5.1 Materials . . . . .	47
4.5.2 Catalyst preparation . . . . .	47
4.5.3 Catalyst characterization . . . . .	48
4.5.4 Partial oxidation test . . . . .	48
4.6 Acknowledgment . . . . .	50
CHAPTER 5 ARTICLE 2 - KINETIC STUDY OF LIGNIN THERMAL AND THERMO- OXIDATIVE DEGRADATION . . . . .	
5.1 Abstract . . . . .	51
5.2 Introduction . . . . .	51
5.3 Experimental . . . . .	53
5.3.1 Thermal and thermo-oxidative degradation . . . . .	53
5.4 Results and discussions . . . . .	54
5.4.1 product distribution . . . . .	54
5.5 Mechanism . . . . .	58
5.5.1 Thermal degradation . . . . .	58
5.5.2 Lignin oxidation . . . . .	64
5.6 Conclusions . . . . .	69
5.7 Acknowledgements . . . . .	71
5.8 Appendix . . . . .	71
5.8.1 Kinetic modeling . . . . .	71

5.8.2	Ea — isoconversional method . . . . .	72
CHAPTER 6 ARTICLE 3 - GAS-SOLID CONVERSION OF LIGNIN TO CARBOXY-		
	LIC ACIDS . . . . .	73
6.1	abstract . . . . .	73
6.2	Broader context . . . . .	73
6.3	Introduction . . . . .	74
6.4	Experimental . . . . .	76
6.4.1	Materials and catalyst preparation . . . . .	76
6.4.2	Catalyst characterization . . . . .	77
6.4.3	Reactor configurations . . . . .	77
6.5	Results and discussions . . . . .	79
6.5.1	Two-step lignin degradation . . . . .	79
6.5.2	Thermo-oxidative steam cracking : catalytic activity . . . . .	83
6.5.3	Discussion . . . . .	88
6.6	Conclusions . . . . .	96
CHAPTER 7 ARTICLE 4 - KINETIC MODELLING OF LIGNIN OXIDATION OVER		
	TITANIA/TUNGSTEN (VI) OXIDE . . . . .	97
7.1	abstract . . . . .	97
7.2	Introduction . . . . .	97
7.3	Experimental . . . . .	99
7.3.1	Materials . . . . .	99
7.3.2	Partial oxidation tests . . . . .	101
7.4	Mechanism and kinetic modeling . . . . .	101
7.5	Results and discussions . . . . .	105
7.5.1	Reaction conditions . . . . .	105
7.5.2	Mechanism and modeling . . . . .	106
7.6	Conclusions . . . . .	110
7.7	Nomenclature . . . . .	111
7.8	Acknowledgements . . . . .	111
CHAPTER 8 GENERAL DISCUSSION . . . . .		
CHAPTER 9 CONCLUSION . . . . .		
9.1	Conclusion . . . . .	116
9.2	Limitations of the solution proposed . . . . .	117

9.3 Recommendations for future research . . . . .	117
LIST OF REFERENCES . . . . .	119



## LIST OF TABLES

Table 3.1	Quantity of lignin linkages Jia et al. (2011) . . . . .	9
Table 3.2	Lignin oxidation . . . . .	16
Table 4.1	Injector behavior in different lignin and solvent concentrations at 648 K. . . . .	35
Table 4.2	Reaction conditions for the production of MA and AA. . . . .	36
Table 4.3	$^{13}\text{C}$ solid NMR spectrometer Almendros et al. (1992) . . . . .	39
Table 5.1	Lignin oxidation aromatic products- GC-MS analysis. . . . .	54
Table 5.2	Lignin pyrolysis characteristic. . . . .	61
Table 5.3	Probable mechanistic function $f(\alpha)$ and the linear regression coefficients ( $R^2$ ) during the thermal decomposition of lignin. . . . .	63
Table 5.4	Kinetic studies of lignin pyrolysis. . . . .	64
Table 5.5	Lignin pyrolysis model. . . . .	64
Table 5.6	Lignin oxidation characteristic. . . . .	66
Table 5.7	Probable mechanistic function $f(\alpha)$ and linear regression coeffi- cients ( $R^2$ ) during the oxidative decomposition of lignin. . . . .	68
Table 5.8	Lignin oxidation model. . . . .	68
Table 6.1	Selectivity vs. reactor configuration . . . . .	82
Table 6.2	Product selectivity vs. catalyst . . . . .	89
Table 6.3	Surface area and pore size of fresh catalysts . . . . .	89
Table 7.1	Kinetic model of lignin oxidation. . . . .	99
Table 7.2	Product selectivity vs. reaction condition, cat. $\text{WO}_3/\text{TiO}_2$ . . .	105
Table 7.3	Estimated kinetic parameters- $k'_{o,i}$ . . . . .	106
Table 7.4	Kinetic parameters–literatures. . . . .	109
Table 7.5	Estimated kinetic parameters– $k_{o,i}$ . . . . .	109

## LIST OF FIGURES

Figure 3.1	Major linkages of lignin – (A) $\beta$ -O-4, (B) 5-5', (C) $\alpha$ -O-4, (D) $\beta$ -5, (E) $\beta$ - $\beta'$ , (F) 4-O-5, and (G) $\beta$ -1. Pandey and Kim (2011) . . . .	9
Figure 4.1	Powder X-ray diffraction patterns of VPP and the indexed materials : $\bullet$ $(VO)_2P_2O_7$ Bordes (1987), $\circ$ $(VO)_2P_4O_{12}$ , $\blacktriangledown$ $VO(PO_3)_2$ , $\triangle$ $VOHPO_4 \cdot 0.5H_2O$ . . . . .	33
Figure 4.2	SEM image of Al-V-Mo and VPP. . . . .	33
Figure 4.3	Softwood lignin TGA, $K\ min^{-1}$ . . . . .	36
Figure 4.4	HPLC curve - $T = 650\ K$ - $R(C : O_2) = 0.7$ . . . . .	38
Figure 4.5	Gas composition, Cat. VPP, $T = 650\ K$ , $C : O_2 = 0.7$ . . . . .	38
Figure 4.6	Acid yield vs. time, Cat. VPP, $T = 650\ K$ , $C : O_2 = 0.7$ . . . . .	39
Figure 4.7	$^{13}C$ solid NMR spectrometer of Lignin and reactor residue catalysed by VPP and Al-V-Mo. . . . .	40
Figure 4.8	Coke formation on VPP, $T = 650\ K$ , $C : O_2 = 0.7$ . . . . .	40
Figure 4.9	vs. time, VPP, $T = 650\ K$ , $R(C : O_2) = 0.7$ , $C_{O_2} = 0.04$ . . . . .	42
Figure 4.10	Gas composition vs. time, VPP, $T = 650\ K$ , $R(C : O_2) = 0.7$ . . . . .	44
Figure 4.11	Al-V-Mo (a) before reaction, (b) after reaction (continuous system) (c) after reaction (oxidation-reduction system), $T = 650\ K$ , $C_{O_2} = 0.04$ . . . . .	44
Figure 4.12	Mechanism proposed for the formation of a) formic acid and acetic acid; b) acrylic acid and lactic acid; c) maleic anhydride and maleic acid. . . . .	45
Figure 4.13	Schematic of the experimental set-up. . . . .	49
Figure 5.1	Lignin thermo-oxidative degradation in the fluidized bed (air)	55
Figure 5.2	GC-MS chromatography. . . . .	56
Figure 5.3	Lignin thermal degradation in the fluidized bed ( $N_2$ ) . . . . .	57
Figure 5.4	Mass loss of lignin as a function of temperature and temperature ramp in a TGA . . . . .	59
Figure 5.5	Lignin degradation behavior– TGA-DTG curve . . . . .	60
Figure 5.6	The TG-DTG curves of thermo degradation of lignin, Ramp= $30\ K\ min^{-1}$ . . . . .	62
Figure 5.7	Frideman model, pyrolysis. . . . .	62
Figure 5.8	Experimental (scatter) vs. model calculated (solid line) data for pyrolysis of lignin . . . . .	65

Figure 5.9	The TG-DTG curves of lignin thermo-oxidation . . . . .	67
Figure 5.10	Frideman model, oxidation. . . . .	68
Figure 5.11	Experimental (scatter) vs. model calculated (solid line) data for oxidation of lignin . . . . .	70
Figure 6.1	Schematic of experimental setup . . . . .	81
Figure 6.2	FTIR spectrum . . . . .	84
Figure 6.3	XRD-V-Mo/TiO <sub>2</sub> , ● anatase TiO <sub>2</sub> , ○ MoO <sub>3</sub> , △ Mo <sub>4</sub> V <sub>6</sub> O <sub>25</sub> , black = before reaction – Blue = after reaction. . . . .	90
Figure 6.4	XRD-VPP, ● (VO) <sub>2</sub> P <sub>2</sub> O <sub>7</sub> Bordes (1987), ▲ VO(PO <sub>3</sub> ) <sub>2</sub> , ▼ VOHPO <sub>4</sub> · 0.5H <sub>2</sub> O, black = before reaction- Blue = after reaction. . . . .	90
Figure 6.5	XRD-V-Mo/ZSM-5, ● HZSM-5 Liu et al. (2015), ■ VMoO <sub>8</sub> , ▼ (V <sub>0.07</sub> Mo <sub>0.93</sub> ) <sub>5</sub> O <sub>14</sub> , black = before reaction- Blue = after reaction Bhattacharyya and Talukdar (2005). . . . .	91
Figure 6.6	WO <sub>3</sub> /TiO <sub>2</sub> . . . . .	92
Figure 6.7	Proposed Mechanism of formation of butyric acid in 3 steps. .	95
Figure 6.8	Proposed mechanism of formation of lactic and malonic acids from syringyl alcohol. . . . .	95
Figure 7.1	scheme of mechanism- . . . . .	100
Figure 7.2	Schematic diagram of the 8 mm quartz reactor, manifold and quench . . . . .	102
Figure 7.3	Scheme 1 – Lignin catalytic oxidation via homogeneous and heterogeneous steps . . . . .	103
Figure 7.4	Scheme 2 – Lignin vapours catalytic oxidation . . . . .	104
Figure 7.5	HPLC trace of test R1 . . . . .	107
Figure 7.6	Experimental (scatter) vs. model calculated (line) . . . . .	108
Figure 7.7	O <sub>2</sub> vs. $\omega - k_{o,B}/k_{o,L}$ – Equation 7.10 . . . . .	110

## CHAPTER 1 INTRODUCTION

Lignocellulosic bio-refineries are a sustainable source of fuels and chemicals that attract attention due to fossil reserve depletion and climate pollution. Forests are one of Canada's most significant resources, covering more than 400 million hectares of land, or approximately half of the total area of the country and 10% of the earth's treed area, while the forest industry is one of the cornerstones of the Canadian economy. It accounts for some 300000 jobs, approximately 600000 indirect jobs, and constitutes 3% of Canada's total gross domestic product (GDP). Producing value-added forest-based products, in addition to traditional, products is one of the main solutions to ensuring a sustainable future for the industry Farag (2013). Lignocellulose contains cellulose, hemicellulose and lignin (Zakzeski et al., 2012). Cellulose and hemicellulose converts to bio-ethanol or bio-butanol and bio-based products (Fan et al., 2013; Ragauskas et al., 2014; Lalitendu et al., 2012). Every year, 50 million tons of lignin is created as waste from the pulp and paper industry. Just in united state alone, it is estimated bio-refinery development will increase lignin residue to 62 million tons by 2022 (Fan et al., 2013; Ragauskas et al., 2014).

Lignin is a bio-polymer made of methoxylated phenylpropane units joint mainly by C-C and ether bonds (Fan et al., 2013). Different linkages of lignin are  $\beta$ -O-4,  $\beta$ -5, 5-5, 5-O-4. Lignin is the only source of aromatics and has a potential to be a sustainable source of chemicals and fuels by acting as an alternative to petroleum chemicals. Lignin constitutes 15-40% of the dry weight of lignocellulose, but the heterogeneity of its structure prevents its commercial use as a chemical, or even as liquid fuel due to low selectivity. Presently, most of the lignin burns in the same industry and only 2% is converted to a value-added chemical. The economic viability of bio-refineries is independent upon lignin valorization (Zakzeski et al., 2012; Ragauskas et al., 2014; Azarpira et al., 2014).

Lignin valorization technologies include the production of carbon fibre, polymeric foam and thermoplastic elastomer as well as the production of fuels and chemicals through pyrolysis, gasification, catalytic hydrogenation, aqueous reforming, oxidation, hydrolysis, enzymatic conversion (Zakzeski et al., 2012; Fan et al., 2013; Ma et al., 2015a) and through its use as a filler (Thielemans et al., 2002). Low molecular weight phenolic compound, carboxylic acids and quinones all are chemicals obtained from the conversion of lignin to chemicals (Ma et al., 2015a). The synthesis of fibre composite material from lignin could be a promising method, but not all lignin has a suitable structure for material application. So, synthetic chemicals and fuels from lignin can cover a vast range of lignin (Ragauskas et al., 2014).

Pyrolysis leaves a mixture of an oxidation compound, phenolic compositions and bio-fuels, Farag et al. (2014a); Azarpira et al. (2014) while oxidation yields mainly vanillin, syringe aldehyde, vanillic acid or simple aldehyde and acids. Acidolytic and reductive methods produce various arylpropanoid monomers and hydrogenolysis tend to produce arylpropanes or arylpropanes Azarpira et al. (2014).

As such, a technology that improves the lignin conversion rate, selectivity and yield will guaranty the economic viability of bio-refineries and will be an alternative to petrochemical based products. The heterogeneity of lignin results in a high rate of products needing an expensive separation processes, preventing its usage as a bio-refinery chemical (Vardon et al., 2015).

The main objective of this project, then, is to introduce the production of carboxylic acids from lignin as a new route for the bio-refinery industry to produce highly valued chemicals while reducing the number of process steps through gas-solids heterogeneous catalysis. This system offers the possibility to sequentially vapourize and react a thermally unstable compound in the presences of a solid catalyst in the gas phase. Target chemicals are carboxylic acids such as maleic acid, butyric acids, acetic acid, lactic acid as well as aromatics. Up until now, this processing route has not been explored.

The development of highly active and selective catalyst for deriving chemicals in one-pot has as of late shown to improve the feasibility, economics, and performance of the bio-refinery process Zakzeski et al. (2010). The presence of untargeted materials increases the importance of the product purification process which affect the economic and environmental impact of the whole process Zakzeski et al. (2010); Fechete et al. (2012). Catalysts improve selectivity but they suffers of fast deactivation rate (Fan et al., 2013).

Solid heterogeneous catalysts in the presence of gas or liquid are used extensively in the industry (Lloyd, 2011). In comparison to homogeneous catalysis, heterogeneous catalysis reduces the problems associated with corrosion, separation and deposal. Porous solid catalysts have shown to offer a high surface area to disperse metal and offer superior thermal stability Fechete et al. (2012). Heterogeneous catalysts play a key role in the polymer, agricultural and pharmaceuticals industries especially in selective oxidation and hydrogenation process (Witsuthammakul and Sooknoi, 2012; Xu et al., 2006; Kadowaki et al.; Kwan et al.). A heterogeneous catalyst decreases catalyst expenses and supports in heterogeneous catalysts permit greater efficiency in the use of an expensive metal by increasing the active surface. Normally, a higher surface area offers higher selectivity and activity (Bagheri et al., 2014).

We ran our experiments in a continuous flow micro-reactor. A continuous flow micro-reactor allowed for less catalyst consumption, providing iso-thermal situation, on-line monitoring

of effluent gas and ease with which to change temperature and gas compositions Yu et al. (2011); Munirathinam et al. (2015). Fluidized-bed are preferred over fixed-beds for reactions in which deactivation (coking) is significant for systems with liquid injection (for gas-solid systems) Raffensberger et al. (2005); Yang (2003). Miniaturized fluidized-bed reactors are suitable for estimating kinetics and investigating reaction characteristics Liu et al. (2008). Agglomeration of powders is problematic in small reactor systems because the heat transfer is lower compared to commercial reactors. Injecting biomass as a solution adds a level of complexity.

Based on the objective of this work, the conversion of lignin to carboxylic acid in the presence of heterogeneous catalyst, one of the main challenges is to discover suitable catalyst which not only properly oxidizes lignin, but also breaks its linkages such as  $\beta$ -aryl and  $\alpha$ -aryl ether. Another major issue is designing a process in accordance with the benefits of gas-solid heterogeneous catalyst's ability to reduce agglomeration and improve performance. To optimize the process and consequently industrialize the technology, a kinetic model will be used to help advance the usability of the process. Therefore, the research is divided into three main parts corresponding to the targeted specific objectives :

– Objective # 1

1. Identify and synthesize the heterogeneous catalysts that are active, and selectively oxidize lignin to carboxylic acids and aromatics. The sub-objectives of this imperative include :

1.1- Designing a process in accordance with the benefits of gas-solid heterogeneous catalysts.

1.2- Synthesize different kinds of catalysts.

1.3- Quality control of synthesized catalysts, characterization and qualification of the catalysts for its usage in fluidized bed reactor.

1.4- Identify the most active and selective catalyst.

– Objective # 2

2. Introduce a gas-solid process to oxidize lignin in gas phase.

2.1- Identify an effective process for partial oxidation of lignin.

2.2- Investigate the performance of catalyst in oxidation of lignin and unwashed lignin.

– Objective # 3

3. Derive a kinetic expression that adequately characterizes the reaction kinetics

The third series of experiments consist of data aimed to kinetic modelling. According to the results of this part, optimum reaction condition will be predicted. The targets include :

3.1- To study the effects of major variables :  $O_2$  concentration, steam concentration and residence time on yield of carboxylic acid.

3.2- To develop a suitable model for lignin conversion.

3.3- To develop a suitable model for gas formation.

3.4- To define a kinetic model for carboxylic acid production.

## CHAPTER 2 COHERENCE OF THE ARTICLES

A brief description of the chapters and the link in between is as follows :

**Chapter 1 & 2 & 3 :** The first two chapters will briefly discuss the principal methods of lignin conversion to chemicals and fuels briefly and review the most significant relevant findings. Common methods will be discussed, in particular the oxidation for conversion of lignin to fine chemicals and catalysts that are active in degradation and oxidation of lignin. Also, common catalysts for conversion of petroleum to carboxylic acids will be demonstrated and their potential to be produced from lignin, mostly  $C_4$  acids such as maleic acids; in addition, describing analysis methods, kinetic modelling and fluidized-bed reactor.

**Chapter 4 :** According to the initial specific objectives, the first paper is "Gas-solid oxidation of lignin" . As there is not data available that target a production of carboxylic acid, firstly, it was important to introduce a catalyst able to cleave lignin linkages, open phenolic rings and oxidize lignin to carboxylic acids in the gas-solid system. Ni, Co, Mo in the presence of  $Al_2O_3$  and  $TiO_2$  especially  $Al_2O_3$  degrade lignin by oxidation, hydrogenation and hydro-deoxygenation. On the other hand, oxides or noble metals are stable for partial oxidation reactions. Vanadium and molybdenum oxides are the most used catalyst in this field.  $V_2O_5$  is a frequently used catalyst due to its suitable redox activity and surface acidity. Supported vanadium oxides form a group of industrially important catalysts for the selective oxidation of hydrocarbons. As a result, catalysts that have Mo and V have been effective in both, partial oxidation and lignin degradation and also VPO that is active for oxidation of n-butane to maleic acid were chosen.

More than just studying the catalyst, process performance is important. Lignin concentration, liquid and injector gas feed rate, and nozzle configuration affect the spray nozzle hydrodynamics. Optimization of the spray injection prevents nozzle blockage and fluidized-bed slumping. We studied the effect of lignin concentration, alkaline solution molarity, solution injection flow rate and nozzle configuration of the jet spray quality. To maximize carboxylic acids (CAs) yield, we evaluated the effect of temperature and C :O<sub>2</sub> ratio on lignin conversion and selectivity. Finally, to reduce catalyst agglomeration we changed the reactor design to alternatively oxidation-reduction system. The new design reduced agglomeration considerably and improved the yield, however, coke still formed on the surface of the catalyst, which could cause problems in a long term reaction. Direct contact of huge molecule of lignin with the catalyst is the main reason in deactivation of the catalyst.

For further reduction of coke formation, a new system we introduced. Degradation of lignin



prior to contact with the catalyst would be a reasonable method. Thermal and thermo-oxidative degradation of lignin leads to monomers. The selective oxidation of monomers to chemicals instead of gas in the presence of the catalyst could provide purer compounds. Reaction temperature, heating rate, degradation atmosphere and kind of lignin all affect product distribution.

**Chapter 5 :** Fundamental knowledge of thermal and thermo-oxidative degradation of lignin helps to control reactions, and therefore, product selectivity. "Kinetic study of lignin thermal and thermo-oxidative degradation" was the topic of the second article in which characterization of the product selectivity and especially product distribution in liquid phase within a micro-fluidized bed reactor operated up to 600 °C in nitrogen and air was demonstrated. Then, with combinations of iso-conversional method, and the model fitting method of the data obtained from TGA at constant heating rate, we drove a precise detailed mechanistic scheme for the whole process. The purpose of this study is to obtain better understanding of kinetics of lignin decomposition by pyrolysis, especially in oxidation atmospheres. Lignin decomposition rate decrease through the increase of the heating rate. Lignin decomposition accelerates at higher than 450 °C. In the presence of air at  $\sim 550$  °C at heating rate of  $10$  °C min $^{-1}$  all lignin decomposes mainly to gas and then liquid, while  $\sim 40$  % char remained in pyrolysis of lignin. Both processes yield  $\sim 20$  % condensable include phenolic compounds. During oxidation there is a competition between liquid and gas and liquid converts to gas with further oxidation. Part of the char in pyrolysis of lignin comes from repolymerization of formed phenolic.

**Chapter 6 :** A new system is introduced that includes thermo-oxidative cracking of lignin, followed by catalytic oxidation of produced evaporated into fine chemicals especially carboxylic acids. We tested four different configurations in order to investigate the performance of system, product distribution and yield in selective oxidation of evaporates yield from pyrolysis, oxidation, thermo-oxidative steamcracking and catalytic degradation in the presence of oxygen and water. We used VPO that converted lignin to maleic acid in the first series of experiments.  $\sim 5$  % coke formed on the catalyst. All lignin converted to gas and liquid. In the next step, we synthesized and tested various catalysts including acidic and basic catalysts and some industrial catalysts. Unwashed lignin we also tested. Solids that remained after removing water from black-liquor, were called unwashed lignin. Black liquor is a direct by-product of the pulp and paper and bio-refinery industry. Using unwashed lignin instead of pure lignin as a feedstock removes the purification costs of lignin and is desired by bio-refinery industries. Surprisingly, unwashed lignin had a higher selectivity to maleic acid.

**Chapter 7 :** The effects of O $_2$ , water concentration and residence time ( $\tau$ ) on product

selectivity in "Kinetics modelling the oxidation of the lignin over  $\text{WO}_3\text{-TiO}_2$ " were tested. A statistical design of experiments was performed on oxygen concentration, water concentration and residence time to develop kinetic modelling. Prediction of the mechanism, kinetic energy and product selectivity of lignin helped to improve the reaction rate and catalyst deactivation rate and led to a better understanding of the underlying processes.

**Chapter 8** is a general discussion and summary of the results.

**Chapter 9** summarized the key conclusions of this study and provides recommendations for future studies.

## CHAPTER 3 LITERATURE REVIEW

### 3.1 Lignin

Lignocellulosic biomass is made of three major components : lignin, cellulose and hemicellulose. Lignin content varies in different types of biomass and decreases as follows : softwood> hardwood> grasses. Lignin is a three dimensional amorphous consisting of hydroxylated, methoxylated, and phenylpropane units (Zakzeski et al. (2010); LanzaLunga and Bietti (2000)); P-coumaryl, coniferyl and sinapylalcohols are the three monomers that connected together with different linkages (Figure 3.1). Composition and quantity of lignin linkages change in different kinds of biomass (Table 3.1) Zakzeski et al. (2010); LanzaLunga and Bietti (2000).

Pretreatment methods used to remove lignin from plants affects the structure of lignin. Physical pretreatment (ball milling), and solvent fraction (organosolve process, ionic liquids, phosphoric acid), chemical pretreatment (aciditic and alkaline) and biological treatment are the four methods of separating lignin from lignocellulose. Lignin pretreatment affects bio-refinery operation in obtaining valuable products Zakzeski et al. (2010). The kraft lignin process is most often employed to separate lignin. Aqueous sodium hydroxide and sodium sulfide solution provide high pH and degrade lignin at 420 K to 460 K.  $\beta$ -Aryl ether that forms 45 % to 60 % of lignin is readily cleaved.

Acidic conditions help to cleave  $\beta$ -O-4 and  $\alpha$  ether linkages Jia et al. (2011). A base such as NaOH with an extra nucleophile like NaHS, anthraquinone, acid-catalyzed hydrolysis and hydrochloric acid or  $\text{AlCl}_3$  in dioxane-water or ethanol-water all are used for the  $\beta$ -O-4 ether linkage cleavage. Lignin C-C bonds are among some of the most difficult bonds to break and they can also be formed by the lignin treatment processes. The bond is broken by fluid catalytic cracking with highly optimized zeolites in the acid-catalyzed reactions Zakzeski et al. (2010). The presence of sulfur in kraft lignin is a barrier in downstream catalytic processes Azadi et al. (2013).

### 3.2 Lignin valorization

Potential high-value products from lignin are materials, fuels and chemicals that are currently sourced from petroleum. The materials include carbon fiber, plastic and composite, or those materials that are used as an additive. Production of carbon fiber composite materials from lignin is a promising product. Fibers driven from lignin have low porosity and a poor graphical structure that diminishes the mechanical properties of these fibers. Plastic and composite such

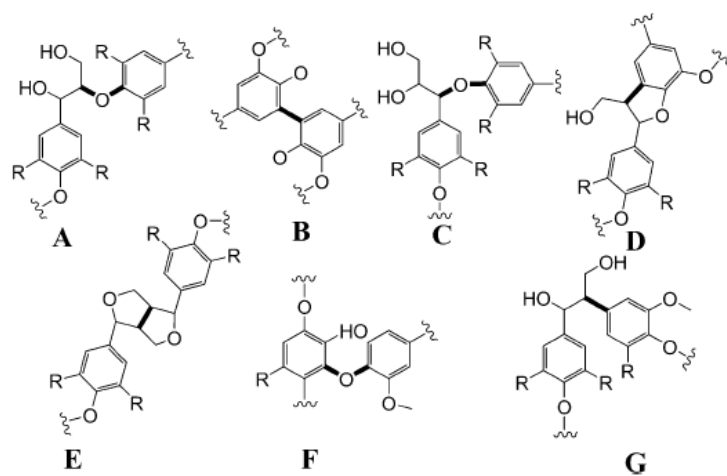


Figure 3.1 Major linkages of lignin – (A)  $\beta$ -O-4, (B) 5-5', (C)  $\alpha$ -O-4, (D)  $\beta$ -5, (E)  $\beta$ - $\beta'$ , (F) 4-O-5, and (G)  $\beta$ -1. Pandey and Kim (2011)

Table 3.1 Quantity of lignin linkages Jia et al. (2011)

Type of linkage	Softwoods	Hardwoods
$\beta$ -Aryl ether ( $\beta$ -O-4)	45–48	60
$\alpha$ -Aryl ether ( $\alpha$ -O-4)	6–8	6–8
Diphenyl ether (4-O-5)	3.5–8	6.5
Biphenyl (5-5')	9.5–17	4.5
Diaryl propane ( $\beta$ -1)	7–10	8
Phenylcoumaran ( $\beta$ -5)	9–12	6

as polyurethane, polymeric foam and membranes have comparable properties to petroleum source products and have a higher market value. However, not all the lignin fraction remains from bio-refineries are suitable for material application. The rigidity of the lignin has limited its market values to such products as dispersing and binding agents (2 % of lignin) or as low value fuel in the same industry Ragauskas et al. (2014). Fundamental efforts to commercialize lignin conversion to chemicals include :

- 1- Modification of cell walls for easy conversion and recovery (Bioengineering).
- 2- Development of analytical skills to understand physical and chemical properties of lignin (genetic engineering) for further processes.
- 3- Improvement of pretreatment technology to recover lignin and promote catalytic conversion technology (Chemistry and chemical engineering) Ragauskas et al. (2014).

A variety of catalysts and processes have been developed to improve lignin conversion and selectivity to specific products Mycroft et al. (2015). Lignin cracking, hydrolysis, catalytic reduction and oxidation reaction all transform lignin to valuable chemicals. Reduction yield simple monomeric compounds such as benzene, toluene and xylene, while, oxidation of lignin leads to platform chemicals or fine chemicals Zakzeski et al. (2010); Mycroft et al. (2015). These methods have not achieved high performance products and have not been appropriate for industrial use. As well, the low reactivity of lignin, especially alkali lignin, which contains high methoxyl groups and low alcoholic hydroxyl groups, prevents the high conversion of lignin and selective product formation Jie-wang et al. (2012). Introducing highly active and selective catalysts will decrease the separation costs and enhance the performance of this process. However, fast catalyst deactivation provides barriers to this technology. The production of chemicals that have a suitable market should be considered for example, the oxidation of lignin to form ring-open organic acids is a potential valuable products.

### 3.2.1 Pyrolysis

Pyrolysis, the thermochemical conversion of lignin in the absence of oxygen, leads to gas, liquid and solid. Thermochemical processes break or rearrange C-H bonds of lignin through heat and pressure. Pyrolysis is one of the most economic ways of yielding low-molecular-weight compounds. Slow pyrolysis ( $T=280^{\circ}\text{C}$  to  $680^{\circ}\text{C}$  and  $t=450\text{ s}$  to  $550\text{ s}$ ) mainly yields solids, while fast pyrolysis ( $T=550^{\circ}\text{C}$  to  $800^{\circ}\text{C}$  and  $t=0.5\text{ s}$  to  $10\text{ s}$ ) and flash pyrolysis ( $T=750^{\circ}\text{C}$  to  $1050^{\circ}\text{C}$  and  $t<0.5\text{ s}$ ) lead to liquids Farag (2013).

Char forms the solid and constitutes of condensed aromatics and reserves up to 50 % of the starting biomass energy. The major gases produced are carbon dioxide, carbon monoxide,

methane and hydrogen; while,  $C_2H_6$ ,  $C_2H_4$ ,  $C_3H_6$ ,  $C_4H_8$ ,  $HCHO$ ,  $CH_3CHO$  have also been detected. Feedstock, heating rate, temperature and additives all affect the yield and selectivity of products Mu et al. (2013); Couhert et al. (2009); Lotfic and Patience (2015). The yield of gas increase higher than  $500^\circ C$ , and  $CH_4$  decrease at higher heating rate. The yield of char decreases from 80 % to 40 % when temperature increases from  $250^\circ C$  to  $750^\circ C$ , while aliphatic OH, carboxyl and methoxyl group cleave at higher temperatures Mu et al. (2013).

Heating lignin degrades it to aromatic hydrocarbon and phenolic compounds Fan et al. (2013). Pure pyrolysis leads to low-molecular weight products. Condensation reaction yields oligomers and catalytic hydrogenation upgrades lignin to fuels and chemicals Ragauskas et al. (2014). The main target product is bio-oil. It takes hundreds of highly oxygenated organic compounds to form the dark brown liquid product. The major compounds of liquid oil are guaiacol, 4-methylguaiacol, syringol, eugenol, and various phenolic compounds. The oil produced during pyrolysis needs to be modified to be used as fuel. It suffers from thermal instability, corrosion, poor volatility, high coking tendency and low heating value Mu et al. (2013). As well, hydrogenation and zeolite cracking are common methods to upgrade the oil.

### 3.2.2 Hydrogenation reduction

While hydrogenation reduction process leads to various products such as phenols, alkanes, and aromatic hydrocarbons (Fan et al. (2013)), selective catalytic hydrogenation mainly targets the production or upgrading of bio-oils or fuels Zakzeski et al. (2010). The hydrothermal process depolymerizes lignin to subcritical or supercritical conditions ( $T \sim 280^\circ C$  to  $400^\circ C$  –  $\sim 20$  Mbar to 200 Mbar), which takes between a few minutes and a few hours. It is affected by its low selectivity and high catalyst deactivation rate Fan et al. (2013).

Generally, lignin converts to a bulk chemical in one or two steps. In the one step-process, the product stream still contains the original building blocks of lignin as phenol, guaiacol and syringol moieties, and catalysts are developed to improve yield and selectivity. In catalytic hydrogenation, conversion and product selectivity depends on reaction conditions rather than the catalyst. Phenol and o-cresol are completely stable under mild reaction conditions ( $T=500 K$  to  $650 K$ ,  $C_{H_2}$ ), while catalyzed by sulfided  $Ni-Mo-SiO_2-Al_2O_3$ . Oxygen free aromatics appears over  $570 K$ . The catalyst deactivation rate accelerates at higher temperature because of higher water release, loss of sulphur and excessive coke formation Zakzeski et al. (2010). The catalyst and support affects the yield of products, and reaction rate as well. Molybdenum-based catalysts tend to have a higher yield of mono-phenol and benzene in the lignin hydrocracking process Zakzeski et al. (2010). And a basic support like  $MgO$  inhibits coke formation. Carbon and silica have three and six times lower activity, respectively, in

comparison with alumina Zakzeski et al. (2010). Platinum-group catalysts are more active than molybdenum, and react at lower temperatures, thus yielding cycloalkenes and methanols caused by full hydrogenation and deoxygenation Zakzeski et al. (2010).

In the two step process, catalysts are developed for further upgrading of the already degraded product of lignin. The conversion of lignin to ethylbenzene occurs in a two-step reaction. First, lignin depolymerized to aromatics with use of HZSM-5, then, these monomers selectively alkylate in the presence of ethanol and ZSM-5 to ethylbenzene. Larger pore size reduced selectivity. The selectivity of benzene, toluene, and xylenes increases at higher acidity. At low acidity, no benzene forms Fan et al. (2013).

The performance of the catalysts varies with different feeding stocks. The reaction condition, source of lignin and its treatment greatly impacts the product distribution and yield of bio-oil Mu et al. (2013); Azadi et al. (2013).

Meier et al. (1993) studied flash pyrolysis of milled wood lignin (MWL) and organocell lignin (OCL) derived from a sulfur-free pulping process. Phenolic compound composition of OCL was less complex than MWL. In addition, the hydropyrolysis of OCL in a semi-continuous reactor, with a mixture of nickel oxide and chromium oxide, supported on aluminium-silicon oxides at 14 MPa and 6 h, yielded up to 80 % oil.

Increasing, the hydrogen pressure from 3 MPa to 12 MPa increases yield of oil from 18 % to 64 % in the presence of nickel-molybdenum and a narrowing of phenolic composition. Increasing the temperature converts lignin fragmentations to phenolic monomers. The hydropyrolysis of OCL lignin yields 15 % liquid and  $\sim 60$  % char at 400 °C and 100 barH<sub>2</sub>. Also, the use of NiMo-Cr<sub>2</sub>O<sub>3</sub> as a catalyst increases the yield of liquid to 71 % and decrease char to 7 %.

Increasing hydrogen pressure to 140 bar in this reaction condition, improves the liquid yield to 80 % and decreases char to 2 %. Decreasing hydrogen pressure to 50 % leads to 28 % and 32 % of liquid and char, respectively. In the presence of other catalysts such as Ni-Mo, (NH<sub>4</sub>)<sub>6</sub>Mo<sub>7</sub>O<sub>24</sub> and Co-Mo at  $\sim 400$  °C and 100 barH<sub>2</sub> liquid and solid yields were  $\sim 60$  % and 2 %, respectively. Pd catalyst was more efficient and increased yield of liquid up to 81 % and almost no char remained Azadi et al. (2013); Matsumura et al. (2006).

In the end, sulfide catalysts (NiMoS/Al<sub>2</sub>O<sub>3</sub>, CoMoS/Al<sub>2</sub>O<sub>3</sub>) and transition metal catalysts (Platinum, palladium, ruthenium, rhodium, etc.) successfully catalyzed the hydrogenation process Mu et al. (2013). Sulfide catalysts are cheap and perform at atmospheric pressure and in the gas phase. However, water and severe coke formation deactivate sulfide catalysts very fast. The studied transition metal catalysts are reusable, need lower temperatures and

have higher reactivity for hydrogenation under either the gas phase or water phase. On the other hand, they are easily poisoned by sulfur and expensive to recover. Thermal/water vapour stability is a major concern for choosing a catalyst. Support and its pore size greatly changes the reaction path. The reactivity of zeolite is higher in mesoporous structure. The desorption rate and the reaction rate are reduced by either too strong an acidity or bonding with reactant. Acidity and surface area of support considerably affects catalyst reactivity.

The ideal hydrolysis catalyst should have a high activity during hydrogenolysis and cracking the lignin linkages, especially  $\beta$ -O-4 and C-C bonds, as they are the main ones. It should also have low activity in hydrogenation of phenolic compounds and substitute alkyl and methoxyl groups that increase hydrogen consumption. Meaningful selectivity (higher than 10%) to one compound or compounds that have close boiling points helps facilitate the separation procedure. High resistance against coke formation, and easy regeneration and recovery of catalysts from the solid residue reduces catalyst cost. In the hydrolysis of kraft or lignosulfonate lignins, high sulfur resistance is necessary. Acidic supports such as zeolite are able to cleave C-C bonds effectively. When they support an active hydrogenation metal work as bio-functional catalysts. In semi-continuous reactors, hydrogen passes through the mixture of lignin and catalyst, removing the desired product through the bed fast and preventing further reaction of undesired products Azadi et al. (2013).

### 3.2.3 Biochemical degradation

In nature, lignin de-polymerizes with powerful oxidative enzymes. Rot fungi and some bacteria deconstruct plant cell wall and release aromatic monomers Vardon et al. (2015). Drawing the same analogy from nature encourages scientists to study the effects of various fungi, and micro-organisms in the degradation of lignin Mycroft et al. (2015); Bugg et al. (2011). Lignin degrades to small compounds in the presence of microorganisms and enzymes Lalitendu et al. (2012). Metallosalen complexes, metalloporphyrins, organorhenium complexes, vanadium complexes and metal-organic frameworks are some organometallic catalysts use for upgrading or converting lignin or lignin model compounds to valuable bio-products Ma et al. (2015a).

Laccase is a multi-copper oxides constituting four copper centers. In the presence of 1-hydroxybenzotriazole, laccase oxidizes lignin to ortho- and para-benzoquinones, as well as, catechol and muconic acid. This process suffers from low yield and selectivity Fan et al. (2013).

Methyltrioxo rhenium (MTO) is an organometallic compound. At mild conditions, MTO activates  $\text{H}_2\text{O}_2$  and, oxidizes substituted phenols to ortho- and para-benzoquinone. Over



oxidation of quinone compounds yields ring opening derivatives such as muconic acid or di- $\gamma$ -lactones. In addition, in the presence of acetic acid, MTO/H<sub>2</sub>O<sub>2</sub> causes oxidative ring cleavage that side-chain oxidation and produces aldehyde and carboxylic acids and aromatics Crestini et al. (2010); Ma et al. (2015a).

Vanadium complexes selectively cleaved C–O and C–C bonds and oxidized lignin to monomeric phenolic compounds include alcohols, aldehydes, ketones, and carboxylic acids Ma et al. (2015a). However, none of these processes are able to achieve a high yield of monomers and high selectivity towards a certain compound simultaneously. But even partial conversion to the group of products that separates easily could be economically viable.

### 3.2.4 Gasification

The gasification process converts lignin to combustion gases such as H<sub>2</sub>, CO, CO<sub>2</sub>, and CH<sub>4</sub>. Inorganics and sulfur could lead to ash and H<sub>2</sub>S formation. Common methods for gasification of lignin are : Conventional gasification at high temperatures and almost atmospheric pressure with oxygen and/or water (>800 °C and 1 bar), pyrolysis and, catalytic gasification in supercritical water at moderate temperatures and high pressures (e.g. 350 °C to 500 °C and 250 bar). Temperature and pressure, steam and oxygen concentration, heating rate, and lignin composition and its impurities affect the yield of products.

These syngas products already have developed applications in various industries. For example, they are the feedstock of liquid fuels and chemicals such as bioethanol and they are used directly in the generation of electricity.

Lignin gasification is mostly focused on the conversion of black liquor, which is the direct by-product of the papermaking process. Black liquor constitutes carbon, oxygen, sodium, sulfur, hydrogen, and potassium. Conventional gasification that runs at high temperatures suffers from high corrosion because of alkali compounds. Decreasing the S/Na ratio of the recovered chemicals increase separation cost. Lignin pyrolysis occurs in a wide temperature range (150 °C to 900 °C) through lots of char remains. Lignin releases more hydrogen than cellulose and hemicellulose. Its yield improves at higher temperatures ( $\sim$  600 °C), through increase of the heating rate and the addition of catalysts such as H-ZSM5 and Co-Mo-Al<sub>2</sub>O<sub>3</sub> Azadi et al. (2013); Haggstrom et al. (2012). The hydrothermal gasification of lignin yields more methane than hydrogen. In this process, phenolic rings open and subsequently C-C bonds cleaves and form C-O bonds, while further cleavage of C-O bonds yields CH<sub>4</sub>. Solid nickel and ruthenium catalysts are widely used but are active in the hydrogenation of CO<sub>2</sub>. Adding promoters, changing the metal-support interaction and crystallite size can control this process Azadi et al. (2013). Monomers produces by depolymerization have a higher economic

value in compare to syngas Azadi et al. (2013).

### 3.2.5 Oxidation

Low molecular weight phenolic compounds, aldehydes and consequently dicarboxylic acids, and quinones are the main products yielded from lignin oxidation, and reaction conditions affect product distribution toward aromatic aldehydes or acids Azarpira et al. (2014). Low molecular weight phenolic compounds are the main products in catalytic oxidation of lignin Ma et al. (2015a). aromatics, alcohols, aldehydes and acids are other products Lalitendu et al. (2012); Zakzeski et al. (2010); Fan et al. (2013).

Ultimately, product selectivity depends on the lignin structure, operating conditions, reactor type and oxidizing reagents— oxygen, peroxide, peroxy acids, chlorine, chlorine dioxide and ozone. Lignin units with hydroxy and methoxy terminal groups are more susceptible to be cleaved because of their higher electron density, as compared to ethyl or propyl groups. Chlorine degrades lignin to mono- and multi-chlorinated phenolic compounds. Chlorine dioxide oxidizes lignin to simple acids, dicarboxylic acids, and quinones. Oxygen is a weak reagent that needs basic conditions to promote electrophilic or radical reactions. Aromatics, carboxylic acids, and biphenyl derivatives are the main products. Hydrogen peroxide cleaves aromatic rings and produces dicarboxylic acids. Ozone is a highly reactive reagent and produces both phenolic and non-phenolic compounds below 300 K. It has the potential to destroy lignin aromatic compounds and form simple carboxylic acids, aldehydes, and ketones. Peroxy acids can convert lignin to phenolic compounds. However, smaller carboxylic acids such as formic, acetic, muconic and maleic/fumaric also form Ma et al. (2015a). Various catalysts oxidise lignin to carboxylic acids (Table 3.2).

However, one should also take into the account the economic value of such products to give a more realistic evaluation of the opportunities.

### Wet oxidation

In wet oxidation, organic compounds react with oxygen; typically, free radicals, at high temperatures and pressures. Vanillin, vanillic acid and syringaldehyde are the main products of lignin wet oxidation Lalitendu et al. (2012). Transition metals, perovskite-type metal oxides, organometal, noble metals and photo- and electro catalysts are common catalysts Lalitendu et al. (2012).

In the wet oxidation of lignin with  $\text{CuSO}_4$ ,  $\text{Cu}^+$  as an electron acceptance accelerates phenoxy radical formation.  $\text{Fe}^{3+}$  in  $\text{FeCl}_3$  catalyst is a oxygen carrier that increases the ionic reaction

Table 3.2 Lignin oxidation

No.	Catalyst	Lignin	T K	P bar	t h	Reactor	Reagent/ Solvent	X %	Main products	Y %	Ref.
1	LaCoO <sub>3</sub>	cornstalk	393	20	3	slurry		17	p-hydroxybenzaldehyde vanillin	2 4.5	Deng et al. (2009)
2	Pd-γ-Al <sub>2</sub> O <sub>3</sub>	sugar-cane bagasse	373	20		wet oxidation 3-phase slurry		12	syringaldehyde vanillin	9.5 5	Sales et al. (2004)
3	Co-Mn-Zr-Br	organosolve	413		10	slurry	water/ethanol	10	syringaldehyde p-hydroxybenzaldehyde aromatics	2 7 4.6	Partenheimer (2009)
4	charcopryrite CuFeS <sub>2</sub>	diluted-acid corn stover	333	1	5	slurry	H <sub>2</sub> O <sub>2</sub> / acetic acid buffer pH=4	14	malonic acid succinic acid malic acid	5 7 0.84	Ma et al. (2015a)
5	charcopryrite CuFeS <sub>2</sub>	steam-exploded spruce	333	1	5	Slurry	H <sub>2</sub> O <sub>2</sub> / acetic acid buffer pH=4	11	malonic acid succinic acid malic acid	4 5.5 0.33	Ma et al. (2015a)
6	-	kraft	403	P <sub>O<sub>2</sub></sub> = 0.28		autoclave	Alkaline O <sub>2</sub>	-	vanilline	11	Lalitendu et al. (2012)
7	-	Softwood	393	10 P <sub>O<sub>2</sub></sub> = 3	1-2	autoclave	NaOH (2M) O <sub>2</sub>	7	vanillin vanillic acid	4.5 2	Lalitendu et al. (2012); Pinto et al. (2011)
8	-	hardwood	393	10 P <sub>O<sub>2</sub></sub> = 3	1-2	autoclave	NaOH (2M) O <sub>2</sub>	5	Syringaldehyde vanillin	2.5 1.2	Lalitendu et al. (2012); Pinto et al. (2011)
9	FeCl <sub>3</sub> CuSO <sub>4</sub>	Steam-exploded hardwood	443			Stirred autoclave	NaOH pH= 10.5-12		syringaldehyde vanillin	9.5 5	Lalitendu et al. (2012); Wu et al. (1994)

by increasing oxygen concentration Wu et al. (1994).

The addition of copper sulphate to phenanthroline under alkaline solution is able to convert lignin model compounds to aldehyde and aromatic acids. The yield of products depends on the pH, molar ratio of ligand/copper, and oxygen partial pressure Azarpira et al. (2014). Azarpira et al. (2014) were able to convert lignin model compounds to vanillin, vanillic acid and veratric acid up to 60 % at 40 psi O<sub>2</sub>. For pine wood lignin, the yield of mentioned acids reduced to 10 %, and some unknown chemicals were produced.

The mixture of CuSO<sub>4</sub> with FeCl<sub>3</sub> improves lignin oxidation at the pH range of 10.5-12, where T is equal to 170 °C. Under high oxygen pressure concentrations, lignin converted to 5 % vanillin and 9.5 % syringaldehyde. But, the yield of aldehydes was very low without a catalyst and in the presence of pure O<sub>2</sub> Wu et al. (1994). The alkaline oxidation of lignin, in the ionized phenolic hydroxyl group, produces quinonemethide and also aldehyde forms Wu et al. (1994).

Aromatic acids and aldehydes have a smaller market, while, ring-open organic acids with suitable purity can open up larger markets Ragauskas et al. (2014). However, depolymerization of lignin leads to fuels rather than chemicals. Also, a complex mixture of molecules were detected. So, there are lots of barriers to introducing a technology that targets the production of commodity and special chemicals Azadi et al. (2013).

### 3.3 Heterogeneous catalyst systems

Solid heterogeneous are widely used in industry and play a key role in the manufacture of polymers, agricultural and pharmaceuticals, especially in the selective oxidation and hydrogenation Lloyd (2011); Hutchings (2009); Ren et al. (2003); Kwan et al.; Deng et al. (2009). In both of these processes, a partial reaction product is required, rather than the products from total hydrogenation or oxidation, and typically  $\text{CO}_2$  and water are produced Hutchings (2009). Oxidation catalysts frequently contain ten or more elements from several phases, and the promotion of micro-structure and catalyst re-usability is a main benefit of the using heterogeneous catalysts Emmett (1960). In addition, supports in heterogeneous catalysts permit greater efficiency in the use of an expensive metal by increasing their active surface. Furthermore, supported catalysts usually have a greater resistance to poisoning and are more stable at elevated temperatures and/or pressures. However, the physical and chemical nature of the support can affect the activity and/or selectivity of the catalyst Nishimura (2001). In heterogeneous systems mass transfer limitations play an important role because of the different reaction phases. In fluidized beds, very fine catalyst particles are fluidized in the reacting gas. The average particle size in fluidized bed applications is less than 0.1 mm. These tiny particles impose severe restrictions on the recovery of entrained material Uraz and Atalay (2007). Thus, the type and concentration of the catalyst can greatly affect conversion and selectivity rates Ren et al. (2003). Supports not only provide a high surface to carry the active metal oxide component and improve the mechanical strength of the catalyst material, but also catalyst in the last decade scientists have unambiguously shown that the activity and selectivity of supported metal oxide catalysts are significantly affected by the properties of the oxide material Weckhuysen and Keller (2003). Accordingly, choosing a support can be as important as choosing the oxidation catalyst itself. Alumina is the preferred support for these kinds of reactions; other common supports are silicon carbide, silica, titanium, fuller's earth, asbestos and kieselguhr. The catalyst can constitute 1 % to 20 % w/w of support Kwan et al.. High surface area supports can give high activity but poor selectivity, while supports with lower surface areas and open porosity can yield more desired products with less over-oxidation. Because of this,  $\alpha$ -alumina is preferred to  $\gamma$ -alumina as a support for vanadium Kwan et al.. The reduction of vanadium decreases with the type of support as follows :  $\gamma\text{-Al}_2\text{O}_3 > \text{SiO}_2\text{-Al}_2\text{O}_3 > \text{SiO}_2 > \alpha\text{-Al}_2\text{O}_3$  Kwan (1985). Catalysts in a suitable condition perform thoroughly.

### 3.4 Catalytic degradation of lignin

Inorganic metal-based catalysts, organo-metallics and organo-catalysts are the three main oxidation catalysts. Inorganic metal-based catalysts include simple metal ions, metal oxides, composite metal oxides and polyoxomethalate.

Transition metal ions are efficient catalysts for oxidation of lignin. Cu, Fe, Mn, Co and Zr in the presence of oxygen or hydrogen peroxide convert lignin to benzaldehyde and benzoic acid in alkaline and acidic (acetic acid–80 %) solution, respectively Ma et al. (2015a). They are also able to cleave side-chain and hydrolysis ether bonds. Transition metal ions facilitate demethoxylation reactions and improve the depolymerization of lignin into low molecular weight aromatic carboxylic/dicarboxylic aromatic acids such as dihydroxyterephthalic acid, 3-hydroxyphthalic acid Ma et al. (2015a); Ferraz et al. (2001); Gierer et al. (2001). Biphenolic structure and non-selective products such as benzoic acid, acetone and carbon dioxide form by increasing the radical coupling reaction rate in the presence of these metal ions Ma et al. (2015a).

Synergic effect increase activity of composite metal oxides. This catalyst, compared to homogeneous metal-ion ones, has a higher reaction rate and aromatic aldehyde yield. During delignification of spruce wood sawdust and wheat straw, the oxidant formed through the interaction between  $\text{MnO}_2$  and oxalate. However, free soluble materials from lignin were not released, and this oxidant led to a 30 % and 10 % decrease in  $\beta$ -O-4 linked to guaiacyl and syringyl units, respectively Lequart et al. (1998); Kurek and Gaudard (2000); Ma et al. (2015a).

Among various metal oxide structures such as corundum, wurtzite, etc., only perovskite type oxides have been studied in the oxidation of lignin.  $\text{LaMO}_3$  ( $M = \text{Fe, Mn, Co}$ ) and  $\text{LaA}'\text{BO}_3$  ( $A' = \text{Sr, Ce}$ ;  $B = \text{Co, Mn}$ ) have a high selectivity in conversion of lignin to phenolic aldehydes and acids Deng et al. (2009); Ma et al. (2015a).

Polymetalates are another promising catalyst for the degradation of lignin to monomeric compounds. They are diverse anionic clusters constituted  $d^0$  by metal cations, mostly,  $\text{W}^{VI}$ ,  $\text{WMo}^{VI}$ ,  $\text{V}^V$ ,  $\text{Nb}^V$  and oxygen anions arranged in  $\text{Mo}_6$  octahedral units. They are commercially available and are able to convert lignin or its model compounds to phenolic aldehydes even at room temperature. Polymetalates cleave  $\beta$ -O-4 and C-C linkages of lignin, directly producing low molecular weight phenolic compounds in various solutions Ma et al. (2015a).

Metal oxide catalysts are highly reactive and are widely used in the petroleum, chemical and environmental industries. They have been studied in oxidation of lignin Otto and Simpson; Ma et al. (2015a). Cupric oxide ( $\text{CuO}$ ) converts 25 % to 50 % of lignin into phenol aldehydes

and acids, acetoguaiacone or acetosyringone Hedges and Ertel (1982); Ma et al. (2015a). CuO cleave aryl ether bonds and release phenolic bonds. However, it has a great potential to selectively oxidize lignin to phenolic compounds with air or oxygen but is unable to completely depolymerize lignin. The product yield depends on lignin structure, too. For example, by increasing the vanyllyl to syringyl monomer ratio, CuO oxidation products decrease Otto and Simpson. The heterogeneous nature of metal oxide allows for a simpler separation/recovery of these catalysts.

Pd/Al<sub>2</sub>O<sub>3</sub> (Sales et al. (2007)), Pt/TiO<sub>2</sub>, TiO<sub>2</sub> were other transition metal oxides studied for the oxidation of lignin to mainly phenolic based products. However, many transition metal oxides have not been studied in the oxidation of lignin. For example, among the first-row transition metals, vanadium oxide supported by alumina has a high activity in the conversion of guaiacol (2-methoxyphenol) to phenol at atmospheric pressure and 350 °C. Less coke formed overall, and it even remained active even in the presence of 20 % coke Filley and Roth (1999).

### 3.5 Carboxylic acids from lignin

Petroleum is the current source of organic acids, so, introducing a biomass source will be very interesting to both the chemical and biorefinery industries Ma et al. (2014). The conversion of lignin to ring-opened carboxylic acids has a higher market but have been neglected. Carboxylic acids and their derivatives have been detected in oxidative delignification (Ma et al. (2014)), pyrolysis (Farag et al. (2014a)) and wet oxidation (Sales et al. (2007)) of lignin. However, they were not the target material Pandey et al. (2015).

An immobilized system based on H<sub>2</sub>O<sub>2</sub> and methylrhenium trioxide heterogeneous catalyst was able to oxidize lignin model compounds into aliphatics, condensed OH groups and mainly carboxylic acid moieties through both side-chain oxidations and aromatic ring cleavage reaction Crestini et al. (2005, 2006); Lange et al. (2013).

In the pyrolysis of bamboo lignin, (Lou and Wu (2011)) investigated the effect of sodium chloride and permutit as a catalyst for liquid yield. The catalyst increased the yield of small molecules such as acetic acid, benzene, phenol and furfural. In the pyrolysis of kraft lignin, acetic acid formed, in addition to benzene and phenol formed. In this process, zeolites, HZSM-5, FCC and olivine as catalysts improved the total yield of liquid but had no effect on small compounds and acid yield Choi and Meier (2013). Acetic acid and propanoic acid also were detected in the production of chemicals in the microwave thermal treatment of lignin Farag et al. (2014a,b). The main liquid product in the pyrolysis of lignin is oil rather than acids.

Unsaturated dicarboxylic acids such as maleic, formic, levulinic and butanedioic, and saturated dicarboxylic acids such as formic and acetic, form in hydrothermal and hydrothermal oxidation of alkali lignin and lignin model compounds at temperatures of  $\sim 280^\circ\text{C}$  to  $400^\circ\text{C}$  and pressures of  $\sim 20$  Mbar to 200 Mbar at times between a few minutes and a few hours Zeng et al. (2014).  $\text{K}_2\text{CO}_3$ ,  $\text{Ca}(\text{OH})_2$  and  $\text{NaOH}$  were also used to avoid coke formation facilitate lignin bonds breakage and enhanced formic and acetic acid formation Zeng et al. (2014); Joffres et al. (2013). The hydrothermal oxidation of lignin reacts at harsh reaction conditions (high temperatures and pressures), causing catalysts to rapidly deactivate.

Carboxylic is a by-product of lignin wet oxidation, as well. In the production of vanillin and aromatic aldehydes – syringe aldehyde and p-hydroxybenzaldehyde – from lignin in an alkaline solution, oxygen is required to break the lignin polymer. A high oxygen concentration or long residence time converts lignin to carboxylic acids such as formic, acetic, lactic, or oxalic acids Fargues et al. (1996); Sales et al. (2007). Sales et al. (2007) monitored formic and lactic acid in the selective wet oxidation of lignin to aromatic aldehydes when the reaction catalyzed by  $\text{PdCl}_3 \cdot 3\text{H}_2\text{O} \gamma\text{-Al}_2\text{O}_3$  at a total pressure of 20 bar and partial oxygen pressure of 2 bar to 10 bar in 370 K to 420 K. The wet oxidation of 2-methoxy phenol and phenol as lignin model compounds in a batch reactor at  $T=300^\circ\text{C}$ , residence time of 10 s to 60 s and 50 % to 100 % oxygen supplies was found to yield mostly  $\text{C}_4$  unsaturated carboxylic acids, such as oxalic, maleic, malonic, succinic, fumaric, formic, acetic and muconic acids Suzuki et al. (2006).

Ma et al. (2014) later used this method to produce dicarboxylic acid. The wet oxidation of corn stover lignin and steam-exploded spruce lignin in the presence of hydrogen peroxide and charcopyrite ( $\text{CuFeS}_2$ )-catalyst yielded 14 % and 11 % liquids, respectively. The product distribution of corn stover lignin after 5 h reached up to 95 % carboxylic acids, including malonic acid, succinic acid, malic acid. Steam-exploded spruce lignin yielded 85 % carboxylic acids after 3 h. While this method has a high selectivity, the residence time is very high.

Vardon et al. (2015) combined biological funnelling, separations and a chemical catalysis reaction to produce adipic acid from lignin derived aromatic molecules (sodium benzoate, coniferyl alcohol, ferulate, vanillin, caffeate, p-coumarate, phenol, etc.). These monomers converted into *cis-cis*-muconic acid with the use of *Pseudomonas putida* KT2440 at  $30^\circ\text{C}$ . The yield of muconate varies from 15 % to 95 % depending on the monomer used. Muconic acid was then recovered (purity  $>97\%$ ). Subsequently, *cis-cis*-muconic acid was converted to adipic acid with hydrogenation in the presence of highly active Pd/C catalyst with  $>97\%$  conversion and  $>97\%$  selectivity. But, there are few studies that target carboxylic acid as the main product, while lignin was converted to acid in several sequential steps, including

biological funnelling, separations and a chemical catalysis reaction.

### 3.6 Carboxylic acid production

Carboxylic acid is produced by oxidation, carbonylation and hydrolysis. Many aromatic hydrocarbons such as benzene, xylene, naphthalene, toluene or durene are used industrially for the production of carboxylic acids Heidemann et al. (2003). Benzoic acid and phthalic acid are generated from cyclic hydrocarbons Hara and Nakamura (2002); Witsuthammakul and Sooknoi (2012). Maleic anhydride (MA), because of its structure is one of the most important anhydrides yielded from benzene. As lignin is constituted by phenyl units, in this research we consider processes that have performed well in the production of  $C_4$  acids. The presence of the double bond and carbonyl groups in the molecule offers several possibilities for further processing such as polymerization or copolymerization with other hydrocarbons like ethylene glycol and vinyl monomers Johannes and Gosselink (2011). MA is widely used for the synthesis of alkyd resins and is an intermediate for chemicals production Paradis et al.. MA is used primarily in the manufacture of alkyd and unsaturated polyester resins, surface coatings, plasticizers, lubricating oil additives, agricultural chemicals, textile chemicals, paper reinforcement, food additives and pharmaceuticals Uraz and Atalay (2007).

MA is produced from n-butane in the presence of VPO catalyst–  $(VO)_2P_2O_7 + 10\% SiO_2$ ,  $VOHPO_4 \cdot 0.5H_2O$  Shekari and Patience (2010); Hara and Nakamura (2002); Witsuthammakul and Sooknoi (2012). A mixture of  $V_2O_5/MgO$  causes oxidative dehydrogenation of crotonaldehyde to produce maleic acid Lochar and Smolakova (2009). Toluene is the other source for the production of MA Tomskii et al. (2008). In the past, MA was commercially produced through the oxidation of the vapor phase of aromatics hydrocarbons such as benzene. However, n-butane and saturated aliphatic hydrocarbons are the other feed for the production of MA in the presence of molybdenum oxide, cobalt oxide, phosphorus-vanadium oxygen Bergman and Frisch (1966); Taheri et al. (2012).  $V_2O_5$ ,  $MoO_3$ , oxides of P, Ag, Na, Li, K, Ti, B, Ta and Sn are industrial catalyst for this purpose Bielanski and Najbar (1997).  $P_2O_5$  decreases the activity of catalysts but its addition with 3% to 4% mole improved MA selectivity. Ag has no effect on activity, but increase MA selectivity, as well Bielanski and Najbar (1997). Also, the addition of boron, particularly in the form of sodium borate, we found to increase the active life of the catalyst and selectivity in producing maleic anhydride Barker (1975). In n-paraffin oxidation V-P offered a higher selectivity in anhydrides than V-Mo Fumagalli et al. (1994). Precise studies on the kinetic reactions show that catalysts based on vanadium are most effective for the partial oxidation of hydrocarbons. Commercially, the combination of  $V_2O_5$  and  $MoO_2$  is used extensively for the partial oxidation of organic



compounds to MA Barker (1975). As well, benzene provides more MA compared to n-butane with a V-Mo catalyst Fumagalli et al. (1994).

In the oxidation of hydrocarbons to CAs, catalyst composition (type and concentration), bed length and its activation, feed type and concentration, reaction temperature and oxygen partial pressure all affect the yield of the desired product. The contrasts and limitations among these parameters demonstrate the need for reaction condition optimization. Generally speaking, an increase in temperature develops feed conversion, but it leads to a reduction in selectivity. Also, the selectivity of MA is reduced at high temperature and relatively higher coke forms. It reveals the promotion of secondary reactions over the acid catalyst by increasing temperature, and longer catalyst life times will be achieved by working at lower temperatures Fumagalli et al. (1994). Partial oxidation temperature ranges from 320 °C to 450 °C, and the best yield is obtained at around 370 °C. In order to avoid forming explosive gases and introducing oxygen in the necessary amount, inactive gases such as nitrogen, argon and steam are commonly added to the system. Preheating the gases also affects the yield of reaction. The range of  $O_2/C_nH_m$  (mol/mol) ratio is between 0.5-20. Some researchers have demonstrated the highest yields when the hydrocarbon and oxygen are fed at their stoichiometric ratio (Patience and Mills (1994)), whereas others have shown the best results when this molar ratio equals one. Catalyst composition, support, reaction conditions including temperature, reactant to oxygen ratio, residence time, etc. are all parameters that affect product selectivity and yield.

### 3.7 Fluidized-bed reactor

The typical applications of fluidized-bed reactors are metallurgical and thermochemical conversion processes (combustion, gasification, and pyrolysis of coal and biomass) Gomez-Barea et al. (2008). The fluidized bed reactor is one of the most important technology for gas-solid heterogeneous process Kunii and Levenspiel (1991). However, its hydrodynamic properties are affected by inter particle forces Shabanian and Chaouki (2015). Reactions between two fluids in the presence of solids are important in industrial processes such as organic compound hydrogenation, coal liquefaction and hydro-desulfurization. Reactions between two fluids in the presence of solids are important in industrial processes such as organic compound hydrogenation, coal liquefaction and hydrosulfurization Sanjay and Tarrer (1994). Bubble slurry reactors are used frequently in gas-liquid processes in the presence of a heterogeneous catalyst, such as oxidation, hydrogenation and hydroformylation Raffensberger et al. (2005). To design a conventional slurry reactor, attempts have been made to increase the mass and heat transfer coefficient, catalyst efficiency, selectivity and reactor performance Sanjay and Tarrer

(1994). The most important parameter is the proper contact between reactants and catalyst. When there are mass transfer limitations, a jet reactor system permits better control of free-radical generation/reaction and provides higher mass-transfer rates. Spraying desulfurized molten naphthalene from above the bed with multiple nozzles and introducing air from below is used for the production of phthalic anhydride in fixed-bed reactor Yang (2003). A jet flow system is particularly suitable for three phase (gas-liquid-solid) processes, it provides rapid and uniform mass distribution Sanjay and Tarrer (1994); Nauman (2002). Moreover, assembling this system with a micro-reactor can considerably reduce catalyst requirements.

### 3.7.1 Micro-fluidized-bed reactor

Micro-reactors are miniaturized chemical reactors in the range of  $10\mu\text{m}$  to  $300\mu\text{m}$  to a few centimetres. They are especially used in studies of fast reactions and unstable materials Yu et al. (2011). There are many kinds of micro-reactors such as micro-wall reactors, micro-channel reactors and meso-reactors that are often called micro-reactors Nauman (2002). In a micro-wall reactor, the catalyst is coated on its wall, which leads to less catalyst loading and a stronger catalyst. The small size of micro-channel reactors brings about heat and mass transfer limitations, so, reactors only a few millimetres in size are preferable because industrially proven catalysts can be used, and catalyst replacement is easy Liu et al. (2008); Fletcher et al. (2002). Micro-reactors work at near isothermal condition, and even with highly exothermic reactions they can lead to excellent selectivity Nauman (2002). Micro-reactors in today's chemical industry provide practical solutions for those who are searching for controllable, information rich, high throughput, and environmentally friendly methods of products formation with a high degree of chemical selectivity Yu et al. (2011). They are useful for studying chemistry and related kinetic modeling. Rapid molecular diffusion and nearly instantaneous cross channel mixing result in effectiveness factors in heterogeneous catalysts Nauman (2002). Also, Guettel and Turek (2010) assert that micro fixed-bed reactors have the potential to significantly intensify large scale industrial processes Guettel and Turek (2010). Their investigation of the partial oxidation of butane to MA and o-xylene to phthalic anhydride in micro-structured fixed-bed reactor reveals 2.5-7 times higher product per unit of reactor volume in comparison to conventional multi-tubular fixed-bed reactors, with a lower pressure drop. In addition, MA selectivity and yield are higher in micro fluidized-bed reactors Liu et al. (2008).

Overall, the advantages of micro-reactors are : " 1. On-line pulse feeding and rapid heating of particle reactant. 2. Effective suppression of the interfacial diffusion via fluidization. 3. The minimization of intra-particle diffusion through the adoption of fine solid reactants. 4.

The on-line monitoring the composition of effluent product gas using, for example, a process mass spectrometer. 5. The quick heating and isothermal conditions Yu et al. (2011). ” Micro-reactors offer superior performance, both operationally and economically, versus standard technologies. The advantageous of the reactor’s present configuration include low inter- and intra- particle mass transfer resistance and high heat transfer ratios that minimize the gas phase parasitic reactions Nauman (2002).

### 3.8 Injection

In the gas-solid conversion of lignin to chemicals, lignin can be introduced to the reactor in solid or liquid form. The form of injection and quality of injection affects the whole process, from hydrodynamics to performance.

#### 3.8.1 Liquid injection

In gas-solid heterogeneous reactions in fluidized-bed reactors, the internal vaporization of reactants improves efficiency by avoiding external heat exchanger costs. Avoiding the formation of hot spots by using the extra heat for vaporizing, too. Further, reactants distribute more uniformly in the reactor Bruhns and Werther (2005). For efficient injection, nozzle shape is also an important parameter. Injector internal diameter, length and liquid/gas ratio greatly affect the quality of atomization Lotfi et al. (2015). There are different models to characterize liquid injection in reactors : one model considers that liquid instantly vaporizes at the injector outlet, and accordingly ; a gas steam enters the bed for the reaction. In another model, atomized liquid exits the injector but it evaporates in the fluidizing gas. In the granulating model, liquid drops are deposited on the catalyst surface, liquid subsequently evaporates, and the reaction takes place in liquid and gas phases Lotfi et al. (2015). In these models catalyst agglomerates in the vicinity of the injector and it evaporates in the bed, so it is desirable to reduce the size of droplets as much as possible. There are two kinds of nozzles. One is an internally mixed nozzle that has a fan spray of  $60^\circ$ , and the other is an externally mixed nozzle that has a full cone spray angle of  $20^\circ$ . The second nozzle has a deeper penetration Bruhns and Werther (2005). The manufacture of internally mixed nozzles is easier and have a smaller outside diameter. The atomization of liquid in a gaseous environment, even without the interaction of injected liquid and the gas-solid flow in the fluidized-bed, greatly complicates the process Bruhns and Werther (2005). And the complex structure of lignin makes it even more complicated. According to the challenges of injecting the lignin solution, both, nozzle design and reactor will need to be optimized.

Liquid feed nozzles for spraying normally consist of four parts : a pre-mixture to combine the liquid feed with the atomization of the steam/gas. This part and second connection affects the stability of feed. The pressure of gas should be much higher than liquid in this section. Next is a venturi that connects that premixture to the body of the nozzle (flow conduit). After that there is a discharge nozzle to create liquid feed droplets of reduced size. The existence of a disperser at the end of the nozzle improves liquid and bed contact but for better penetration into the bed it is often neglected. Reducing the average mean diameter to a relatively fine size for proper contact between the components of the fluidized-bed and the injected fluid is useful for injecting heavy oils such as petroleum residues and bitumen into fluid coking reactor. The design of the fluid injection nozzle must consider the convergence/divergence of the parts Chan et al. (2013). In particular, the convergence section accelerates the flow mixture and elongation and shear stress flow, reducing droplet size. At the diffuser, the velocity of the effluent is reduced before entering the second contractor, while the second contraction reduces the size of the droplets Chan et al. (2013).

The design of the nozzle depends on feed characteristics (mainly viscosity) and the required flow rate. These parameters induce change on the convergence angle at the entry to the throat, its diameter and angle, divergence angle from the throat and entry and exit diameter, which can be adjusted empirically. Throat size is dependent on flow rate, while the pressure drop across the nozzle body induces a shearing force to establish a fine and uniform droplets feed. The produced momentum is sufficient For the spray to penetrate the bed of solids Chan et al. (2013).

Injectors affect the contact efficiency between reactants and thus the yield. Poor mixing of the two streams brings about lower yields due to combustion on surface of the catalyst. Although, the effectiveness of liquid spraying as aerosol into fluidized bed reactor is established, it is unknown in micro-fluidized-bed reactors Chan et al. (2013); Chen et al. (2006).

### **3.8.2 Solid injection**

One of the main challenges in continuous systems that use solid feedstock is solid injection. During pyrolysis raw biomass particles is injected through the fluidized-bed reactor. Conveying the most particles with least energy is critical.

Dilute phases pneumatic transport feeders, dense phase pneumatic transport feeders, and screw/auger feeders are three kinds of feeder have been used by industry. Dilute phase pneumatic transport feeders use a huge amount of gas to suspend and inject particles in the feeding tube, and this system consumes a high amount of energy. In screw/auger feeder system, pneumatic screw feeders slowly force particles into the reactor. In this system, there is

the potential for chemical change prior to entering the reactor and plugging the feed tube, especially with temperature-sensitive feedstocks such as kraft lignin or dried distiller's grains. In a flash pyrolysis process, where the temperature of the reactor is high (450 °C to 550 °C), coupling high temperature with pressure fluctuations can lead to severe injection line plugging, and cohesive solid particles increase the plugging rate Berruti et al. (2012).

Intermittent solid slug feeders effectively inject biomass materials into fluidized bed reactors, preventing plugging and undesired reactions in the injection line; raw biomass particles effectively penetrate and spread in the bed, and consume less gas, compared to screw feeders. ICFAR introduced this system recently for the injection of highly cohesive biomass materials like lignin. In the intermittent slug method, gas pulses propel loosely packed particles and transport them along horizontal or inclined feeding pipes into the fluidized bed section of the reactor Berruti et al. (2012).

### 3.9 Analytical method

Differences in lignin structure and the liquidification method necessitate the use of a reliable analysis method to characterize lignin products.

Gas chromatography alone, or coupled with mass spectroscopy, is a good analytical tool to quantify and qualify lignin degradation products Lange et al. (2013). Nuclear magnetic resonance spectroscopy (NMR) is also a versatile tool to characterize various samples of lignin, from solid lignin to valorization liquid products Lange et al. (2013). FT-IR can also give insight into the whole portion of pyrolysis oil Mu et al. (2013). The complex structure and variety of produced chemicals create barriers in the analysis of formed chemicals.

A simple and fast method for the analysis of organic acids in the hydrolysate is liquid chromatography/mass spectrometry (LC/MS). An ion exchange column based on a polystyrene-divinylbenzene polymer is also frequently used in biofuel research. In liquid chromatography, samples can easily be prepared with only filtration and dilution, as it only needs a small injection volume as low as 2  $\mu$ L. It can analyze vast series of chemicals such as phenolic compounds; it also calibrates easily and leads to accurate results Ibanez and Bauer (2014); Wang et al. (2014); Nollet and Toldra (2012).

The complicated structure of lignin, presence of carboxylic acid in feed and products, use of distilled water for gathering sample and low concentration of products all are critical issues. In our system, to meet these challenges we used HPLC, LC-MS and GC-MS for analysis.

High performance liquid chromatography (HPLC) can quantify the liquid. In HPLC, the sample and a pressurized mobile phase pass through a column filled with a sorbent. During

their transit, the sample components are separated due to their absorption intensity with the sorbent. Finally, the quantity and quality of the samples are identified according to the signals generated by various detectors such as av/vis or photodiode array. We are using a Metacarb 87HPN5210- 250\*046mm column which is appropriate for acid analysis. The mobile phase is phosphoric acid 0.02N with a flow of  $0.5 \text{ mL min}^{-1}$  at ambient temperature.  $20 \mu\text{L}$  of the sample is injected every time, and is then diluted in water. Each sample analysis is repeated 4-5 times. Gas chromatography mass spectroscopy (GC-MS) Agilent technology 5975C VL-MSD is able to distinguish the unknown aromatic products, while HPLC is used for the quantification of the products.

The analysis of the produced gases as well as unreacted oxygen is carried out by using an online Hiden and Pfeiffer mass spectrometer connected to the gas absorber. The lag time before the reaction species could be detected by a mass spectroscopy detectors is in the order of 30 seconds at normal feed flow rates (e.g.  $40 \text{ ml/min}$ ). The evolved species will be detected by mass spectroscopy according to their most abundant mass to charge ( $m/e$ ) ratios. Relative sensitivities for calibration purposes are calculated every day before and after each experiment. The gas calibration concentration should be close to the operating concentrations of the components during reaction.

### 3.10 Kinetic modeling

Ascertaining rate laws and kinetic parameters are essential for the design of reactors, estimating product distribution, and providing insight into the operation conditions of the new process. The wet oxidation of lignin in the presence of various catalysts, reaction conditions and product distributions has been previously investigated Fargues et al. (1996); Sales et al. (2007); Kindsigo et al. (2010). However, there are very few kinetic models in literature. The wet oxidation of organic compounds even with a pure compound such as phenol, goes through very complicated pathways and leads to the formation of various intermediates Zhang and Chuang (1999).

The generalized kinetic model cannot describe the catalytic wet oxidation process, since the activity of the catalyst for intermediate oxidation is unknown and intermediate's reactivity is different Zhang and Chuang (1999). To describe the effect of all components, a micro-kinetic model needs a large number of chemical equations and experimental data even for a simple component Roohollahi et al. (2012). A lumped reaction can accurately model complicated reactions including the production of various intermediates Zhang and Chuang (1999). In the catalytic and non-catalytic degradation of lignin that various intermediates form, a lumped model can accurately predict the degradation mechanism. This model considers lignin

conversion to various products with parallel pathways like  $\text{CO}_2$  for the complete oxidation and aldehyde with partial oxidation. Farag (2013) considered a first order mechanism, and parallel reactions decomposed lignin into gases, volatiles and solids Farag (2013).

Araujo et al. (2009) simulated the oxidation of lignin to vanillin with a detailed mathematical model in a packed bed and bubble column reactor (BCR). Their simulation covers variables such as liquid feed flow rate, gas feed flow rate, the set point of the thermostatic bath, and the oxygen partial pressure. The mass transfer parameters also affect the rate of the reaction. This is one of the rare models to characterize the oxidation of lignin Araujo et al. (2009, 2010). Catalytic surface reactions, as well as the heat and mass exchange between the catalyst surface and gas phase, make the heterogeneous gas-solid catalytic process very complex. Micro-reactors are suitable for kinetic modeling because of the improvement of transport across the channel.

The as mentioned, lignin oxidation reactions a yield variety of intermediary products (Sales et al. (2007)) and provide a highly complex reaction mechanism, so, we used a lumped model to predict lignin oxidation in our system as well.

## CHAPTER 4    ARTICLE 1 - GAS PHASE PARTIAL OXIDATION OF LIGNIN TO CARBOXYLIC ACIDS OVER VANADIUM PYROPHOSPHATE AND ALUMINUM-VANADIUM-MOLYBDENUM

**Samira Lotfi, Daria C. Boffito, and Gregory S. Patience\***

*Department of Chemical Engineering, Ecole Polytechnique de Montreal, Montreal, Quebec, Canada*

Corresponding author : Tel. : +1-514-340-4711 X 3439 ; fax : +1-514-340-4159.

E-mail address : gregory-s.patience@polymtl.ca

(Published in ChemSusChem 8 (2015) 3424–32)

### 4.1 Abstract

Lignin is a complex polymer that is a potential feedstock for aromatic compounds and carboxylic acids by cleaving the  $\beta$ -O-4 and 5-5' linkages. In this work, a syringe pump atomizes an alkaline lignin solution into a catalytic fluidized bed operating above 600 K. The vanadium heterogeneous catalysts convert all the lignin to carboxylic acids (up to 25 % selectivity), coke, carbon oxides and hydrogen. Al-V-Mo mostly produced lactic acid (together with formic acid, acrylic acid and maleic anhydride) ; vanadium pyrophosphate catalyst (VPP) produces more maleic anhydride.

### 4.2 Introduction

Lignin is a three-dimensional amorphous polymer consisting of hydroxylated, methoxylated, and phenylpropane units Zakzeski et al. (2010). The pulp and paper industry generates several million tons of waste lignin annually Flores and Dobado (2010). The production of biofuels from the agricultural biomass will increase waste lignin Dwivedi et al. (2009). Currently, only 2 % is converted to chemicals. Most of the lignin serves as a fuel, which has a lower value. Producing chemicals from lignin and waste lignocellulosic biomass would contribute substantially to the economic viability of a bio-refinery Zakzeski et al. (2010); Johannes and Gosselink (2011); Vardon et al. (2015).

The composition of lignin and the number of linkages between the hydroxylated, methoxylated and phenylpropane units varies with biomass type.  $\beta$ -O-4 constitutes  $\sim 50$  % of the linkages and 5-5' (phenyl units) constitutes  $\sim 12$  % Zakzeski et al. (2010); LanzaLunga and Bietti (2000).  $\beta$ -O-4 is the easiest bond to cleave. Either a base such as NaOH (with an



extra nucleophile like NaHS or anthraquinone) or acid-catalyzed hydrolysis (HCl or  $\text{AlCl}_3$  in dioxane-water or ethanol-water) cleaves the  $\beta$ -O-4 ether linkage Jia et al. (2011). Functionalized zeolites can crack biomass C–C bonds Zakzeski et al. (2010). Lignin C–C bonds such as the biphenyl 5–5' are among the most difficult to break and can even form during lignin treatment processes. Depolymerizing lignin is challenging because the resulting compounds can react to form even more stable species Ragauskas et al. (2014).

Lignin aromatic monomeric units remain an elusive but attractive feedstock for the chemical industry. At 20 bar and 393 K,  $\text{LaCoO}_3$  catalyses lignin to p-hydroxybenzaldehyde ( $\sim 2\%$ ), vanillin ( $\sim 4.5\%$ ), and syringaldehyde ( $\sim 9.5\%$ ) Araujo et al. (2010); Nikiema et al. (2009); Fargues et al. (1996). Maximum yield of lignin wet oxidation was 12% at 413 K and 20 bar in a three-phase slurry reactor in the presence of supported Pd on  $\gamma\text{-Al}_2\text{O}_3$  Sales et al. (2004). Dissolved lignin in water/ethanol solutions at 470 K and 30 bar gives 6% cyclic hydrocarbon and aromatics over transition metal catalysts Zakzeski et al. (2012).

Metal ions oxidize lignin to carboxylic acids and phenolics in the presence of oxygen, hydrogen peroxide, ozone or peroxy acids. Separating the metal ions from the compounds is costly even for highly selective processes. Solid metal oxides also catalyse these reactions with lower separation costs. Composite metal oxides have synergistic effects resulting in higher activity and selectivity than isolated metal oxides. Perovskites produce phenolic compounds while composite metal sulfites form dicarboxylic acids. Polyphenol, phenolic acids, and other phenol compounds are the main products in the oxidation of lignin or lignin model compounds in the presence of metal ions such as  $\text{Cu}^{II}$ ,  $\text{Fe}^{II}$ ,  $\text{Mn}^{II,III}$ ,  $\text{Co}^{II}$ , and  $\text{Zr}^{IV}$  Ma et al. (2015a).

Yadav et al. Yadav and Garg (2014) wet oxidize lignin model compounds with Cu/Mn/Ce supported on alumina. However, catalysts that cleave lignin model compounds like Brønsted acid catalysts in 1-ethyl-3-methylimidazolium triflate are not necessarily active for real lignin Binder et al. (2009). Co–Mo/ $\text{Al}_2\text{O}_3$  reduces lignin by cleaving oxygen.  $\text{TiO}_2$ , Ni–MgO and Pt– $\text{TiO}_2$  are photochemical oxidation catalysts. They form  $\text{H}_2$ ,  $\text{CH}_4$  and  $\text{CO}_2$  rather than higher molecular weight compounds Zakzeski et al. (2010).

Deriving carboxylic acids - maleic acid (MAc), fumaric acid (FA), acrylic acid (AA), lactic acid (LA) and phthalic acid (PA) - from lignin is an attractive economic alternative to burning it in kilns. These acids are broadly used as chemical reagents Xing et al. (2011). Annual production rates of acrylic acid, phthalic anhydride, maleic anhydride exceed 5000 kt, 4000 kt, and 2000 kt, respectively. Production rates are an order of magnitude lower for lactic acid. Propane, propene, glycerol, and acrolein are common raw materials to produce AA Hara and Nakamura (2002); Witsuthammakul and Sooknoi (2012). The preferred catalysts for these reactions include  $\text{Mn}_2\text{O}_3$ ,  $\text{V}_2\text{O}_5$ ,  $\text{MoO}_3$  and mixtures of Mo, Bi, Ni, Co, Fe, Na, Mn,

B, K, Si Kadowaki et al.. Recently, Ma et al. (2015b) found that vanadium catalysts were effective at cleaving C-C bonds of a lignin model compound to (2-phenoxy-1-phenylethanol) to form acetic acid. In general, V and Mo oxides on alumina or silica are the most selective oxidative catalysts for AA Witsuthammakul and Sooknoi (2012).

Vanadium pyrophosphate (VPP) converts *n*-butane to maleic anhydride at 675 K Shekari and Patience (2010); Diedenhoven et al. (2012); Rownaghi et al. (2010). Mixtures of  $V_2O_5$ –MgO oxidatively dehydrogenate croton aldehyde to produce maleic anhydride (MA) Lochar and Smolakova (2009). Benzene was the main feed-stock for MA before 1980 Barker (1975); Robinson (1963).  $V_2O_5$  catalyses this reaction as well as ortho-xylene and naphthalene to phthalic anhydride Chen et al. (2004). Transition metal oxides catalysts are common for partial oxidation of hydrocarbons but this is the first time that their activity and selectivity for lignin have been tested.

The product selectivity depends on the oxidizing agent as well as operating conditions and reactor type — oxygen, peroxide, peroxy acids, chlorine, chlorine dioxide and ozone. Lignin units with hydroxy and methoxy terminal groups are more susceptible to be cleaved because of their higher electron density, compared to ethyl or propyl groups. Chlorine degrades lignin to mono- and multi-chlorinated phenolic compounds. Chlorine dioxide oxidizes lignin to simple acids, dicarboxylic acids, and quinones. Oxygen is a weak reagent that needs basic conditions to promote electrophilic or radical reactions : aromatics, carboxylic acids, and biphenyl derivatives are the main products. Hydrogen peroxide cleaves aromatic rings and produces dicarboxylic acids. Ozone is a highly reactive reagent and produces both phenolic and non-phenolic compounds below  $\sim 300$  K. It has the potential to destroy lignin aromatic compounds and form simple carboxylic acids, aldehydes, and ketones. Peroxy acids can convert lignin to phenolic compounds. However, smaller carboxylic acids such as formic, acetic, muconic and maleic/fumaric also form Ma et al. (2015a).

Lignin could be a sustainable source of aromatic compounds, carboxylic acids and other chemicals if a catalyst can be identified to selectively activate it Ma et al. (2015a). Temperature, feed and oxidant concentration, and contact time also affect selectivity and yield Witsuthammakul and Sooknoi (2012).

Here, for the first time, we introduce a gas-solid system to convert lignin to carboxylic acids catalyzed by vanadium oxides. We dissolved lignin in a basic solution to model black liquor. A sparger atomizes the solution directly into a  $\mu$ -fluidized bed of vanadium oxide catalyst. VPP and an Al-V-Mo catalyst partially oxidize the lignin in a single step. Choosing an active and selective catalyst and the experimental conditions is critical to convert biomass to chemicals in a one-pot processes. Volatile species vaporize and the lignin reacts with the solid

catalysts. Fluidized-bed reactors are ideally suited for highly exothermic reactions because of their superior heat transfer characteristics compared to fixed bed reactors. Moreover, it is easier to regenerate catalyst (combust coke) in a fluidized bed Raffensberger et al. (2005); Yang (2003).

Our first objective was to optimize the nozzle spray conditions in order to avoid slumping the fluidized bed. This was challenging because the reactor contained less than 1 g of catalyst and the nozzle diameter of the sparger that atomized the solution was only 0.7 mm. Solvent, lignin concentration, feed rate at the injector, and nozzle configuration affect the spray nozzle hydrodynamics. The second objective was to maximize carboxylic acids (CAs) yield. We evaluated the effect of temperature and C :O<sub>2</sub> ratio on lignin conversion and selectivity towards the target compounds and finally, optimized the reactor design to reduce catalyst agglomeration.

## 4.3 Results and Discussion

### 4.3.1 Catalyst characterization

Based on XRD analysis, the Al–V–Mo is amorphous and both (VO)<sub>2</sub>P<sub>2</sub>O<sub>7</sub> and (VO)<sub>2</sub>P<sub>4</sub>O<sub>12</sub> phases are predominant with secondary phases of VO(PO<sub>3</sub>)<sub>2</sub> and VOHPO<sub>4</sub> · 0.5H<sub>2</sub>O in the VPP catalyst (Figure 4.1) Dong et al. (2005); Rihko-Struckmann et al. (2006).

The  $\gamma$ -Al<sub>2</sub>O<sub>3</sub> average particle diameter was 112  $\mu$ m, which increased to 120  $\mu$ m after impregnation with V and Mo. SEM images of the Al–V–Mo (Figure 4.2) confirm the particles size measured by laser diffraction. Al–V–Mo bulk density was 1000 kg m<sup>-3</sup>. The BET surface area of the  $\gamma$ -Al<sub>2</sub>O<sub>3</sub> was 150 m<sup>2</sup> g<sup>-1</sup>, whereas the SSA of the catalyst was 120 m<sup>2</sup> g<sup>-1</sup>. Al–V–Mo is a standard catalyst to produce MA from benzene and thus is a candidate to produce fine chemicals from lignin that have many phenolic compounds.

A powder with a low minimum fluidization velocity ( $U_{mf}$ ) is desirable : bubbles are smaller and the gas-solid contact is better. The ideal  $U_{mf}$  of a Geldart Group A powder varies from 2 mm s<sup>-1</sup> to 3 mm s<sup>-1</sup>. The  $U_{mf}$  of the Al–V–Mo catalyst powder was 6 mm s<sup>-1</sup> at ambient conditions and 4 mm s<sup>-1</sup> at 650 K. The minimum fluidization velocity decreases with increasing gas viscosity Lorences et al. (2003); Jiliang et al. (2013).

SEM-EDS spectra of the Al–V–Mo catalyst detected Al, Mo, V and O, as well as traces of Cl and Na. For VPP, the main components were P, followed by V and Si. We sieved commercially activated VPP to between 100  $\mu$ m to 180  $\mu$ m ( $\bar{d}_p$  = 140  $\mu$ m). Its bulk density was 960 kg/m<sup>3</sup> with a  $U_{mf}$  of 7 mm s<sup>-1</sup> and its SSA was 36 m<sup>2</sup> g<sup>-1</sup>. According to the particle

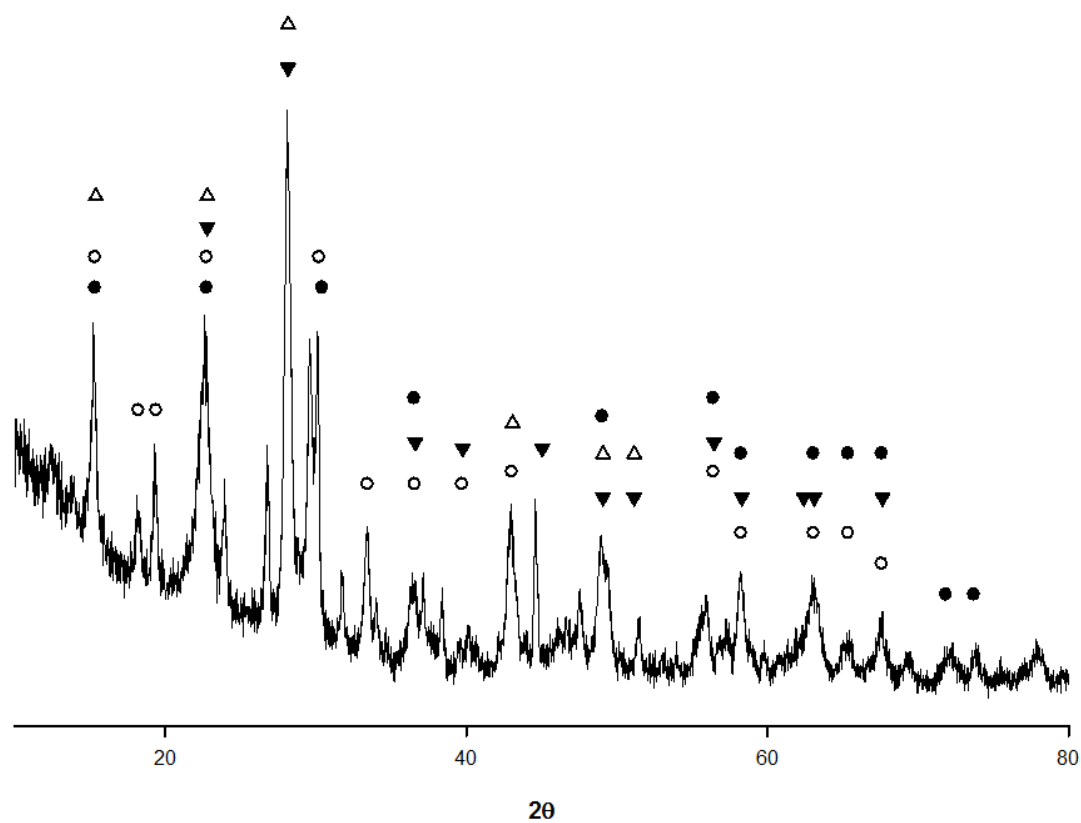


Figure 4.1 Powder X-ray diffraction patterns of VPP and the indexed materials :  $\bullet$   $(VO)_2P_2O_7$  Bordes (1987),  $\circ$   $(VO)_2P_4O_{12}$ ,  $\blacktriangledown$   $VO(PO_3)_2$ ,  $\triangle$   $VOHPO_4 \cdot 0.5H_2O$ .

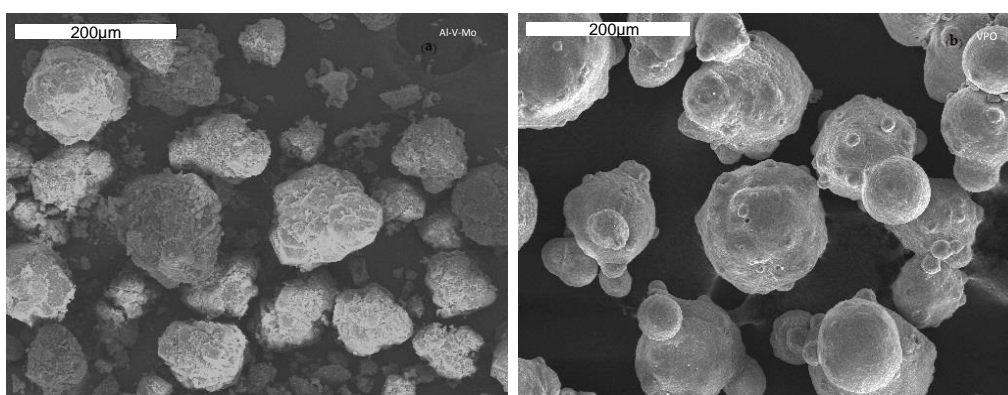


Figure 4.2 SEM image of Al-V-Mo and VPP.

size and particle density, both Al–V–Mo and VPP are Geldart Group A powders.

### 4.3.2 Spray atomization

Fluid catalytic cracking, thermal cracking Latifi et al. (2014), and aniline synthesis rely on high heat transfer rates to vaporize liquids into commercial fluidized bed reactors. Working at the laboratory scale with liquid feeds is more challenging than at the commercial scale. Heat and mass transfer rates are lower and the reactor and lines plug more frequently. Another difficulty for lignin was to identify a suitable solvent to dissolve it. It must be capable of dissolving lignin at near ambient temperature but, it should have a low volatility so that it does not evaporate in the line upstream of the nozzle tip. We tested many solvents, lignin concentrations, volumetric flow rates and sparger configurations.

Lignin dissolves in 1-butyl-3-methylimidazolium chloride (an ionic liquid) but this compound degrades at high temperature. Bases and acids extract lignin from lignocellulosic biomass near 375 K Kumar et al. (2009). The softwood kraft lignin was soluble in NaOH, KOH and aqueous ammonia solutions at ambient temperature. The maximum solubility of lignin in  $\text{NH}_{3(\text{aq})}$  was 10 % but the boiling point was low (300 K). NaOH and KOH solutions dissolved lignin at ambient temperature and boil at a higher temperature. Consequently, we chose sodium hydroxide as the solvent and tested concentrations in the range of  $10 \text{ g L}^{-1}$  to  $120 \text{ g L}^{-1}$  and lignin concentrations between  $10 \text{ g L}^{-1}$  to  $70 \text{ g L}^{-1}$ . The injector blocked at NaOH concentrations below  $70 \text{ g L}^{-1}$  and  $50 \text{ g L}^{-1}$  in less than 5 min when the lignin concentration was  $30 \text{ g L}^{-1}$  and  $15 \text{ g L}^{-1}$ , respectively.

At concentrations greater than  $100 \text{ g L}^{-1}$ , NaOH crystals deposited on the reactor wall. At lignin concentrations in the range of  $10 \text{ g L}^{-1}$  to  $30 \text{ g L}^{-1}$ , the injector remained clear for several hours of operation.

The solution flow rate is another important parameter to maintain the line clear. We tested lignin solution feed rates of  $90 \mu\text{L min}^{-1}$  and  $125 \mu\text{L min}^{-1}$  (Table 4.1). At flow rates lower than  $125 \mu\text{L min}^{-1}$  the injection line blocked in less than 5 min after starting the experiment.

We tested orienting the injector upwards and downwards. In the upward direction, the sparger passed through the centre of the distributor from below the fluidized bed. The contact time between the fluidized bed and liquid solution exiting the nozzle was instantaneous. In the downward facing direction, small droplets formed at the tip and sprayed on top of the fluidized bed. In this orientation, the sparger blocked when crystals formed in the line. In the upward configuration, the line temperature was lower so crystals would form less frequently ; however, catalyst agglomerated at the tip. Furthermore, solids entered the sparger at times

Table 4.1 Injector behavior in different lignin and solvent concentrations at 648 K.

No.	$C_{\text{lignin}}$ $\text{g L}^{-1}$	$C_{\text{NaOH}}$ $\text{g L}^{-1}$	$Q_{\text{solution}}$ $\mu\text{L min}^{-1}$	Injector state	Observations
1	15	50	90	downward	line blocked
2	15	50	125	downward	line blocked
3	15	70	90	downward	line blocked
4	15	70	125	downward without catalyst	no line blockage
5	15	70	125	downward without catalyst	no line blockage
6	15	70	125	downward	no blockage poor fluidization
7	15	120	125	downward	no line blockage salt formation at reactor <sup>-</sup>
8	15	70	125	upward with argon	line blockage
9	30	50	90	downward	line blockage
10	30	70	125	downward	no line blockage

(particularly in the case of pressure fluctuations induced by the pulsating flow of the pump).

### 4.3.3 VPP partial oxidation of lignin

In nitrogen, lignin loses 45 % of its mass in a TGA heated to 670 K, regardless of the heating rate (Figure 4.3). Beyond 670 K it continues to lose weight slowly and approaches a mass fraction of 55 at 1070 K. In air, lignin loses weight at a similar manner as nitrogen, up to 670 K and thereafter loses weight almost linearly with increasing temperature until there is virtually nothing left. Accordingly, even at a maximum operating temperature (700 K), some of the lignin remains as a solid. Operating the reactor at a higher temperature could react this lignin thereby increasing conversion but selectivity might drop. When the volume fraction of oxygen is below 4 %, unreacted lignin could build-up in the reactor (TGA data). If we draw an analogy from other oxidative processes, the oxygen feed concentration should be higher than stoichiometric (Table 4.2).

In fixed bed reactors, to convert n-butane to maleic anhydride, the oxygen to n-butane ratio is 10 :1. The stoichiometric ratio to produce maleic anhydride at 100 % selectivity is 3.5 ; it is 4.1 at 70 % selectivity. In the fluidized bed reactor, the oxygen to n-butane ratio is approxi-

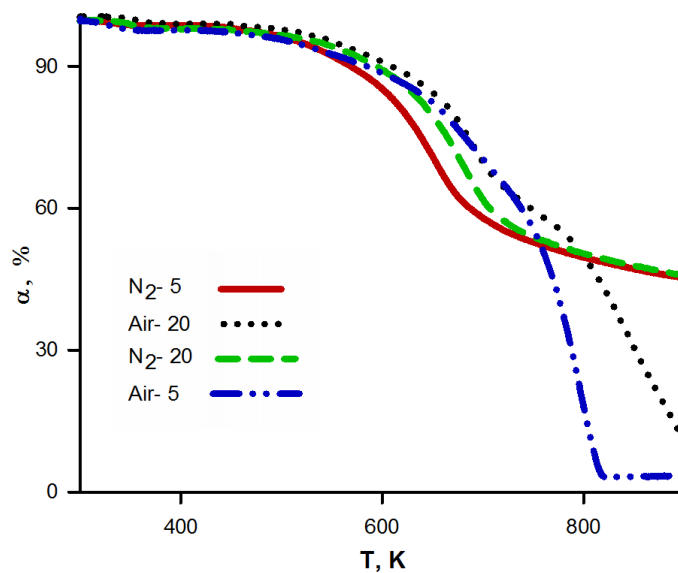


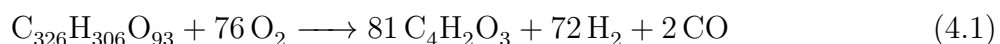
Figure 4.3 Softwood lignin TGA,  $\text{K min}^{-1}$ .

Table 4.2 Reaction conditions for the production of MA and AA.

Feed	Product	Catalyst	% $\text{O}_2/\text{C}_n\text{H}_m$ mole ratio	T K	P atm	Conversion $C(\%) - S(\%)$	Reactor
Propylene	AA Kadowaki et al.	$\text{Mo}_a\text{Bi}_b\text{Ni}_c\text{Co}_d\text{Fe}_e\text{Na}_f\text{Mn}_g\text{K}_i\text{Si}_j\text{O}_x$	1.2-1.8	533-623	1	98-84	Fixed bed
n-Butane	MA Paradis et al.	VPP	-	648-698	1.5-3	90+	Fixed bed
n-Butane	MA Patience and Bockrath (2010); Shekari (2011)	VPP	5-15	623-673	4	30-60	CFB
Benzene	MA Bayne et al. (1972)	$\text{Al}_2\text{O}_3\text{-MoO-V}_2\text{O}_5\text{-P}_2\text{O}_5$	9.1	623-723	1	34-65	Fixed bed
Benzene	MA	Silica-NaO <sub>3</sub> -NiO	8	598-673	1	-	Fixed bed

mately 5 :1. In forced concentration cycling (DuPont's Circulating Fluidized Bed process), the optimum ratio is about 1 Shekari and Patience (2010). Selectivity to maleic anhydride decreases with higher oxygen concentration. At concentrations lower than stoichiometric, coke begins to form on the VPP, which deactivates it.

For lignin, we adopted a  $O_2:C$  molar ratio of 1.4 and 2.8, corresponding to a lignin : $O_2$  molar ratio of 0.001 and 0.002. To calculate the required oxygen we considered the formula  $C_nH_mO_l$  for lignin. The feedstock was softwood lignin with a molecular weight of  $5800 \text{ g mol}^{-1}$ . Based on the lignin composition, 76 mol oxygen react to form maleic anhydride (our model compound)(equation 4.1).



In a blank test, we injected the lignin solution (0.7 C : $O_2$ ) over 300 mg of sand operating at 650 K. The quench was virtually free of any organic products : An HPLC trace of the liquid had only a few small peaks (Figure 4.4).

A trace from a test with VPP at the same conditions is superimposed on the blank test : malonic acid 1.4 % is the predominant compound followed by maleic anhydride 0.7 % and acrylic acid 0.1 % and then traces of acetic acid, fumaric acid and vanillic acid. There were two small unknown peaks. Based on GC-MS analysis of the compounds extracted with ethyl ether, the peaks were a mix of aromatics such as cyclopentene 1-ethyl-2-(4-methylpentyl), cyclohexene, ethyl and benzene, 1,3-dinoethyl.

#### 4.3.4 Al-V-Mo partial oxidation of lignin

The acid yield was higher with Al-V-Mo compared to VPP. The Al-V-Mo produced more  $C_3$  compounds whereas the VPP made more  $C_4$  compounds (Figure 4.4). After initiating the lignin pump, the MS signal of the  $O_2$  effluent gas dropped by 1 % and the CO (0.02 %) and  $CO_2$  (0.1 %) signals rose. Coincidentally,  $H_2$  increased and reached 1 % (Figure 4.5) and then dropped abruptly. The carboxylic acid production rate followed the same trend (Figure 4.6), which implies that catalyst reacts the lignin to produce carboxylic acids and hydrogen.

Selectivity to CO and  $CO_2$  is low. We sampled the solids from the reactor (catalyst + residual carbon) and, based on TGA, tests demonstrated that more than 90 % of the carbon in lignin remained in the reactor, either as coke or aromatic compounds (Figure 4.7). The coke deactivated the catalyst (Figure 4.8).

The Al-V-Mo catalyst produces several compounds including acetic acid (0.2 %), acrylic



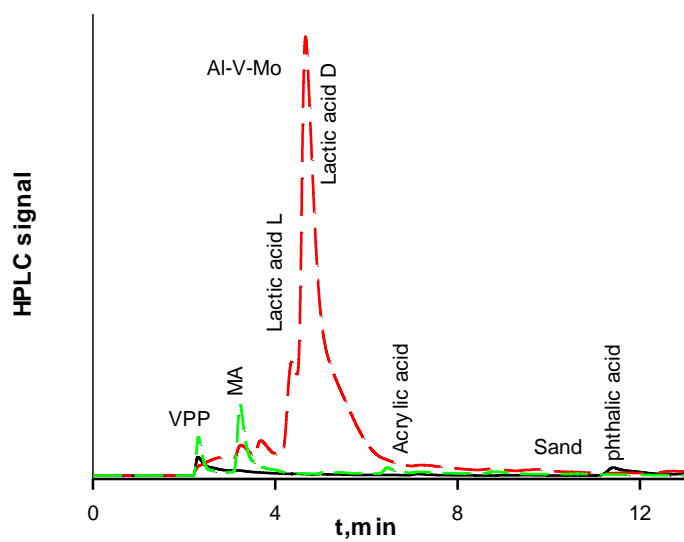


Figure 4.4 HPLC curve -  $T = 650\text{ K}$  -  $R(C : O_2) = 0.7$ .

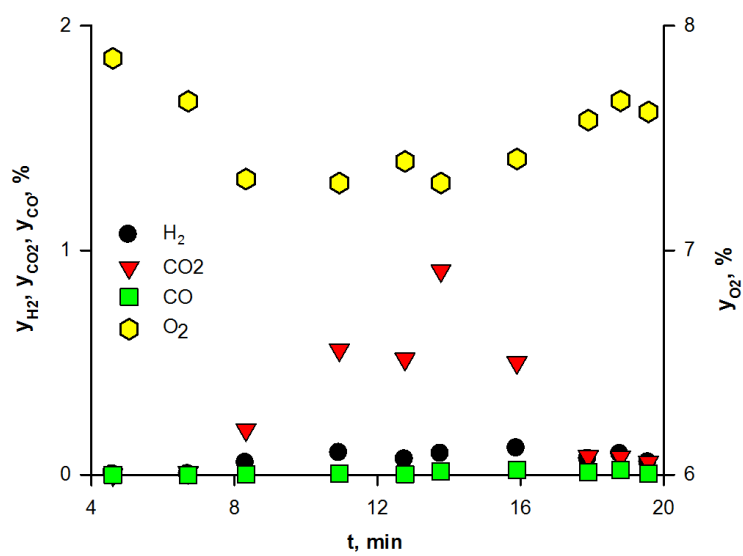


Figure 4.5 Gas composition, Cat. VPP,  $T = 650\text{ K}$ ,  $C : O_2 = 0.7$ .

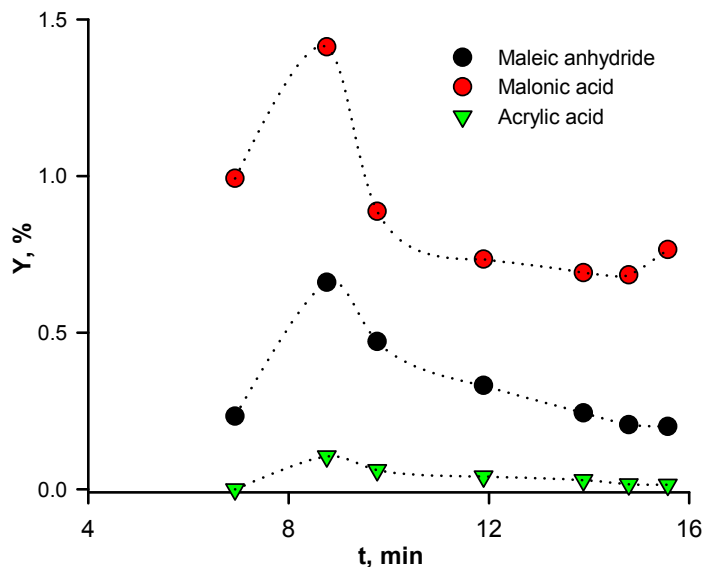


Figure 4.6 Acid yield vs. time, Cat. VPP,  $T = 650\text{ K}$ ,  $C : O_2 = 0.7$ .

acid (0.04 %) and maleic anhydride (0.6 %) but the predominant compound was lactic acid (6 %) (Figure 4.4). Lactic acid represented 86 % of all the acids detected. At 650 K and a  $C : O_2$  molar ratio of 0.7, the HPLC detected both phthalic acid and fumaric acids. The product selectivity was appreciable at a single condition : 650 K and  $C : O_2$  ratio of 0.7. At higher and lower temperatures, organic acid yield was less than 1 %.

NMR identified various non-volatile organic compounds that remained with the catalyst (Table 4.3).

The high  $C=O$  signal between 164 – 168 ppm represents aromatic acids. These acids are produced as a consequence of breaking the  $C_\alpha - C_\beta$  bonds (Figure 4.7) Almendros et al. (1992). The spectral region from 164 – 200 ppm corresponds to  $C=O$  that represents aldehydes, acids

Table 4.3  $^{13}C$  solid NMR spectrometer Almendros et al. (1992)

$^{13}C$ Shift ppm	Probable assignment
178	$C=O$ in aliphatic acid
148	$C_3$ and $C_4$ in etherified guaiacyl
117	$C_5$ in guaiacyl and $C_3$ and $C_5$ in p-hydroxyphenyl
72	$C_2$ in xylose internal unit and $C_\alpha$ in $\beta$ -O-4-linked unit
55	aromatic methoxy group

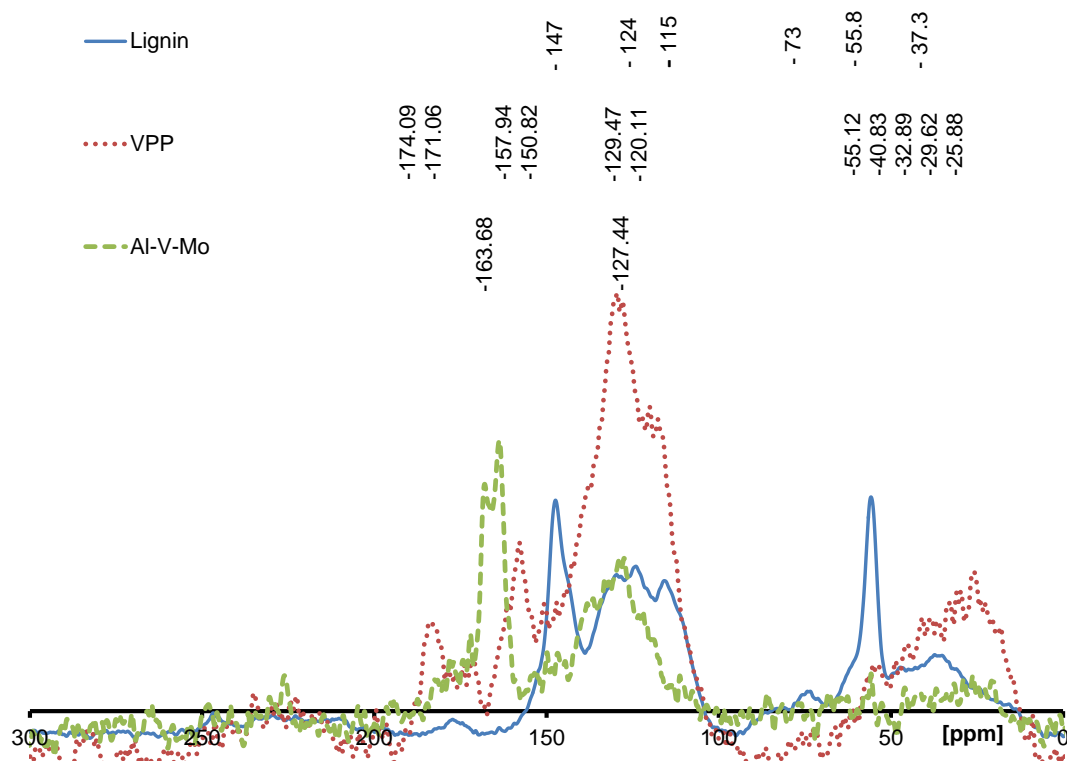


Figure 4.7  $^{13}\text{C}$  solid NMR spectrometer of Lignin and reactor residue catalysed by VPP and Al-V-Mo.

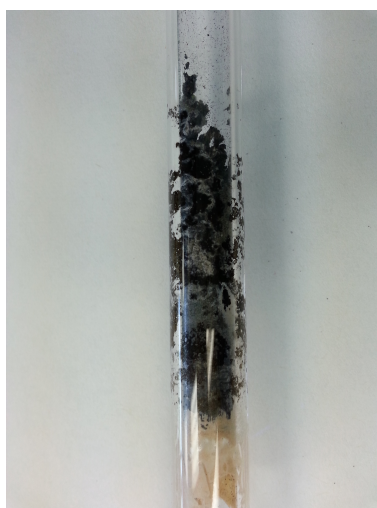


Figure 4.8 Coke formation on VPP,  $T = 650\text{ K}$ ,  $\text{C}:\text{O}_2 = 0.7$ .

and aroxyacetic structures. The intensity of the signal at 128 ppm belongs to  $C_2$  and  $C_6$  of the p-hydroxyphenyl species. We attribute the peaks at 17 ppm to the terminal  $CH_3$  group. The Al–V–Mo completely degraded lignin since their associated signals were absent in the NMR spectrum.

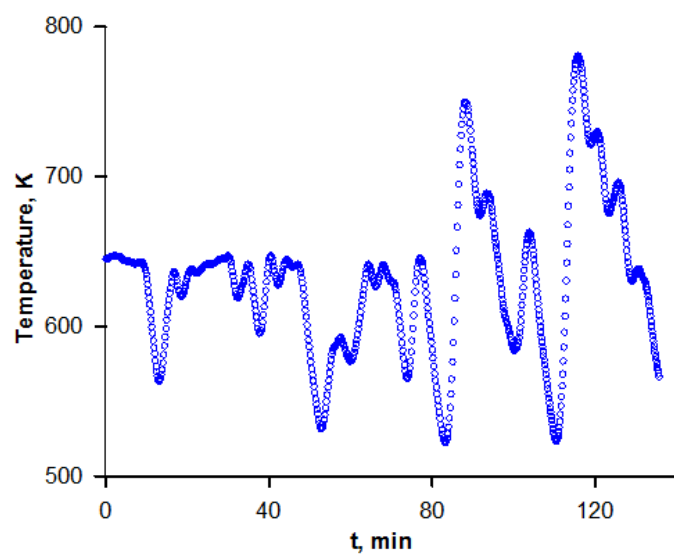
In the case of VPP, aromatic methoxy groups are still detected after reaction (Figure 4.7-VPP). Peaks at 171, 174 and 183 suggest the presence of C=O groups. Peaks at 151, 128 and 122 are attributable to  $C_3$  and  $C_5$  (p-hydroxyphenyl species), and  $C_2$  and  $C_6$  in p-hydroxyphenyl and  $C_6$  in guaiacyl units, respectively. Also, peaks between 26 and 40 ppm belong to  $CH_2$  and  $CH_3$  groups. Al–V–Mo catalyst is more effective than VPP to degrade lignin.

#### 4.3.5 Oxidation-reduction system

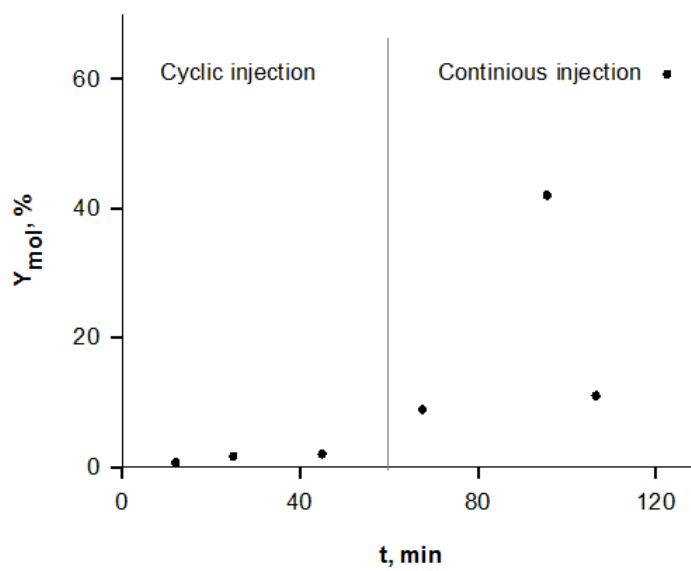
Agglomeration of powders is problematic in small reactor systems because heat transfer is lower compared to commercial reactors. Injecting biomass (in solution) adds a level of complexity. The atomized fluid cools the reactor and the droplets can coat the powder and create liquid bridges. Even in the absence of liquids, powders cluster due to Van der Waals forces and electrostatic forces Bartels et al. (2008). Alkali components form adhesive silicates such as  $K_2O-Al_2O_3-SiO_2$ , which have a low melting point. However, their melting point is much higher than the 700 K, which was the maximum operating temperature in our experiments. Mechanical stresses in large reactors are much higher than micro-reactors, which will easily break the weak Van der Waals forces and electrostatic forces. Liquid bridging will also be less prominent in the larger reactors. Further to these physical phenomena, coking and catalyst deactivation accelerated powder agglomeration (Figure 4.8). The micro-reactor operated for a maximum of 16 min after which the bed would slump and liquid would accumulate inside. Deactivation and coking were the likely causes.

To address catalyst deactivation, we shortened the lignin injection time and periodically regenerated the catalyst in air. This operating mode is referred to as forced concentration cycling. We intermittently fed the lignin solution, purged the sparger line with water for 45 s and then stopped liquid injection. The sequence helped keep the line clear and we could operate for several hours uninterrupted.

The temperature dropped 75 K to 150 K when the solution was injected (Figure 4.9a). The temperature recovered thereafter to the set-point of 650 K. The temperature swings became larger with time-on-stream. The peak temperature approached 800 K, whereas, the minimum temperature approached 500 K. At larger temperature swings, more coke accumulated on the catalyst (Figure 4.9b).



(a) Temperature profile

(b)  $Y_C$  in gas phaseFigure 4.9 vs. time, VPP,  $T = 650 \text{ K}$ ,  $R(\text{C} : \text{O}_2) = 0.7$ ,  $C_{\text{O}_2} = 0.04$ .

The concentration of  $\text{CO}_2$  increased while the  $\text{O}_2$  concentration decreased proportionately (Figure 4.10). The MS traces  $\text{CO}$  and  $\text{H}_2$  followed the  $\text{CO}_2$  trace.

In the oxidation-reduction system, the syringe pump sprayed lignin solution into the middle of the catalyst (500 mg) from the bottom of the reactor. To spray lignin, a syringe pump injected liquid ( $0.09 \text{ mL min}^{-1}$ ) to argon by flow of  $50 \text{ mL min}^{-1}$ . To improve the quality of the lignin solution spray we reduced the internal diameter of the injector at the top.

Catalyst oxidation removes coke from the catalyst and decreases the catalyst deactivation considerably. In the oxidation-reduction cycle, we injected twice as much lignin and the catalyst remained active (Figure 4.11).

Moreover, the acid product selectivity was superior. We operated the reactor with VPP at 600 K and 650 K and oxygen volume fractions of 4 % ( $\text{C}:\text{O}_2$  0.7), 7 % ( $\text{C}:\text{O}_2$  0.35) and 21 % ( $y_{\text{O}_2}$ ). The HPLC identified maleic acid, acrylic acid and an aromatic compound in the quench. The maximum yield of MA was 3 % at  $y_{\text{O}_2} = 4$  %,  $T=650$  K and the yield of AA was 0.5 %. Less MA was produced while co-feeding air but the HPLC detected trace quantities of fumaric acid and lactic acid.

With Al–V–Mo the maximum yield of lactic acid was 7 % at  $y_{\text{O}_2} = 4$  % and  $T = 600$  K. MA yield at this condition was 1 % and it was 7 % for formic acid, 3 % for acetic acid, 1 % for acrylic acid and 4 % for phthalic. The mass conversion of the lignin approached 25 % and 17 % of the carbon gave carboxylic acids. Ma et al. achieved a 14 % yield for a diluted-acid corn stover lignin and 11 % yield for steam-exploded spruce lignin Lochar and Smolakova (2009). The selectivity to dicarboxylic acids after 5 h at 333 K was 95 %. In comparison, in the fluidized bed, the yield to carboxylic acids was almost twice as high.

#### 4.3.6 Lignin degradation pathways

Most of the reactions leading to carboxylic acids initiate with the rupture of the  $\beta$ -O-4 bonds, which are the easiest to cleave. This rupture makes either an anion (phenolate) or a phenol radical. These negative charges re-distribute across the ring to re-establish the aromaticity. Depending on the type of terminal groups of the polymeric chains of lignin, which are usually in para position with respect to the phenolic oxygen, the products are different. As a result of the re-distribution of the charge across the ring, the alkylic side chains in para position with the respect to the phenolic O, if any, are released. In the presence of  $\text{O}_2$ , the oxidative degradation of the side alkylic chains occurs, passing through alcohols as intermediates. The final products are formic acid and acetic acid when the alkyl side chains are methyl or ethyl chains (Figure 4.12a).

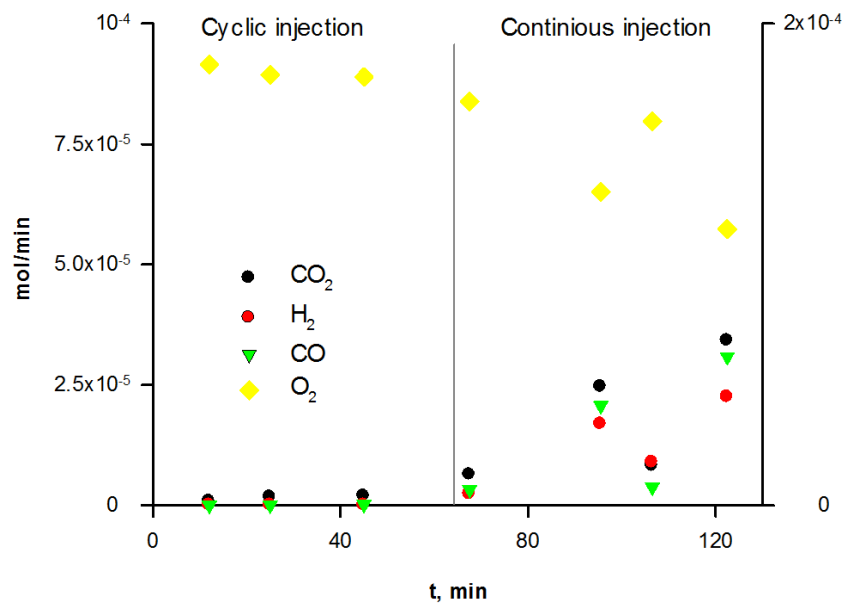


Figure 4.10 Gas composition vs. time, VPP,  $T = 650$  K,  $R(\text{C} : \text{O}_2) = 0.7$ .



Figure 4.11 Al-V-Mo (a) before reaction, (b) after reaction (continuous system) (c) after reaction (oxidation-reduction system),  $T = 650$  K,  $C_{\text{O}_2} = 0.04$ .

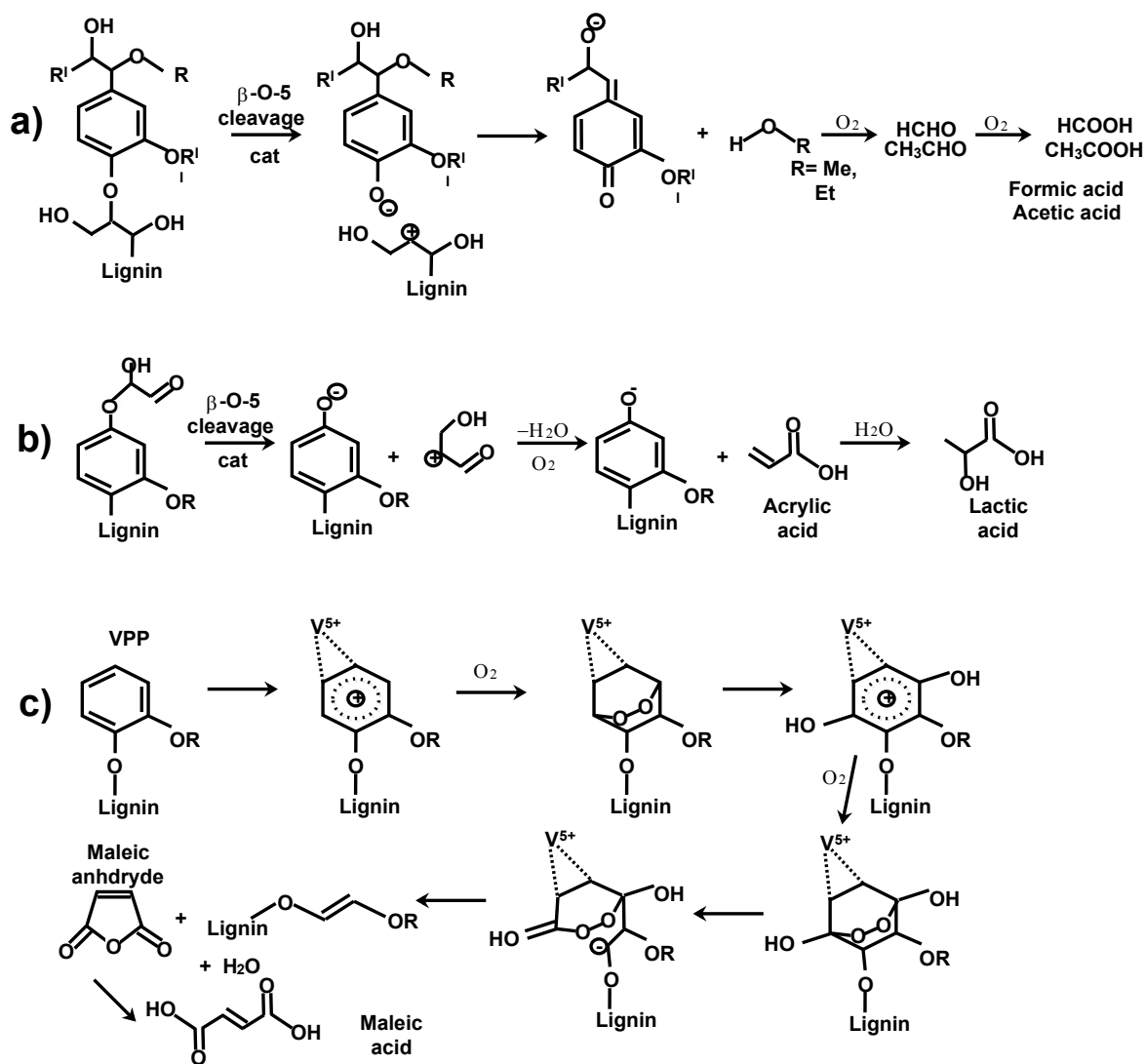


Figure 4.12 Mechanism proposed for the formation of a) formic acid and acetic acid; b) acrylic acid and lactic acid; c) maleic anhydride and maleic acid.



Side alkyl chains containing double bonds can hydrate and then crack to form acetic acid Hasegawa et al. (2011).

We detected more lactic acid than any other compound with Al–V–Mo. We attribute the formation of lactic acid to the hydration of acrylic acid, which we have also detected. Acrylic acid may form from the scission of a phenolic unit and one of the numerous aldehydes with which the lignin polymeric chains terminate. Acrylic acid forms in the presence of O<sub>2</sub> and at high temperature (Figure 4.12b).

VPP produces maleic anhydride from many substrates Shekari and Patience (2010); Ghaznavi et al. (2014).

In the presence of an aromatic ring, the ion V(V) activates lignin attracting the p-electrons of the double bonds and generating a positive charge displaced on the ring. The ring opens by successive attack of 2 O<sub>2</sub>, thus producing maleic anhydride (Figure 4.12c). H<sub>2</sub>O insertion - instead of O<sub>2</sub>- might also cause the aromatic ring cleavage to form maleic anhydride Umezawa and Higuchi (1987).

Maleic anhydride hydrolyses to the acid in water (Figure 4.12c). Phthalic anhydride proceeds from the reaction between maleic anhydride and 5 carbon atoms rings with at least one oxygen.

The reason why VPP produces maleic anhydride rather than lactic acid is because V<sub>5</sub><sup>+</sup> is able to uniquely activate the aromatic rings leading to their cleavage. Due to the charge imbalance among the metals, Al–Mo–V is more acidic than VPP. Therefore, its activity towards the  $\beta$ -O-4 bonds cleavage is higher compared to VPP. As a consequence, in the presence of Al–Mo–V, a higher number of aldehydic units will make lactic acid.

We attribute the hydrogen produced to lignin decomposing to the carbon (e.g. forming coke on the catalyst) partly to gasification, as Furusawa and co-authors report at supercritical water conditions Furusawa et al. (2007).

## 4.4 Conclusions

Vanadium-oxides are promising catalysts to activate lignin at atmospheric pressure and below 700 K. Al–V–Mo and VPP catalysts convert a small fraction of lignin to carboxylic acids in one step in a gas-solid system. Reaction kinetics are higher in the gas phase and convert lignin in minutes rather than hours in the liquid phase. Lactic acid predominates with Al–V–Mo while VPP mostly gave malonic acid and maleic anhydride. The yield to lactic acid was 6 % over Al-V-Mo but yield to acids over VPP was only 2 %. Assuming fuel value for lignin, a

maleic anhydride process would be economically attractive above 50 % selectivity (weight basis), which is equivalent to the current commercial maleic anhydride process based on n-butane as a feedstock. Yields versus n-butane are necessarily higher because the distillation train would be more complex due the higher concentration of by-products.

Catalyst agglomeration and liquid injection of lignin were challenging and contributed to the yield loss. We expected cycling catalyst between the lignin solution and air increase yields. Our tests with forced concentration cycling (switching between air and the lignin solution) reduced coke formation and catalyst deactivation thereby increasing the yield to organic compounds to 25 % at 600 K and O<sub>2</sub> of 4 %. Increasing the reactor scale (to improve the heat transfer) and using multi-functional catalysts that cleave the  $\beta$ -O-4 and 5-5' linkages more effectively to phenolic compounds and C<sub>3</sub> compounds are other options that we are going to investigate in future work.

## 4.5 Experimental Section

### 4.5.1 Materials

Softwood kraft lignin was provided by FPIInnovations (Quebec, Canada). It was recovered from the Resolute Forest Products mill in Thunder Bay, Ontario via the LignoForce System (with a mass fraction of 66.9 % carbon, 5.2 % hydrogen, 0.1 % nitrogen, 25.4 % oxygen, 92 % total solids) Kouisni et al. (2012); Kouisni and Paleologou.

DuPont synthesized the VPP to convert n-butane to MA Patience and Bockrath (2010). Laboratoire MAT provided the NaOH (97 % purity). The catalyst reagents included : HCl (Fischer Scientific, 37 %), ammonium molybdate(VI) tetrahydrate (Acros, 99 %), sodium tetraborate decahydrate (Fisher Scientific, 99.5 %), sodium phosphate (Sigma-Aldrich, 96 %), ammonium metavanadate (ACS reagent grade,  $\geq 99$  %). We did not further purify any reagents.

### 4.5.2 Catalyst preparation

We impregnated  $\gamma$ -alumina (specific surface area (SSA) = 140 m<sup>2</sup> g<sup>-1</sup>) with V-Mo Barker (1975). A 50 mL solution of 37 % HCl and 4 mL of water at 350 K dissolved 5.3 g of ammonium molybdate(VI) tetrahydrate and 0.6 g of sodium tetraborate decahydrate. We prepared two solutions : (i) 0.4 g of sodium phosphate in 3 mL of distilled hot water ; and (ii) 8.4 g of ammonium metavanadate ACS reagent grade in 25 mL of hydrochloric hexahydrate and 11 mL of distilled water at 300 K. We added the first solution to the second while conti-

uously stirring and finally adding the support. A rotary evaporator operating at 500 mmHg vacuum and 358 K removed most of the water. The powder dried completely at 370 K and atmospheric pressure for 12 h. It then calcined at 675 K for 2 h.

#### 4.5.3 Catalyst characterization

A Quantachrom Autosorb 1 MP system measured the surface area following the standard multi point Brunauer-Emmet-Teller (BET) method. The samples were degassed at 575 K for 3 h under vacuum.

A Philipps X'pert diffractometer with a Cu-K radiation source ( $1.5406 \text{ \AA}$ ) at 50 kV and 40 mA generated the diffraction patterns (XRD). The instrument operated at room temperature with an incidence angle of  $0.5^\circ$ . It scanned at a diffraction angle between  $20^\circ$  and  $90^\circ$  and a divergence slit of  $1^\circ$ .

A Horiba LA-950 measured the particle size distribution (PSD).

A scanning electron microscope (SEM) generated images of the catalysts. An SEM-JSM-840A (JOEL Company) energy-dispersive X-ray spectroscopy (SEM-EDX) coupled with an electronic X-ray diffraction (EDX) detector identified the principal elements.

#### 4.5.4 Partial oxidation test

We conducted all experiments in a 7 mm quartz  $\mu$ -fluidized bed with 300 mg of catalyst powder. In the first series of experiments, a syringe pump injected the lignin-NaOH solution to the top of the reactor at  $0.125 \text{ mL min}^{-1}$  through a 1/16" (ID= 0.8 mm) SS tube. The nozzle tip sprayed the solution downwards 0.5 cm above the bed surface (Figure 4.13). The concentration of lignin was  $30 \text{ g L}^{-1}$  and NaOH (in distilled water) was  $70 \text{ g L}^{-1}$ .

Ar and Ar/O<sub>2</sub> mixtures entered the reactor from the bottom to fluidize the powder and partially oxidize lignin. The effluent gases passed through an ice-cooled absorber containing distilled water to trap the condensate. Heat tape maintained the lines upstream of the absorber at 395 K. A thermocouple monitored the bed temperature. Brooks mass flow controllers maintained the volumetric flow rate of the fluidization gas and the Ar/O<sub>2</sub> at  $70 \text{ mL min}^{-1}$  ( $25^\circ\text{C}$  and 1 bar). A Hiden mass spectrometer (QIC-20) monitored the non-condensable effluent gas concentrations on-line at a frequency of 3 Hz. A Varian HPLC (Prostar) with a Metatherm column and a 0.02 N phosphoric acid solution measured the liquid product distribution off-line. We calculated the yield of products by dividing the produced acids by total injected lignin. To calibrate the HPLC, we prepared 100 ppm standard solution for different acids. We obtained the HPLC calibration curve by injecting standard solution at 6 levels.

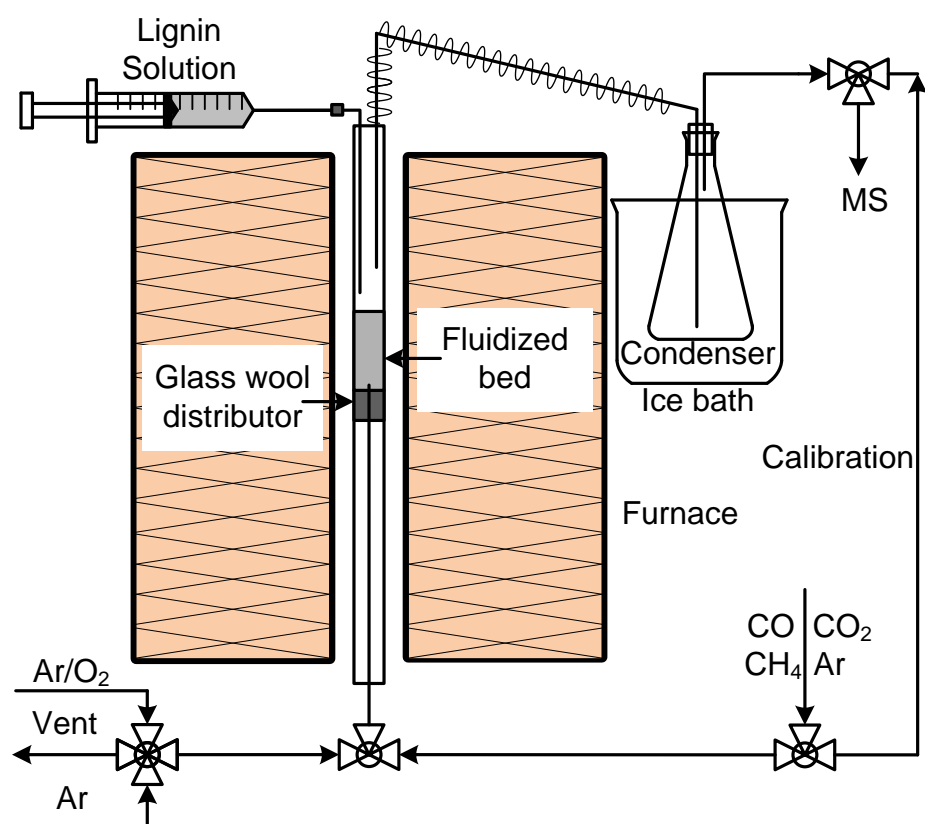


Figure 4.13 Schematic of the experimental set-up.

We analysed each sample three times. To verify repeatability of the analysis, we randomly tested several samples one or two weeks after completing the experiments. Also, we injected the standard solution in between HPLC runs to ensure the instrument was stable.

An AVANCE 200 MHz solid state NMR spectrometer (1 ms  $^{13}\text{C}$  CPMAS contact, spinning speed of 5 kHz and recycle delay of 2 s) analysed the solid residue.

The fresh catalyst fluidized well but the hydrodynamics of the bed became poorer with time-on-stream while feeding the lignin/NaOH solution. Eventually, the bed would slump as liquid filled the tube and the catalyst agglomerated. The agglomeration accelerated when the exit line temperature dropped below 100 °C and water and reaction products condensed and dropped into the bed.

We established the  $\text{O}_2$ :lignin molar ratio assuming syngas ( $\text{H}_2$  and  $\text{CO}$ ) was the end product. Literature studies have tested  $\text{O}_2$  to hydrocarbon molar ratios of 1 to 14 (Table 4.2) and temperatures from 530 K to 725 K.

We tested C: $\text{O}_2$  ratios between 0.35 and 0.7 and 600 K, 650 K and 700 K.

Each test was repeated at least two times and most were repeated three times.

The lower explosion limit of hydrocarbon gases in air is 2 %. Since the mole fraction of oxygen was at most 3 %, there was no risk of deflagration or other particular safety hazard.

## 4.6 Acknowledgment

The authors acknowledge NSERC for financial support and DuPont for supplying the VPP catalyst and FPInnovation for supplying lignin and analytical assistance. In addition special thanks to to the NSERC Biomaterials and Chemicals Strategic Network([www.lignowork.ca](http://www.lignowork.ca)), especially Dr. Facey and Dr. Baker from University of Ottawa for analytical assistance.

## CHAPTER 5    ARTICLE 2 - KINETIC STUDY OF LIGNIN THERMAL AND THERMO-OXIDATIVE DEGRADATION

**Samira Lotfi and Gregory S. Patience\***

*Department of Chemical Engineering, Ecole Polytechnique de Montreal, Montreal, Quebec, Canada*

Corresponding author : Tel. : +1-514-340-4711 X 3439 ; fax : +1-514-340-4159.

E-mail address : gregory-s.patience@polymtl.ca

(Submitted to Biomass and Bioenergy)

### 5.1 Abstract

Lignin is a complex biopolymer that is exploited for its fuel rather than for valuable phenolic compound content. Lignin is the glue that binds hemicellulose and cellulose to form a rigid structure but is chemically inert except at high temperature or at basic and acidic solutions. Thermal and oxidative degradation are two methods to convert lignin into chemicals. We characterized the lignin product yield and selectivity with in a micro-fluidized bed reactor operated up to 900 K in nitrogen and air. The liquid product yield (predominantly aromatics) was  $\sim 20\%$  for both cases. In air, oxygen reacted with lignin to form CO, CO<sub>2</sub> and CH<sub>4</sub> while in nitrogen char was the principal product. We derived a two-step model from based on thermogravimetric analysis at a heating rate of 5 K min<sup>-1</sup> to 30 K min<sup>-1</sup>.

### 5.2 Introduction

Lignocellulosic compounds are a potential source of chemicals and fuels as an alternative to petroleum, whose environmental foot print is greater and whose price fluctuates widely on the global market. Lignin has been largely ignored as a feedstock even though it constitutes up to 40 % of the lignocellulosic because it is difficult to activate except at extreme conditions resulting in low selectivity to target compounds (Zakzeski et al., 2012; Ragauskas et al., 2014). It is a three dimensional amorphous polymer and the only source of aromatic compounds from biomass (Shen et al., 2009). Various linkages connect hydroxylated, methoxylated and phenylpropene units of lignin.

Lignin is the main waste product from the pulp and paper industry and Bio-refineries (Shen et al., 2009). The US Department of Energy recommends that bio-refineries concentrate on converting lignin to selective products. However, lignin is a heterogeneous compound and

their composition and physico-chemical properties vary geographically and with pretreatment methods (Ma et al., 2015a).

Thermal processes — pyrolysis, gasification, liquefaction and combustion — with lignin as a feedstock produce bio-oils, chemicals, charcoal and heat. Thermo-catalytic conversion of lignin to valuable chemicals is a promising alternative to add value to the product portfolio of bio-refineries (Ragauskas et al., 2014). A better understanding of the fundamental reaction mechanism of lignin is necessary to develop efficient processes (Shen et al., 2009). Catalysts reduce the activation energy allowing processes to operate at lower temperatures thereby increasing the selectivity to phenolic compounds and carboxylic acids.

Pyrolyzing lignin produces incondensable gases, liquids and coke (Farag et al., 2014a). Thermo-catalytic processes break and rearrange the lignin C-H bonds (Lalitendu et al., 2012). Reaction temperature, heating rate, gas composition and type of lignin affect product profile (Brebú and Vasile, 2010; Shen et al., 2009). Gas versus liquid production increases with higher H/C ratio. Low heating rates yield oxygen-containing compounds while fast heating rates tend to produce hydrocarbons and alkyl-phenol derivatives (Brebú and Vasile, 2010). The product distribution depends on the biomass composition Pasangulapati et al. (2012a) but the reaction rate and activation rate are somewhat independent of the composition. The lignin structure, moisture content, impurities, heating rate, and reaction temperature affect the product yield as well as selectivity (Brebú and Vasile, 2010). The oxygen functional group react over a wide temperature range (Brebú and Vasile, 2010). Stable low molecular weight compounds form when lignin depolymerizes (Ragauskas et al., 2014; Brebú and Vasile, 2010).

Whereas thermo processes of lignin have been studied, oxidative processes have received less attention ((Elder, 2014; Kumar et al., 2009; Farag et al., 2014a; Brebú and Vasile, 2010; Faravelli et al., 2010)) The scarce data come from studying gasification of lignocellulose—cellulose, hemicellulose, and lignin Poletto et al. (2012); Kumar et al. (2009); Lv et al. (2010).

Shen et al. (2009) proposed a two step kinetic model for wood oxidation in the range of 450 K to 800 K. In the first step, lignin decomposed to gas and char and in the second step the remaining fraction produced gas ( $\text{CO}_x$ ) and char. Wet oxidation hydrolyses lignin to aromatic aldehyde and acids through a consecutive reaction and simultaneously to CO and  $\text{CO}_2$  and water. The activation energy of lignin conversion and aromatic aldehyde production were  $44 \text{ kJ mol}^{-1}$  and  $65 \text{ kJ mol}^{-1}$ , respectively (Sales et al., 2007). Chen et al. (2014) determined the kinetic model parameters for the decomposition of lignocellulose under an  $\text{CO}_2$  environment. A two step mechanism best fit lignin decomposition, where the surface reaction rate was limiting, with an activation energies of  $150 \text{ kJ mol}^{-1}$ , Blasi et al. reported  $86 \text{ kJ mol}^{-1}$  for

the rapid decomposition of lignin in air Chen et al. (2006).

Identifying the reaction mechanism could help maintain the catalyst activity and develop strategies to target specific chemicals. Catalyst composition and morphology, heating rate and temperature are the factors that determine the rate at which volatile compounds evolve and are key to prevent compounds from fragmenting, condensing and agglomerating. Oxygen converts most of the lignin to gas and liquids, while after pyrolysis a large fraction remains as char. Here we tested both an inert atmosphere and air ((Jankovic, 2013)) to gauge the product selectivity in a micro-fluidized bed and TGA. We characterize the data with a two-step kinetic model.

## 5.3 Experimental

### 5.3.1 Thermal and thermo-oxidative degradation

In the first series of experiments, we monitored product selectivity versus temperature in a 8 mm ID quartz micro-fluidized-bed while we heated lignin at  $5\text{ K min}^{-1}$  under argon and 21 % oxygen. Softwood kraft lignin was provided by FPIInnovations (Quebec, Canada). It was recovered from the Resolute Forest Products mill in Thunder Bay, Ontario via the LignoForce System (with a mass fraction of 66.9 % carbon, 5.2 % hydrogen, 0.1 % nitrogen, 25.4 % oxygen, 92 % total solids) Lotfi et al. (2015); Kouisni et al. (2012); Kouisni and Paleologou. The effluent passed through a quench filled with water. When the bed temperature reached 500 K, we sampled the quench every 10 min. A Varian HPLC (Prostar) with a Metatherm 87H column and a 0.02 N phosphoric acid solution as a carrier analyzed the liquid products. To identify unknowns, we extracted samples from the quench with ethyl ether and injected it in a GC-MS (Agilent5975C VLMSD) with a capillary column (Br-1MS 15 m x 0.25 mm x 0.25  $\mu\text{m}$ ). A Hanna electrical conductivity instrument measured the concentration of the ionizable solutes present in the quench to assess the lignin liquefaction rate. A ThermoStar Pfeiffer Vacuum mass spectrometer monitored the gas phase composition at the exit of the quench.

A Thermo-Gravimetric Analyser (TA-Q50) measured the weight loss versus temperature. The resolution of the balance was 0.1  $\mu\text{g}$  with an accuracy better than 0.1 %. We modelled the reaction kinetics based on multiple temperature ramps ( $5\text{ K min}^{-1}$  to  $30\text{ K min}^{-1}$ ) and iso-thermal tests at 900 K under nitrogen (pyrolysis) and air (oxidation). We loaded 20 mg sample to a platinum crucible and heated to 350 K at  $10\text{ K min}^{-1}$  under  $40\text{ mL min}^{-1}$  flow of nitrogen, we held it at 350 K for 15 min to evaporate water. For the isothermal tests, we ramped the dried sample at  $100\text{ K min}^{-1}$  up to 950 K. For the constant heating rate tests, we



ramped at 5, 10, 20, 30 K min<sup>-1</sup> to 950 K.

## 5.4 Results and discussions

### 5.4.1 product distribution

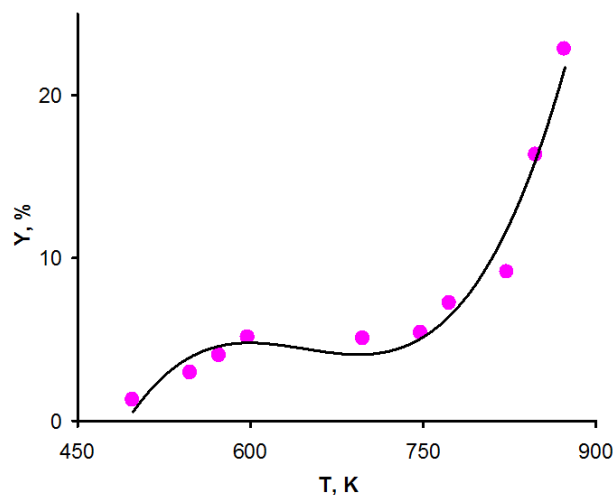
#### Lignin oxidation

Temperature affects liquid yield and the product distribution. We monitored the gas composition of the effluent of a fluidized-bed that was subjected to a 5 K min<sup>-1</sup> temperature ramp. At  $\sim 450$  K oxygen began to react in the fluidized bed. The oxygen concentration reached a minimum at  $\sim 500$  K and both the CO and CO<sub>2</sub> and H<sub>2</sub> concentrations reached a plateau. At this temperature, the MS detected a low concentration of CH<sub>4</sub> (Figure 5.1d). We suppose that at  $\sim 500$  K weak aryl-ether bonds degrades.  $\alpha$ -O and  $\alpha$ - $\beta$  have lower breakage enthalpies; however, their bond dissociation enthalpy varies with lignin source. Increasing the temperature increased the liquid yield slightly (Figure 5.1a). The liquid yield increased considerably beyond  $\sim 750$  K. The CO concentration increased and CH<sub>4</sub> and H<sub>2</sub> detected, also.

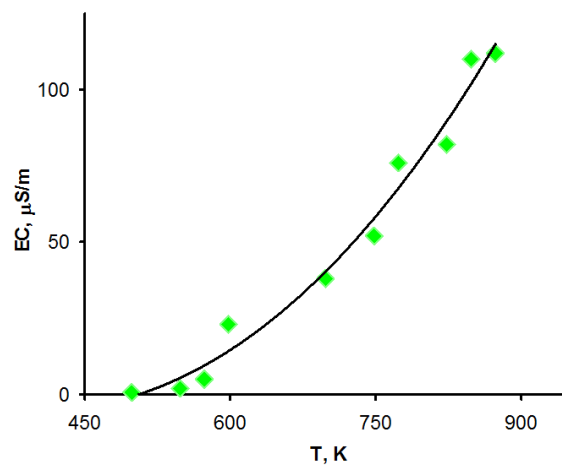
Aromatics and carboxylic acids (maleic, formic, fumaric, butyric, acetic, succinic and phthalic) were the main liquid products detected by HPLC and GC-MS (Figure 5.2, Table 5.1) Liquid yield for the oxidation and pyrolysis test were similar but the conductivity signal was higher for the oxidation tests (Figure 5.1b). Most acids form at 550 K to 850 K. The gas, liquid and solid carbon yield were 79 % and 20 % and 1 % between 900 K, respectively (Figure 5.1c).

Table 5.1 Lignin oxidation aromatic products- GC-MS analysis.

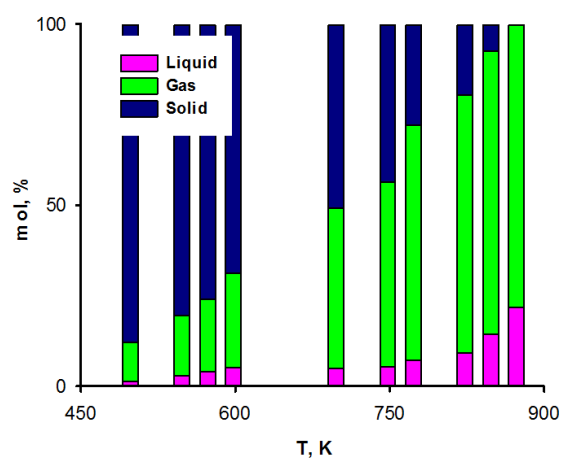
No.	Name
1	o-Guaiacol
2	4 Ethyl 1,3-benzenediol (4-Ethylresorcinol)
3	Creosol
4	4-Ethyl-2-methoxy-phenol(4-Ethylguaiacol)
5	2-Acetyl-4-methylphenol
6	Benzaldehyde, 3-hydroxy-4-methoxy, oxime
7	Vanillin
8	Apocynin
9	Butylated Hydroxytoluene



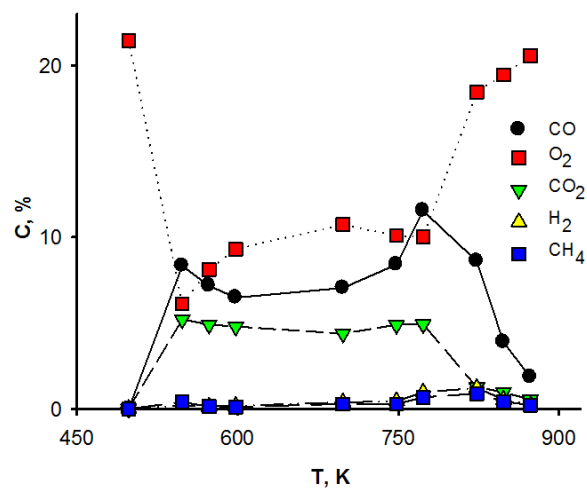
(a) Yield



(b) Electro-conductivity



(c) Carbon balance



(d) Gas concentration

Figure 5.1 Lignin thermo-oxidative degradation in the fluidized bed (air)

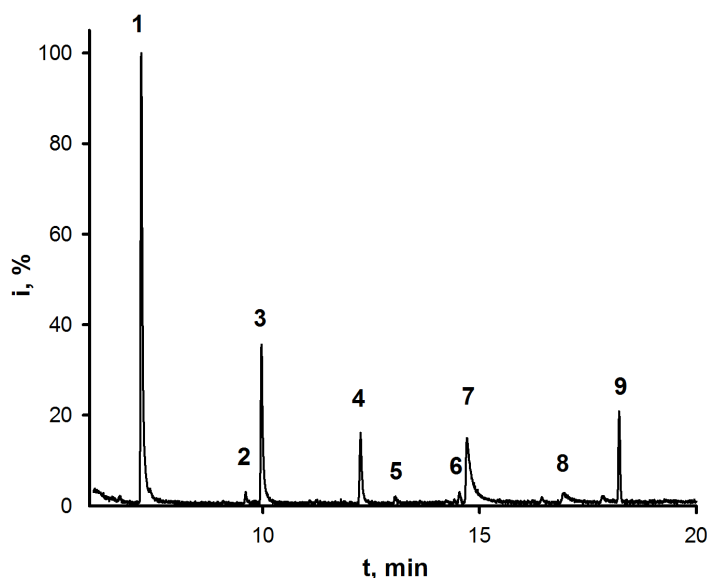


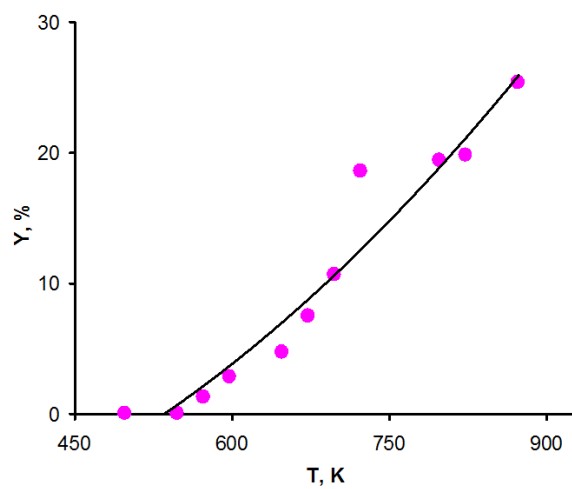
Figure 5.2 GC-MS chromatography.

### Thermal degradation

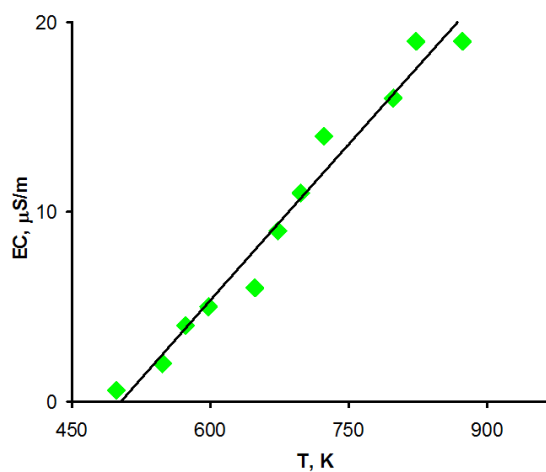
We followed the lignin degradation in the micro-fluidized bed reactor by collecting and analysing the gas and liquid phases. Pyrolysis of lignin gives coke, gases and liquids including phenolics, non-phenolic, aromatics, and aliphatic compounds Farag et al. (2014a); Brebu and Vasile (2010). The various oxygen functional groups in lignin react over a broad temperature range (550 K to 1000 K). Ledesma et al. (2014) cracked of 4-vinylguaiacol (2-methoxy-4-vinylphenol) model lignin compounds and produced oxygenates (phenols, cresols, furans, ketones, and aldehydes) and aromatic hydrocarbons (single-ring aromatics, and polyaromatics). Temperature had a remarkable effect on product distribution.

The softwood kraft lignin structure began to crack at  $\sim 550$  K (Figure 5.3). First,  $\text{CO}_2$ ,  $\text{CO}_2$  and  $\text{CH}_4$  evolve;  $\text{CO}_2$  and  $\text{CH}_4$  reach a maximum at 550 K and 600 K, respectively. The maximum CO was between 600 K to 750 K (Figure 5.3d). The aryl-ether bonds have a lower thermal stability and began to cleave at 580 K Brebu and Vasile (2010). At 600 K aromatics formed (Figure 5.3a). The conductivity signal increased sharply at this point as well (Figure 5.3b). Lignin propanoic side chains yield methyl-, ethyl- and vinyl guaiacol and vanillin between 500 K to 550 K Brebu and Vasile (2010).

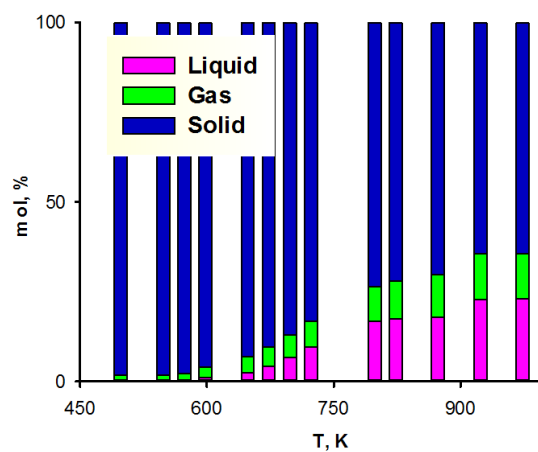
Increasing temperature beyond 700 K dropped the CO concentration from 1.5 % to 1 % while at the same point the  $\text{H}_2$  concentration began to increase and reached 0.5 % at 900 K. The



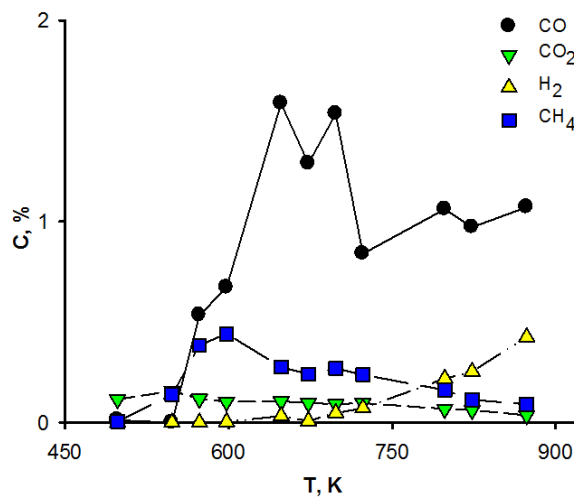
(a) Yield



(b) Electro-conductivity



(c) Carbon balance



(d) Gas concentration

Figure 5.3 Lignin thermal degradation in the fluidized bed (N<sub>2</sub>)

liquid yield increased up until  $\sim 900$  K and thereafter remained almost constant (Figure 5.3c, 5.3b). Based on the TGA traces, the rate lignin degraded beyond 800 K was constant (Figure 5.4b). The liquid yield was very low until 600 K. The major peaks belonged to  $C_5$ – $C_8$  aromatics. At 650 K, the yield of  $C_5$ – $C_8$  doubled and more aromatics like vanillin and benzoic acid as well as lactic acid formed. Aromatics formed from the cleavage of the O–C(alkyl) and O–C(aryl) at  $\sim 700$  K Brebu and Vasile (2010). Increasing temperature to 850 K doubled yields of  $C_5$ – $C_8$  aromatics. At 950 K, besides the phenolic compounds, acetic, vanillic, acrylic and gallic acid were detected. At 1000 K, the HPLC detected traces of formic and fumaric acids. Normally, higher than 800 K aromatic rings rearranges or condenses and  $H_2$  forms Ferdous et al. (2002). CO forms from ether bridge joining sub-units at lower temperature and from diaryl ether at higher temperature Ferdous et al. (2002). Methoxy group ( $-OCH_3$ ) yields  $CH_4$ .  $CO_2$  groups forms from carboxyl group Brebu and Vasile (2010).

The gas and liquid carbon fraction reached 15 % and 25 % at 900 K, respectively. Klein and Virk (2008) reported 10 % to 20 % gas production during lignin pyrolysis. Phenolic fraction typically is 3 % to 30 % Klein and Virk (2008). The product selectivity changes with temperature and time Klein and Virk (2008). Beis et al. (2010) reached 16–22 % liquid yield. The aromatic fraction depended on type of lignin Beis et al. (2010).

## 5.5 Mechanism

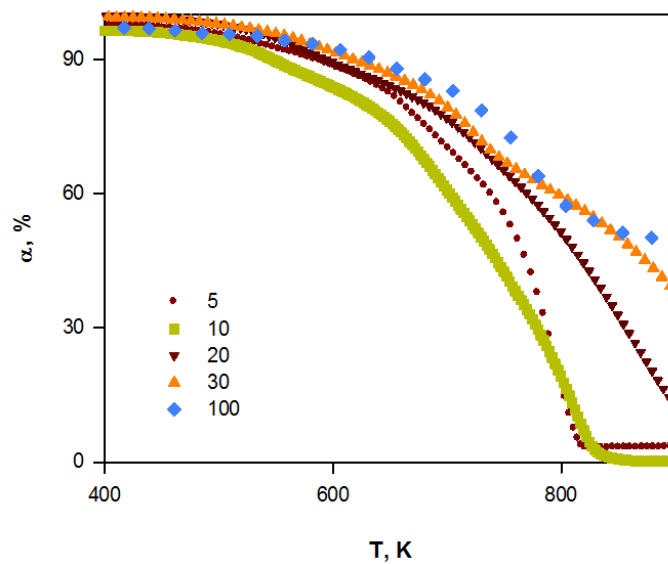
In the TGA lignin oxidation tests at heating rates of 5, 10, 20, 30, and 100  $K\ min^{-1}$  0.3 %, 3 %, 27 % and 37 % solids remained at 850 K (Figure 5.4a). In the lignin pyrolysis tests  $42\% \pm 2\%$  solids remained even up to 950 K for all heating rates (Figure 5.4b). Increasing the heating rate shifted the maximum degradation rate to the higher temperatures (Figure 5.5a, 5.5b). Pre-exponential factor reduced by increase of heating rate (Table 5.2).

### 5.5.1 Thermal degradation

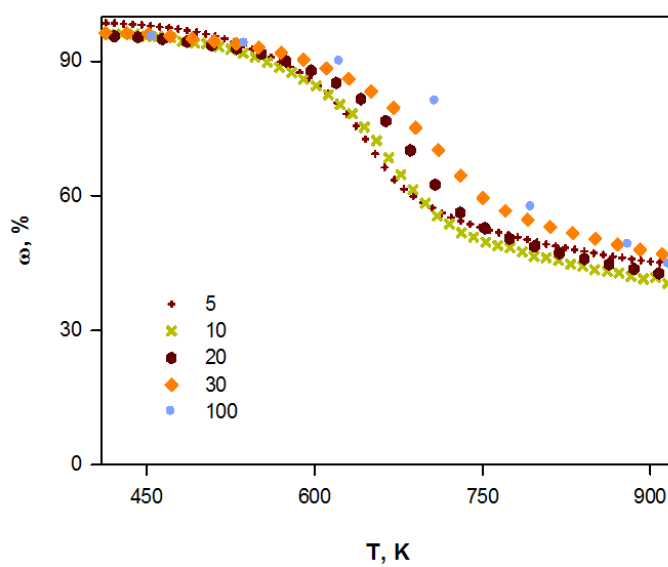
Characterizing the lignin thermal degradation kinetics, product selectivity and mechanism will help optimize the reaction to achieve high selectivity of valuable compounds.

## Stability

The differential thermogravimetric curves (DTG) and TG curves (Figure 5.6) exhibit two distinct temperature regions in which lignin reacted — 400 K to 550 K (Zone 1) and 260 to 950 K (Zone 2). In Zone 1, lignin degrades forming phenolic compounds while in the second one it releases — CO,  $CO_2$  and probably  $CH_4$ ,  $C_2H_4$  — and char Brebu and Vasile (2010).

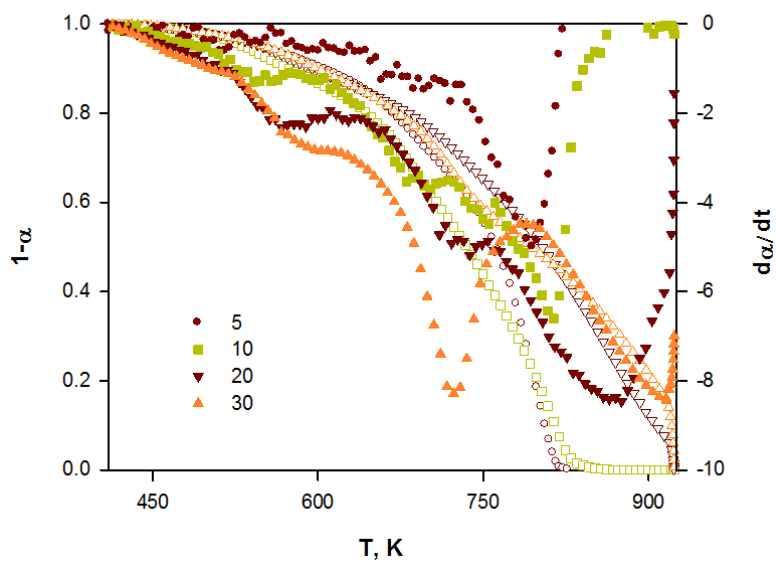


(a) Oxidation

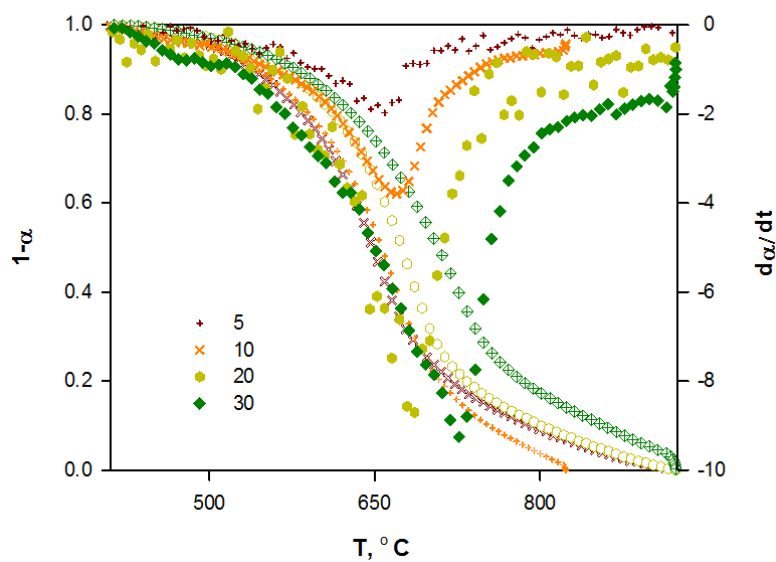


(b) Pyrolysis

Figure 5.4 Mass loss of lignin as a function of temperature and temperature ramp in a TGA



(a) Oxidation



(b) Pyrolysis

Figure 5.5 Lignin degradation behavior– TGA-DTG curve

Brebu and Vasile (2010) reported between 550 K to 650 K, C-C and  $\beta$ - $\beta$  compounds cleave and guaiacols and syringols form. They claimed two competitive reaction pathways that produce monomers and gases.

In our experiments, the most of the lignin reacted in Zone 2. The DTG curves were asymmetric with a shoulder, which suggests multiple reaction pathways exist. The shoulder could be related to the production of aromatics. Decomposition of these aromatics to char and gas gave the sharp peak. By increasing the heating rate, the main peak (peak II) shifted to higher temperature and degradation rate ( $\frac{d\alpha}{dt}$ ) increased.

Comparing the fluidized-bed results with the TG curves suggests that until 750 K most of the lignin reacted to form light gases while after 750 K it produced more liquids. Farag et al. (2014a) observed the same product selectivity. Up to 750 K yield of non-condensable gas was higher than liquids and most aliphatic hydroxyl side chains degraded. Increasing temperature cleaved the strong chemical bonds and yielded more liquid rather than gas. With an isoconversional analysis we estimated the activation energy and mechanism.

### Isoconversional analysis

Isoconversional method gives  $E_a$  at different  $\alpha$  without considering any reaction model Vyazovkin et al. (2011); Brown et al. (2000); Nassar et al. (2014). We applied the Friedman analysis to estimate activation energy of lignin pyrolysis (Figure 5.7). First,  $E_a$  increased sharply up to  $\sim 23 \text{ kJ mol}^{-1}$ . Increasing the temperature, increased the activation energy slightly between  $0.2 < \alpha < 0.8$ .

Since the activation energy varies with temperature, we conclude that lignin pyrolyses in multiple steps, which substantiates our fluidized bed data. We consider two parallel and independent reactions Jankovic (2013); Nassar et al. (2014). Farag et al. (2014a) proposed a kinetic model assuming lignin degraded to solid, gas and liquids. Assuming first order reaction kinetics the activation energies for solids, liquids and gas were 19, 29 and  $22 \text{ kJ mol}^{-1}$ ,

Table 5.2 Lignin pyrolysis characteristic.

$\frac{dT}{dt}$	Peak I		Peak II	
	T(K)	$\frac{d\alpha}{dt}$	T(K)	$\frac{d\alpha}{dt}$
5	553	0.58	648	1.83
10	544	0.62	667	4.59
20	504	0.7	702	7.3
30	499	0.94	728	9.3



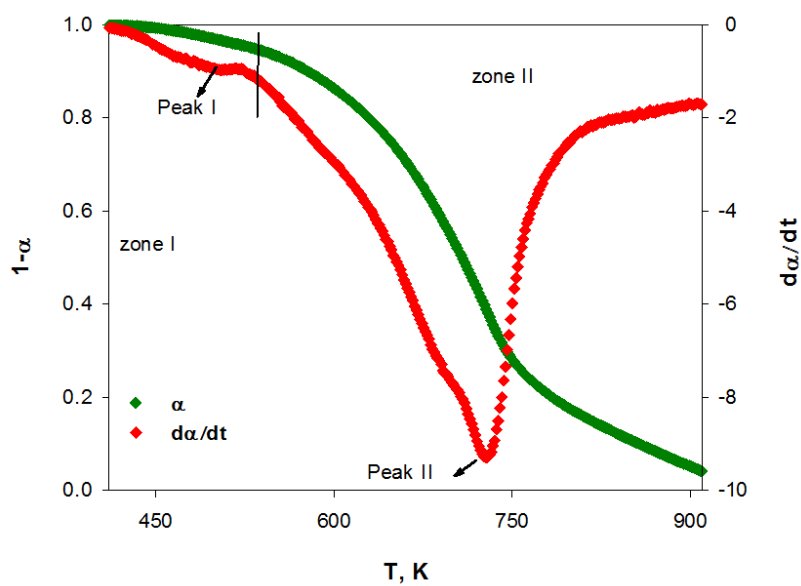


Figure 5.6 The TG-DTG curves of thermo degradation of lignin, Ramp=30 K min<sup>-1</sup>.

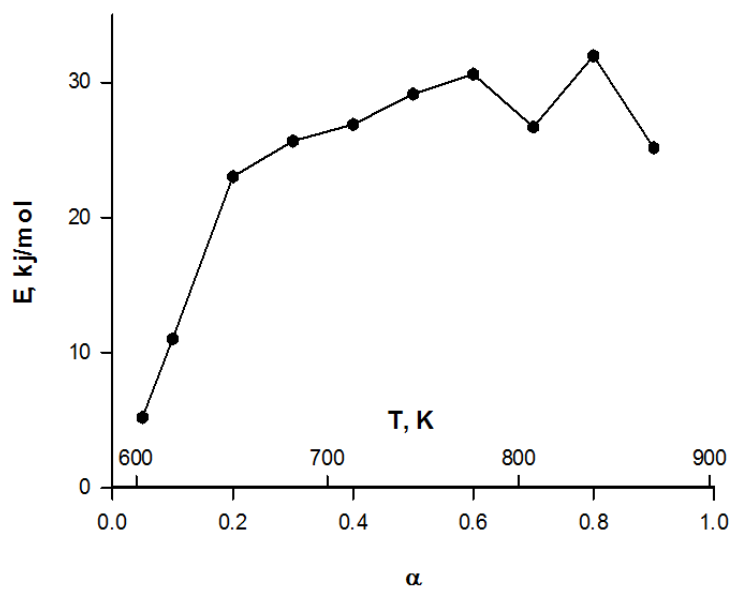


Figure 5.7 Frideman model, pyrolysis.

respectively, which, is close to the values we derived based on the isoconversional method.

We compared the experimental data to standard methods to identify possible mechanisms (Table 5.3). Single step mechanisms poorly characterised the experimental data, as expected, so we considered two parallel first order reactions.

A two step first order fit the experimental data well (Figure 5.8). Activation energy (Table 5.5) was independent of heating rate but the pre-exponential factor decreased from 0.00195, 0.00372 to 0.00058 and 0.0015 when increasing the heating rate from 5 K min<sup>-1</sup> to 30 K min<sup>-1</sup> in the higher and lower temperature range (zone I and zone II). The pre-exponential factor represents the frequency of vibration of the activated complex Vyazovkin et al. (2011). This variation could be attributed to heat and mass transfer phenomena or a combination of both. The activation energies for the first and second step were 47 kJ mol<sup>-1</sup> and 95 kJ mol<sup>-1</sup>, respectively. The pre-exponential factor and  $E_a$  increase as conversion increases in polymer and complex organic materials Vyazovkin et al. (2011). Brebu and Vasile (2010) considered two competitive reaction pathways for thermal degradation of lignin.

We can derive pre-exponential factors, activation energies, and the reaction mechanism of lignin thermal degradation by fitting standard models to the experimental data (Table 5.4). At lower temperature, the activation energy is  $\sim 25$  kJ mol<sup>-1</sup> that increases to  $\sim 70$  kJ mol<sup>-1</sup> at higher temperature Brebu and Vasile (2010); Kumar et al. (2009). Activation energy of fast pyrolysis of lignin at 800 K for Indulin AT, acetocell lignin and lignoboost were 43, 47 and 37 kJ mol<sup>-1</sup>, respectively Beis et al. (2010). Activation energy of lignin torrefaction ( $T_{max}=600$  K) was 38 kJ mol<sup>-1</sup>. Most literature models assume first-order reaction kintetics Brebu and Vasile (2010); Ferdous et al. (2002). Ferdous et al. (2002) used a distributed activation energy model and considered that lignin decomposes following irreversible first-order reactions with multiple activation energies. Our results are close to the former models

Table 5.3 Probable mechanistic function  $f(\alpha)$  and the linear regression coefficients ( $R^2$ ) during the thermal decomposition of lignin.

Mechanism	$f(\alpha)$	$g(\alpha)$	Slope	$R^2$	$B$
Reaction controlled by phase boundary, Jimenez et al. (2013)	$3(1 - \alpha)^{2/3}$	$3(1 - (1 - \alpha)^{2/3})$	-0.16	0.99	0.74
Contracting sphere	$(3/2)(1 - \alpha)^{1/3}$	$1 - (1 - \alpha)^{1/3}$	-0.1	0.99	0.45
One and a half order, Nassar et al. (2014)	$2(1 - \alpha)^{3/2}$	$(1 - \alpha)^{-1/2} - 1$	-0.28	0.98	1.1
Second order, Nassar et al. (2014)	$(1 - \alpha)^2$	$(1 - \alpha)^{-1} - 1$	-0.83	0.97	3.03
Third order, Nassar et al. (2014)	$(1/2)(1 - \alpha)^3$	$(1 - \alpha)^{-2} - 1$	-3.6	0.94	12.08
Fourth order, Nassar et al. (2014)	$(1/3)(1 - \alpha)^4$	$(1 - \alpha)^{-3} - 1$	-12.14	0.91	38.02
First order reaction pursue instantaneous nuclei growth, Jimenez et al. (2013)	$1 - \alpha$	$-\ln(1 - \alpha)$	-0.39	0.99	1.62

Table 5.4 Kinetic studies of lignin pyrolysis.

Mechanism	$T$ K	$E$ kJ mol <sup>-1</sup>	$k_0$ min <sup>-1</sup>	method	Ref.
First order	520-580	54-79		TGA	Brebu and Vasile (2010)
	600-1440	81	$3.4 \times 10^{-5}$		
First order	430-950	25	$4.7 \times 10^{-2}$	microwave	Brebu and Vasile (2010)
Fractional kinetic modeling	500-900	72-174		fast pyrolysis	Brebu and Vasile (2010); Atadana (2010)
Pseudo-first order	-	34-65	$10^{-0.3}-10^3$	TG-DSC	Brebu and Vasile (2010)
Parallel and competitive reaction					
First order (SA lignin)	500-1000	63-113	$5-2 \times 10^4$	TGA	Kumar et al. (2009)
First order (MWV lignin)	500-670	34	47	TGA	Kumar et al. (2009)
First order	450-900	17-89		fixed-bed reactor	Brebu and Vasile (2010)

Table 5.5 Lignin pyrolysis model.

Heat rate K min <sup>-1</sup>	$k_{0,1}$ 10 <sup>-3</sup>	$E_1$ kJ mol <sup>-1</sup>	$k_{0,2}$ 10 <sup>-3</sup>	$E_1$ kJ mol <sup>-1</sup>	RSS
5					0.22
10	2		3.7		0.1
20		47		95	0.37
30	0.58		1.5		0.06

that were developed for thermal degradation of lignin (Table 5.4, Figure 5.4).

### 5.5.2 Lignin oxidation

#### Stability

The TG curves to derive the the activation energies for lignin oxidation have a sigmoidal shape. The mass loss increased slowly at the beginning; it increased rapidly in the range of 600 K to 750 K, at which point 80 % of the mass has reacted and finally the residuals reacted. Increase of heating rate had a significant effect on oxidation of lignin (Figure 5.9b).

Three peaks at  $\sim 510$ ,  $\sim 660$  and  $\sim 780$  K are evident in the differential TG curves. But, the shape of the curves also change with temperature ramp. The peaks shifts towards higher temperature with increasing ramp rates (Table 5.6). The second peak was noticeable at high heating rate but almost disappeared at low heating rate. We assign this peak to char. TGA result shows  $\sim 40$  % char remains at the higher heating rate Shen et al. (2009). The lower mass loss at the higher heating rate indicates that the processes is limited by heat transfer Cardona et al. (2015).

Comparing the fluidized-bed results with the TG-DTG curves, and the other studies indicates that first weak bonds break, aromatics form and non-condensable gases evolve. The second

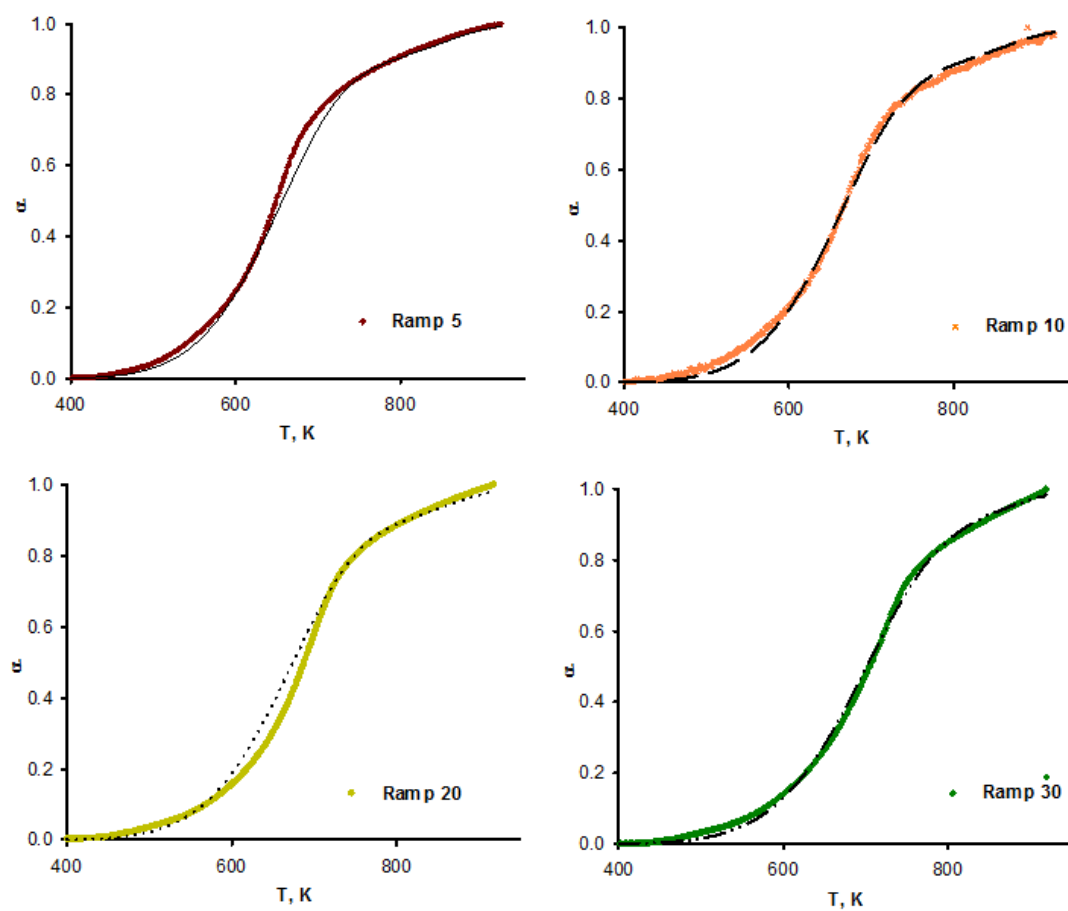


Figure 5.8 Experimental (scatter) vs. model calculated (solid line) data for pyrolysis of lignin

peak belongs to tar and char. The third peak comes from primary tar degradation and aromatic production that has a lower activation energy according to the iso-conversional analysis.

Increasing the heating rate produces more gas and char and decreases aromatic compounds Faravelli et al. (2010). Adjusting the heating rate in oxidation and thermal degradation has a considerable effect on selectivity to liquids Faravelli et al. (2010).

### Isoconversional analysis

The trends we show in the isoconversional tests (Figure 5.10) match what we expected based on the DTG curves and product yields. The highest activation energy were about ( $\sim 90 \text{ kJ min}^{-1}$ ) between 550 K to 650 K which corresponds to gas formation. The activation energy was essentially constant from 550 K to 750 K and it drops at 900 K. The wide range of activation energy implies that thermal oxidation is more complex than pyrolysis. The activation energy of phenolics, heavy-molecular weight compounds, single ring non-phenolic group and aliphatics are 38, 35, 40, and  $47 \text{ kJ mol}^{-1}$ , respectively. Farag et al. (2014a)

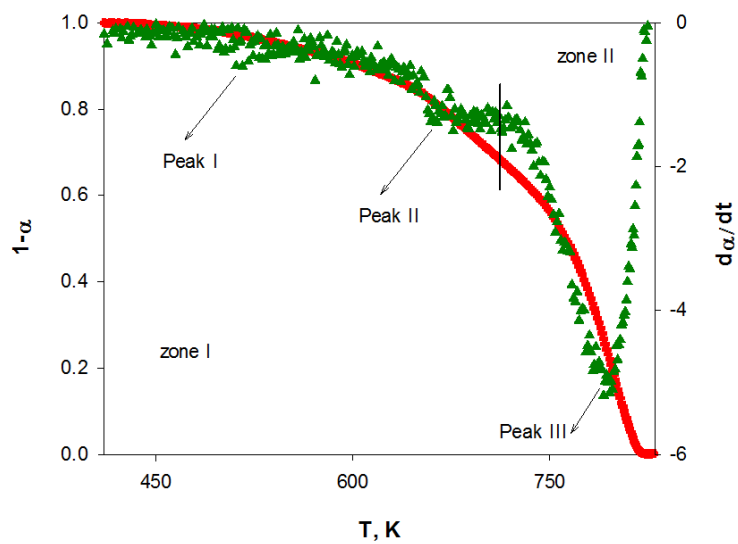
### Kinetic modelling

We fit the experimental data with common chemical reaction mechanisms. As with pyrolysis, no model fit the data well (Table 5.7). Second order models were better but a single model was incapable of capturing all of the features of the data. Rather than fitting the data over the entire range, we can assign global reaction rates to each peak and shoulder — a total of three steps. However, under certain circumstances a single rate expression may adequately approximate multi-step processes adequately Vyazovkin et al. (2011). In this case, we were able to fit the data with only two kinetic rates (Table 5.8, Figure 5.11).

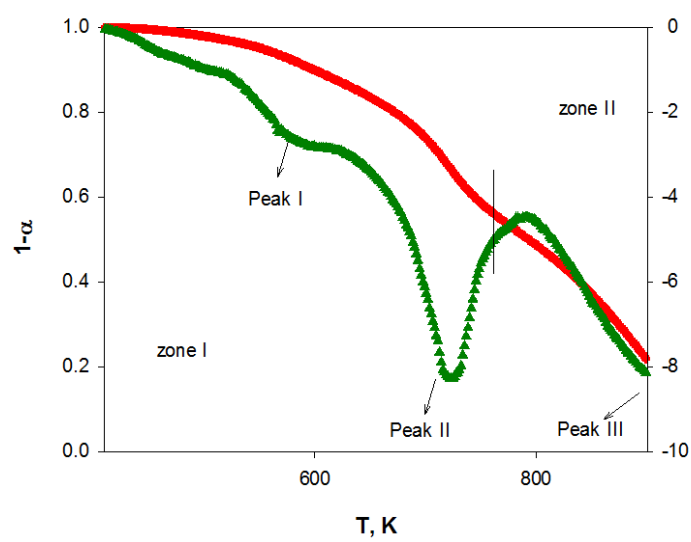
Similar to pyrolysis, activation energy was independent of heating rate but the pre-exponential factor decreased with increasing heating rate. The variation was low in the first zone :  $k_{0,1}$

Table 5.6 Lignin oxidation characteristic.

	Peak I		Peak II		Peak III	
$\frac{dT}{d\alpha}$	T(K)	$\frac{d\alpha}{dt}$	T(K)	$\frac{d\alpha}{dt}$	T(K)	$\frac{d\alpha}{dt}$
5	510	0.32	380	1.25	780	4.9
10	530	1.44	400	3.6	800	6.6
20	560	2.2	440	4.9	840	8.5
30	570	2.83	430	8.3	900	8.5



(a) Ramp= $5 \text{ K min}^{-1}$



(b) Ramp= $30 \text{ K min}^{-1}$

Figure 5.9 The TG-DTG curves of lignin thermo-oxidation

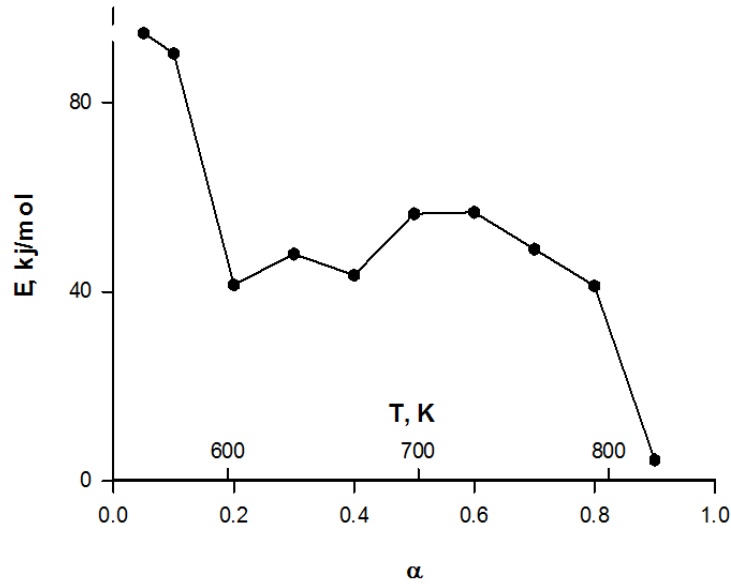


Figure 5.10 Frideman model, oxidation.

Table 5.7 Probable mechanistic function  $f(\alpha)$  and linear regression coefficients ( $R^2$ ) during the oxidative decomposition of lignin.

Mechanism	$f(\alpha)$	$g(\alpha)$	Slope	$R^2$	$B$
Reaction controlled by phase boundary Jimenez et al. (2013)	$3(1 - \alpha)^{2/3}$	$3(1 - (1 - \alpha)^{2/3})$	-0.24	0.99	0.87
Contracting sphere	$(3/2)(1 - \alpha)^{1/3}$	$1 - (1 - \alpha)^{1/3}$	-0.14	0.99	0.53
One and a half order Nassar et al. (2014)	$2(1 - \alpha)^{3/2}$	$(1 - \alpha)^{-1/2} - 1$	-0.39	0.97	1.36
Second order Nassar et al. (2014)	$(1 - \alpha)^2$	$(1 - \alpha)^{-1} - 1$	-1.16	0.95	3.9
Third order Nassar et al. (2014)	$(1/2)(1 - \alpha)^3$	$(1 - \alpha)^{-2} - 1$	-5.4	0.91	16.7
Fourth order Nassar et al. (2014)	$(1/3)(1 - \alpha)^4$	$(1 - \alpha)^{-3} - 1$	-19.4	0.87	57.45
First order reaction pursue instantaneous nuclei growth Jimenez et al. (2013)	$1 - \alpha$	$-\ln(1 - \alpha)$	-0.52	0.98	1.95

Table 5.8 Lignin oxidation model.

Heat rate K min <sup>-1</sup>	$k_{0,1}$ *10 <sup>-3</sup>	$E_1$ kJ mol <sup>-1</sup>	$k_{0,2}$ *10 <sup>-3</sup>	$E_1$ kJ mol <sup>-1</sup>	RSS
5	0.79		1.33		0.04
10	0.76		0.95		0.1
20	0.74	40	0.84	200	0.11
30	0.35		0.03		0.06

decreased from  $0.79 \times 10^{-3}$  to  $0.35 \times 10^{-3} \text{ min}^{-1}$  with increasing heating rate from  $5 \text{ K min}^{-1}$  to  $30 \text{ K min}^{-1}$ . The variation was higher in the second zone :  $k_{0,2}$  decreased from  $1.33 \times 10^{-3}$  to  $0.03 \times 10^{-3} \text{ min}^{-1}$  with increasing the heating rate from  $5 \text{ K min}^{-1}$  to  $30 \text{ K min}^{-1}$ . The activation energy in the first zone was  $40 \text{ kJ mol}^{-1}$  and in the second zone it was  $200 \text{ kJ mol}^{-1}$ .

Oxidizing lignin produces more gas and less liquid than pyrolysing it. Low activation energy leads to char,  $\text{H}_2\text{O}$ ,  $\text{CO}$  and  $\text{CO}_2$  while higher activation energy produces monomers Brebu and Vasile (2010). Considerably higher activation energy in oxidation of lignin in compare to pyrolysis, could be due to forming monomer followed by oxidizing them to  $\text{CO}_x$ . Pasangulapati et al. (2012b) characterized the devolatilization of cellulose, hemicellulose and lignin under  $\text{N}_2$  and air from 550 K to 650 K Pasangulapati et al. (2012b). The activation energy of switchgrass degradation in air ( $122 \text{ kJ mol}^{-1}$ ) was higher than in  $\text{N}_2$  ( $103 \text{ kJ mol}^{-1}$ ) Pasangulapati et al. (2012b). In air ( $Q=20 \text{ ml min}^{-1}$ ) lignin degrades slowly from 480 K to 120 K. They reported the lowest activation energies from 550 K to 610 K ( $67 \text{ kJ mol}^{-1}$ ) and the highest between 1110 K to 1200 K ( $160 \text{ kJ mol}^{-1}$ ). The activation energy increased from  $33 \text{ kJ mol}^{-1}$  in pyrolysis to between  $353 \text{ kJ mol}^{-1}$  to  $200 \text{ kJ mol}^{-1}$  in gasification of MWV lignin Kumar et al. (2009). Our results agree with these previous studies particularly with respect to oxygen and activation energy.

## 5.6 Conclusions

Lignin is the only source of aromatics from biomass; it is a residue of bio-refineries and pulp and paper industry and remains under-exploited The lignin market is limited to low value products such as dispersing and binding agent (2 % of lignin) or as a fuel. Converting lignin to valuable chemicals has been hindered by the lack of suitable technology, low yield and low selectivity. Introducing a selective process to produce value-added chemicals from lignin would guarantee the viability of bio-refineries. This study characterized the lignin degradation in inert and oxidative environments. Monomers are one of the first products during the degradation but they react further to form carbon-oxides or re-polymerize during pyrolysis. Selective oxidation of these monomers to chemicals instead of gas or solid will improve product selectivity. Our results demonstrate the lignin degradation process proceeds during two broad mechanisms. In both, oxidation and pyrolysis, the yield of liquid increases sharply at temperatures greater than 600 K. First, the weak bonds break and char and gas forms. The remaining lignin depolymerizes and reacts to aromatics and char. Lignin conversion, liquid yield and selectivity varies with temperature. A two step mechanism characterizes the thermal degradation reaction rate. The activation energy at low temperature was  $47 \text{ kJ mol}^{-1}$  and it was  $95 \text{ kJ mol}^{-1}$  at higher temperature. The pre-exponential factor varied with hea-



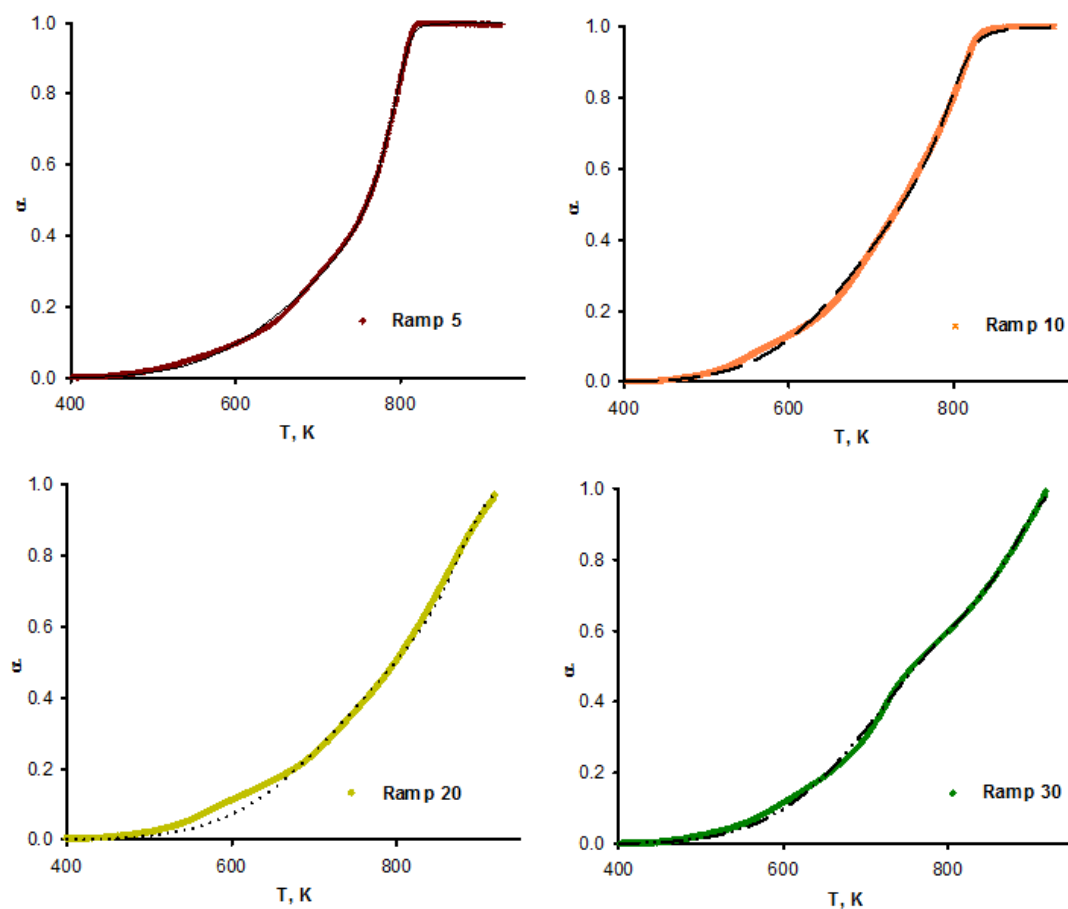


Figure 5.11 Experimental (scatter) vs. model calculated (solid line) data for oxidation of lignin

ting rate. Lignin oxidation proceeds through three main steps but a two stage mechanism characterizes the data adequately. The activation energy of lignin oxidation during the first stage was lower compared to pyrolysis ( $40 \text{ kJ mol}^{-1}$ ) but considerably higher ( $200 \text{ kJ mol}^{-1}$ ) in the second step.

## 5.7 Acknowledgements

The authors acknowledge NSERC for financial support, FPInnovation for supplying lignin and analytical assistance. In addition we give special thanks to the NSERC Biomaterials, Chemicals Strategic Network ([www.lignowork.ca](http://www.lignowork.ca)) and FIBRE Network ([www.fibrenetwork.org](http://www.fibrenetwork.org)).

## 5.8 Appendix

### 5.8.1 Kinetic modeling

Reaction kinetics :

In thermal processes, temperature (T), extent of conversion ( $\alpha = \frac{m_0 - m_i}{m_0 - m_f}$ ) (Equation 5.1), weight (m), and pressure (P) define the rate of a equation Vyazovkin et al. (2011). Under no baric condition we have :

$$\frac{d\alpha}{dt} = k(T)f(\alpha) \quad (5.1)$$

Multistep process take the following form (equation 5.2) Vyazovkin et al. (2011) :

$$\frac{d\alpha}{dt} = k_1(T)f_1(\alpha_1) + k_2(T)f_2(\alpha_2) \quad (5.2)$$

It could be necessary to use more complex multi-step process. Sestak and Bergren developed an empirical model (equation 5.3) that is reliable to represent data include mix of various models Vyazovkin et al. (2011).

$$f(\alpha) = \alpha^n (1 - \alpha)^m [-\ln(1 - \alpha)]^p \quad (5.3)$$

The relationship between  $\alpha$  or  $\frac{d\alpha}{dt}$  and t or T provide accounts for accelerating reactions, decelerating reactions and auto-catalytic (Sigmoidal) Vyazovkin et al. (2011). In the decelerating type reactions, the rate decreases as conversion increases and power law models characterize the rates well. Power law expressions of the following form  $f(\alpha) = n\alpha^{(1-\frac{1}{n})}$  represent the

accelerating reaction rate models. In Sigmoidal type reactions, the rate begins slowly at the beginning then it ends rapidly, or vice versa. The rates obey Arrhenius law with respect to temperature (Equation 5.4).

$$k(T) = k_o \exp \left[ -\frac{E_a}{R} \left( \frac{1}{T} - \frac{1}{T_o} \right) \right] \quad (5.4)$$

Where  $k_o$  is the rate constant at the reference temperature,  $k_o$  pre-exponential factor and  $E_a$  is the activation energy and  $R$  is universal gas constant. We select the fitted parameters by minimizing the sum of squares of the error (Equation 5.5) :

$$RSS = \sum (y_{\text{exp}} - y_{\text{cal}})^2 = \min \quad (5.5)$$

### 5.8.2 Ea — isoconversional method

Logarithmic derivative of equation 5.6 at constant  $\alpha$  while temperature or heating rate change can be used for activation energy calculation :

$$\left[ \frac{\partial \ln \left( \frac{d\alpha}{dt} \right)}{\partial T^{-1}} \right]_{\alpha} = \left[ \frac{\partial \ln k(T)}{\partial T^{-1}} \right]_{\alpha} + \left[ \frac{\partial \ln f(\alpha)}{\partial T^{-1}} \right]_{\alpha} \quad (5.6)$$

We derive the activation energy for different  $\alpha$  by taking the logarithm of Equation 5.1 versus temperature (Equation 5.6). Plot of  $\ln[\beta \frac{d\alpha}{dT}]$  versus  $\frac{1}{T}$  will give  $\frac{E_{\alpha}}{R}$  (equation 5.7–Frideman).

$$\ln \left[ \beta \frac{d\alpha}{dT} \right] = \ln [A f(\alpha)] - \frac{E_{\alpha}}{RT} \quad (5.7)$$

$\alpha$  should be in the range of 0.05–0.95 while the step is not larger than 0.05 Jankovic (2013); Vyazovkin et al. (2011); Brown et al. (2000).

## CHAPTER 6    ARTICLE 3 - GAS-SOLID CONVERSION OF LIGNIN TO CARBOXYLIC ACIDS

**Samira Lotfi, Daria C. Boffito, and Gregory S. Patience\***

*Department of Chemical Engineering, Ecole Polytechnique de Montreal, Montreal, Quebec, Canada*

Corresponding author : Tel. : +1-514-340-4711 X 3439 ; fax : +1-514-340-4159.

E-mail address : gregory-s.patience@polymtl.ca

(Submitted to Energy & Environmental Science)

### 6.1 abstract

Lignin represents 15 % to 40 % of the dry weight of lignocellulosic biomass but remains under exploited as a sustainable feedstock for chemical and fuels even though it is the only bio-polymer with aromatic units. Technology that selectivity converts lignin to value added specialities would improve the economics of the burgeoning bio-refinery industry. Here we introduce a two stage gas-phase catalytic process that produces carboxylic acids and aromatics from lignin while minimizing coke and char and maintaining catalyst activity. In the first step, a mixture of 50 % water vapour in air crack and partially oxidize this complex macromolecule ( $<550^{\circ}\text{C}$ ). The effluent gas contacts heterogeneous mixed-metal oxides or metal catalysts in the second step. The product profile from the second step included aromatic compounds but mostly  $\text{C}_4$  carboxylic acids such as maleic acid and butyric acid. Vanadium catalysts cleave lignin bonds, open aromatic rings and oxidize lignin to carboxylic acids, especially maleic acid.  $\text{WO}_3/\text{TiO}_2$  mostly gave butyric acid. Basic catalysts produced more aromatic compounds. The maximum amount of coke was 5 % of the total carbon in lignin.

### 6.2 Broader context

Lignin is an aromatic biopolymer that constitutes up to 40 % of the total plant mass. It is a potential feedstock for both chemicals and fuels. However, its complex structure and heterogeneity render it inert except for non-selective thermo-chemical processes that produce syngas and oils, both of which require further processing.

We combine thermo-chemical processes with oxidative catalysis to convert lignin to aliphatic carboxylic acids whose market value is twice as much as fuels. In our tests, water vapour and oxygen crack and partially oxidized lignin to volatile monomers. These vapours contact

a catalytic fluidized bed positioned immediately above the thermo-oxidative steam-cracking reactor. The catalysts — mainly supported metals or metal oxides — produced C<sub>4</sub> carboxylic acids, mainly butyric acid and maleic acid.

### 6.3 Introduction

Bio-refineries that convert lignocellulosic biomass into fuels and chemicals represent a paradigm shift versus the pulp and paper industry that dominates the market. Lignocellulosics contains cellulose, hemicellulose and lignin macromolecules (Zakzeski et al., 2012). Cellulose and hemicellulose are raw materials for bioethanol, bio-butane and other chemicals (Fan et al., 2013; Ragauskas et al., 2014; Lalitendu et al., 2012). The pulp and paper industry combusts as much as 40 % of their lignin. Only 2 % is converted to value-added chemicals ((Ragauskas et al., 2014)) and the rest is waste — 50 million tons per year (Fan et al., 2013; Ma et al., 2015a). To comply with the 2007 U.S. Energy Security and Independence Act production of 79 Mm<sup>3</sup> of biofuels release 62 million tons of lignin a year to produce (Ragauskas et al., 2014).

Methoxylated phenylpropane units linked by C–C and ether bonds constitute the skeleton of lignin as a bio-polymer (Fan et al., 2013). Lignin accounts for 15 % to 40 % of lignocellulose, but the heterogeneity of its structure inert and is thus an uncommon feedstock for chemicals or even liquid fuels (Vardon et al., 2015; Feghali et al., 2015). Moreover, process requires a homogeneous feedstock to minimize multiple purification trains that engender costs and complexity for biorefiners (Vardon et al., 2015; Fan et al., 2013).

Pyrolysis, gasification, hydrogenation, oxidation, aqueous reforming, hydrolysis and enzymatic processes convert lignin to aromatic compounds (Zakzeski et al., 2012; Fan et al., 2013; den Bosch et al., 2015; Song et al., 2013; Rahimi et al., 2014). The products include low molecular weight phenolic compounds, carboxylic acids and quinones. Oxidatively cleaving the lignin aromatic rings yields dicarboxylic acids. Organic acids dominate the pharmaceutical, food, petrochemical and polymer industry while aromatic compounds constituent an important but smaller market segment Ragauskas et al. (2014); Ma et al. (2015a); Vardon et al. (2015)

H<sub>2</sub>O<sub>2</sub> and chalcopyrite-CuFeS<sub>2</sub> in an acetic acid buffer oxidized lignin to malonic, succinic, malic and maleic acid at 333 K. Ma et al. propose a molecular pathway where HO<sup>+</sup> initiates the ring hydroxylation to depolymerize lignin. The reaction also produced aromatic compounds — benzoic acid, vanillin and vanillic acid. Further oxidation yield p- and o-quinone, which can undergo ring opening to give C<sub>4</sub> acids such as maleic, fumaric and muconic acid. Hydrolyzing

these acids gave stable endpoint acids (malonic, succinic, malic and trace of maleic acid) (Ma et al., 2015b). Vardon et al. (2015) produced adipic acid from lignin model compounds. First, fed-batch biological cultivation process converted the model compound to *cis-cis* muconate acid. Then PdC catalyst hydrogenated the recovered acid to adipic acid.

Heterogeneous catalysis plays a key role in the manufacture of polymers, agricultural and pharmaceuticals, especially in selective oxidation and hydrogenation (Witsuthammakul and Sooknoi, 2012; Xu et al., 2006; Kadowaki et al.; Kwan et al.). Catalysts improve the selectivity to target molecules and reduces the activation energy so that the process operates at lower temperature. However, lignin forms coke and char and other compounds that deactivate catalysts (Fan et al., 2013; Brebu and Vasile, 2010). Developing a selective catalytic process to convert lignin to chemicals and fuel represents a paradigm shift with respect to current practice in the pulp and paper industry ((Ma et al., 2015b)) and could ensure the economic viability of biorefineries.

Olcese et al. (2013) improved the quality of lignin pyrolysis bio-oil hydrotreating the vapours over iron-silica (Fe/SiO<sub>2</sub>) and iron-activated carbon (Fe/AC) catalysts in a fixed bed at 400 °C and 1 bar. The products were benzene, toluene, xylenes, phenol, cresols, and alkyl phenols. Coke plugged the micropores of Fe/AC but not the mesopores of the Fe/SiO<sub>2</sub> Olcese et al. (2013).

Fan et al. (2013) converted lignin to ethylbenzene in a two-step process. In the first step, zeolites depolymerized lignin to aromatics (mainly benzene). In the second step, HZSM-5 (with ethanol) selectively alkylated the aromatic compounds to ethylbenzene. Large pores reduced the benzene selectivity and yield of benzene, toluene, and xylenes increased with catalyst acidity. The catalyst deactivated after 3 uses : the selectivity to benzene dropped from 23 % to 7 % but a 4 h oxygen treatment restored the original catalytic activity Fan et al. (2013). Alternating reaction/regeneration cycles is a successful strategy to maintain catalyst activity overtime and reduce deactivation (Lotfi et al., 2015).

We developed four micro-reactor configurations to activate lignin involving air, steam and heterogeneous catalysts. Based on screening tests, passing the effluent gases after a thermo-oxidative steam cracking step produced the most organic acids and phenolic compounds. This configuration reduced the susceptibility of coking and thus reducing the regeneration cycles.

## 6.4 Experimental

### 6.4.1 Materials and catalyst preparation

#### Lignin

FPIinnovations (Quebec, Canada) supplied softwood kraft lignin for all the experiments. It was recovered with the the LignoForce System from the Resolute Forest Products mill in Thunder Bay (Ontario). The softwood kraft lignin had a mass fraction of 66.9 % carbon, 5.2 % hydrogen, 0.1 % nitrogen, 25.4 % oxygen, with 92 % total solids. The impurities were <0.05 % Na, 1.4 % S and 1.5 % suger (Lotfi et al., 2015; Kouisni et al., 2012; Kouisni and Paleologou). Total solids of the Thunder Bay softwood black liquor (unwashed lignin) was 29 %. The main solid components were lignin (43 %) and NaOH (32 %). The unwashed lignin had a mass fraction of 40 % carbon, 4 % hydrogen, 0.1 % nitrogen, 35 % oxygen and 2.15 % sulfide as sulphur%.

#### Catalysts

In a first set of experiments, vanadium pyrophosphate (VPP) converted lignin to carboxylic acid in four reactor configurations. DuPont designed VPP to partially oxidize n-butane to MA (Patience and Bockrath, 2010). In a second set of experiments, we selected on of the reactor configurations *iii* and tested 8 supported metal and mixed-metal oxides (Figure 6.1c) :

- C1 : V–Mo/Al<sub>2</sub>O<sub>3</sub>(Lotfi et al., 2015)
- C2 : V–Mo/TiO<sub>2</sub>
- C3 : V<sub>2</sub>O<sub>5</sub>/MnO<sub>2</sub>
- C4 : MgO (Sigma-Aldrich — we did not purify it further)
- C5 : Mg–K (Pingxiang Xingfeng Chemical Packing Co., Ltd(fen))
- C6 : WO<sub>3</sub>/TiO<sub>2</sub>(Dubois et al.; Dalil et al., 2015)
- C7 : V–Mo/ZSM-5
- C8 : V–W/ZSM-5

C2 : We impregnated a commercial TiO<sub>2</sub>-IV with the metal salts and followed the same procedure as in C1 but we replaced Al<sub>2</sub>O<sub>3</sub> with TiO<sub>2</sub>.

C3 : To synthesize V<sub>2</sub>O<sub>5</sub>/MnO<sub>2</sub> we added 1 g of MnO<sub>2</sub>-IV powder to the aqueous ammonium metavanadate (1.3 g ) and ammonium hydroxide (0.07 g) solution at 80 °C Lochar and Smolakova (2009). After impregnation, a rotary evaporator removed most of the water at 500 mmHg and 85 °C. The powder dried at 100 °C and atmospheric pressure for 12 h. A static air muffle furnace calcined the V<sub>2</sub>O<sub>5</sub>/MnO<sub>2</sub> sample at 500 °C for 6 h.

C7 : We impregnated HZSM-5 with V and Mo salts and followed the same procedure as C1 but replaced  $\text{Al}_2\text{O}_3$  with ZSM-5.

C8 : For V-W/ZSM-5 we impregnated HZSM-5 with salts of V and W : 10 % tungsten and 30 %.

The catalyst reagents included : HCl (Fischer Scientific, 37 %), ammonium molybdate(VI) tetrahydrate (Acros, 99 %), sodium tetraborate decahydrate (Fisher Scientific, 99.5 %), sodium phosphate (Sigma-Aldrich, 96 %), ammonium metavanadate (ACS reagent grade,  $\geq 99\%$ ),  $\text{V}_2\text{O}_5$  (99.6 %). The supports were HZSM-5 (Alfa Aesar,  $\text{SiO}_2/\text{Al}_2\text{O}_3$  molar ratio 50 :1), Titanium(IV) oxide (Alfa Aesar, 99.5 %-metals basis), activated aluminum oxide (ACROS), manganese(IV) oxide and magnesium oxide (Sigma-Aldrich). We did not further purify any reagents.

#### 6.4.2 Catalyst characterization

A Quantachrom Autosorb 1 MP porosimeter measured the surface area and porosity with 21 points, following the standard multi point Brunauer-Emmet-Teller (BET) method. Prior to the test, a heated bag degassed the samples at 200 °C for 3 h under vacuum.

A Philipps X'pert diffractometer with a Cu-K radiation source (1.5406 Å) at 50 kV and 40 mA generated the diffraction patterns (XRD). The instrument operated at room temperature with an angle of incidence of 0.5°. It scanned diffraction angles between 20° and 90° with a divergence slit of 1°.

A scanning electron microscope (SEM) generated images of the catalysts. An SEM-JSM-840A (JOEL Company) energy-dispersive X-ray spectroscopy (SEM-EDX) coupled with an electronic X-ray diffraction (EDX) detector identified the principal elements in the catalytic samples.

A Perkin Elmer infrared spectrometer (FTIR) with a spectral resolution of 4  $\text{cm}^{-1}$  scanned the catalysts at 16 kHz. The data were collected in the range from 4000  $\text{cm}^{-1}$  to 600  $\text{cm}^{-1}$ . The surface composition of the samples was investigated using attenuated total reflectance (ATR) mode.

#### 6.4.3 Reactor configurations

In a first set of experiments, vanadium pyrophosphate (VPP) catalyst converted lignin to carboxylic acids in four reactor configurations in two steps. In the first step coincided lignin decomposed to volatile compounds these compounds reacted with the heterogeneous catalysts



in the second step

- i) lignin pyrolysis + oxidation over VPP (Figure 6.1a)
- ii) lignin thermo-oxidation + oxidation over VPP (Figure 6.1b)
- iii) lignin thermo-oxidative steamcracking + oxidation over VPP (Figure 6.1c)
- iv) lignin thermo-oxidative steamcracking over V-Mo/HZSM-5 + oxidation on VPP (Figure 6.1d)

Reactor configuration *iii* maximized the yield of carboxylic acids and therefore we selected it to assess catalyst performance — yield, conversion, selectivity, product profile - in the second set experiments *iii* (Figure 6.1c). The reactor was an 8 mm ID quartz tube 600 mm long with two glass wool distributors positioned 350 mm and 500 mm from the bottom. Placing the catalyst bed near the top of the reactor minimizes product degradation.

In all the experiments we loaded 250 mg of lignin above the lower distributor and 500 mg above the top distributor. The gas contact time in the catalyst bed was 0.2 s.

Two thermocouples monitored the temperature in each zone. A syringe pump injected water into the reactor from the bottom through a 0.15 mm nozzle. Argon entered the nozzle at 22 mL min<sup>-1</sup> to help atomize it into small droplets.

The mole fraction of oxygen in the feed bottle was 33 % (balance Ar) at a flowrate of 38 mL min<sup>-1</sup>. The temperature ramp for all experiments was :

- 15 °C min<sup>-1</sup> up to 150 °C
- 5 °C min<sup>-1</sup> up to 350 °C
- 5 °C min<sup>-1</sup> up to 450 °C, (75 min from the beginning of the reaction)
- 5 °C min<sup>-1</sup> up to 550 °C (105 min from the beginning of the reaction)

The choice of the heating rate was dictated by TGA experiments in air, which showed that lignin lost  $\sim 40\%$  of its weight above  $\sim 500\text{ }^{\circ}\text{C}$ . We repeated selected tests two and three times.

## Analytical

An ice bath trapped the condensable product from the catalyst and we sampled the liquid at each temperature step. A Hanna electrical conductivity measured the concentration of ionizable solutes present in the sample to monitor the productivity Lorences et al. (2003).

A Varian HPLC (Metacarb 87H column) analyzed the liquid sample offline. We calibrated the HPLC with standard solutions for each product we detected, building a calibration curve with six concentrations. We repeated each analysis three times. A Pfeiffer mass spectrometer (MS) monitored the permanent gases online.

At the end of the last temperature ramp and hold at 550 °C no solids remained above the first distributor. We calibrated the MS with a mixture of hydrocarbons and oxygen at four concentrations. The carbon balance was the sum of the carbon in the gas phase (MS) + the carbon in the liquid phase + the carbon remained on the catalyst surface. The mass of carbon remaining on the catalyst we measured by TGA. The MS detected CO, CO<sub>2</sub> and CH<sub>4</sub>. We calculated the carbon trapped in the water-ice quench as the difference between the carbon loaded to the reactor and that detected on the catalyst and in the gas phase and by HPLC. We assumed that the response factors for the unknown aromatics (detected by GC-MS) were the same as other known aromatics that we had previously evaluated. These two methods differed by less than 10 %

## 6.5 Results and discussions

### 6.5.1 Two-step lignin degradation

#### Configuration i : Lignin pyrolysis + oxidation on VPP

In reactor configuration i, the lignin in the first step pyrolyzed (Figure 6.1a) and oxygen entered the reactor just below the second distributor. The catalyst in the second stage oxidized the pyrolysis vapours into aromatics and aliphatic carboxylic acids. Pyrolyzing lignin produces 10 % to 20 % gas and 3 % to 30 % phenolic compounds Farag et al. (2014a); Klein and Virk (2008). The phenolic monomers can either condense to oligomers that are the precursors of char or form compounds that are precursors to fuels and chemicals by catalytic hydrogenation (Ragauskas et al., 2014). In configuration i, the temperature breaks the  $\beta$ -O-4 bonds and produces the phenolic monomers in the first stage. Some of these phenolic compounds reach the second stage (VPP bed), whereas 46 % form char and remains in the lower bed. The catalyst and oxygen open the rings of the phenolic compounds and oxidize the compounds of which maleic acid was the most abundant product.

We proposed a reaction pathways to form maleic acid from lignin : the  $V^{5+}$  ion activates lignin to attract  $\pi$  electrons of the double bonds and generate a positive charge displaced on the ring. The ring opens by successive attack of 2O<sub>2</sub> Lotfi et al. (2015).

Here, 19 % of the carbon in the lignin converted to liquid. The selectivity to maleic acid was 84 %. The production of light monomers during pyrolysis could account for the high maleic acid selectivity. Other products were aromatics (6 %) acrylic acid (2.6 %), malonic acid (2.6 %), followed by formic, lactic, acetic acid and vanillin. The solid residue remaining above the first distributor was the highest among the four configurations (46 %) due to the char (Table 6.1).

### **Configuration ii : lignin thermo-oxidation + oxidation on VPP**

In configuration ii, a stream containing a mole fraction of 21 % oxygen degrades the lignin (Figure 6.1b). VPP oxidized the vapours formed in the first step and 36 % of the products were C<sub>5</sub>-C<sub>8</sub> aromatics. The other compounds included : Maleic acid (32 %), fumaric acid (4.5 %), malonic acid (6 %), gallic acid, lactic and formic acid.

We attribute the large gas fraction produced in this configuration (73 %) to either the decarbonylation of lignin monomeric units, lignin gasification, or to combustion of coke on the catalyst to CO and CO<sub>2</sub>. (Table 6.1).

### **Configuration iii : lignin thermo-oxidative steamcracking + oxidation on VPP**

In the third system, steam and oxygen cracked the lignin cracked (Figure 6.1c). The vapours produced in the first step passed through the VPP and scavenged the remaining oxygen. This configuration converted the most lignin to liquid products with 48 % selectivity to maleic anhydride, 31 % to aromatics, 7 % to acrylic acid, followed by malonic, gallic and lactic acid. This configuration produced as much gas as in reactor configuration ii (Table 6.1).

### **Configuration iv : lignin thermo-oxidative steam cracking over V-Mo/HZSM-5 + oxidation on VPP**

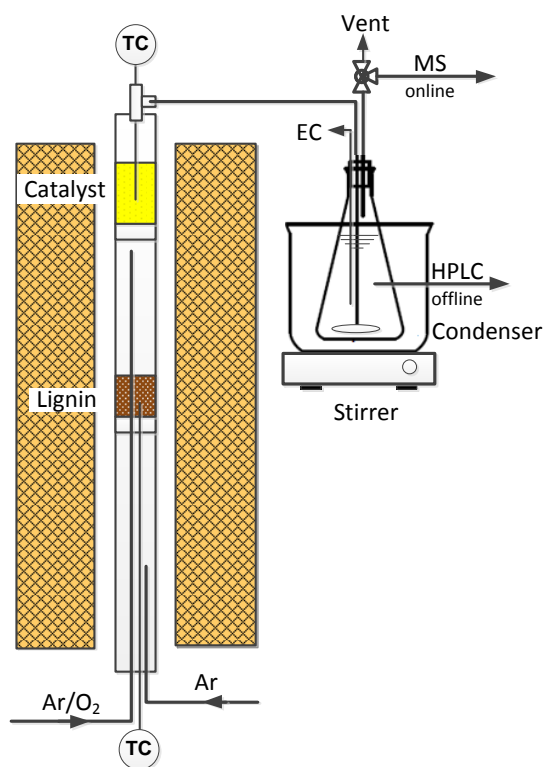
In the fourth configuration (Figure 6.1d) V-Mo/HZSM-5 and steam cracked and partially oxidized the lignin in the first step ( $Q_{water}=5\text{ cm}^3\text{ min}^{-1}$  and a mole fraction of 21 % O<sub>2</sub>). VPP partially oxidized the intermediates formed in the first step in the second step. Most of the lignin formed gas (81 %) and only 13 % was recovered in the quench including : 16 % aromatics, 47 % maleic acid, 12 % malonic acid, 10 % butyric acid, 7 % phthalic acid followed by acetic, formic acid and vanillin (Table 6.1).

The high cracking activity of V-Mo/HZSM-5 is responsible for the high yield of gases, as well as the combustion of the coke on the catalyst during the reaction.

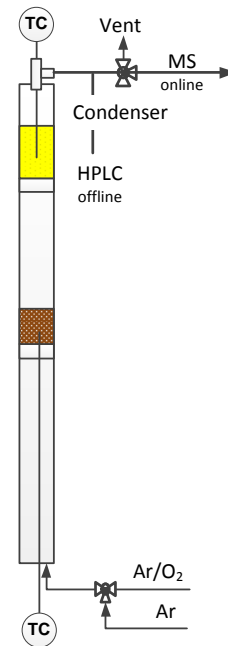
Beside lignin, we tested unwashed lignin in the same condition as conf. iv. 19 %, 76 %, 5 % of carbon converted to liquid, gas and solid, respectively. MA selectivity reached up to 68 % and we detected 9 % aromatic, 5 % malonic, 1.5 % phthalic and formic acid.

### **FTIR of the reaction residues**

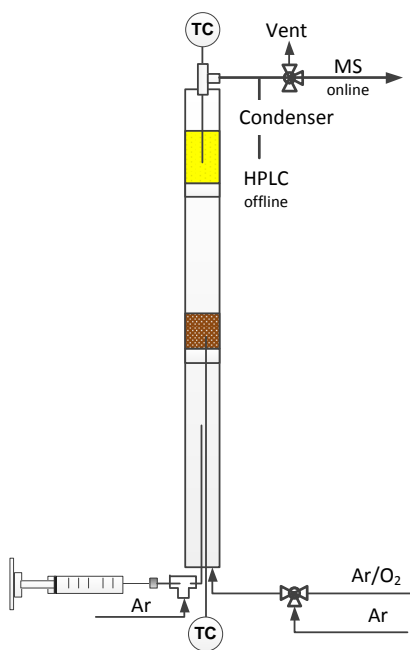
The pure lignin FTIR spectra (Figure 6.2a) are typical of lignin derivatives. Adsorption at 3420 cm<sup>-1</sup>, 2944 cm<sup>-1</sup> and 2833 cm<sup>-1</sup> corresponds to the stretching of O-H, aromatic C-H and



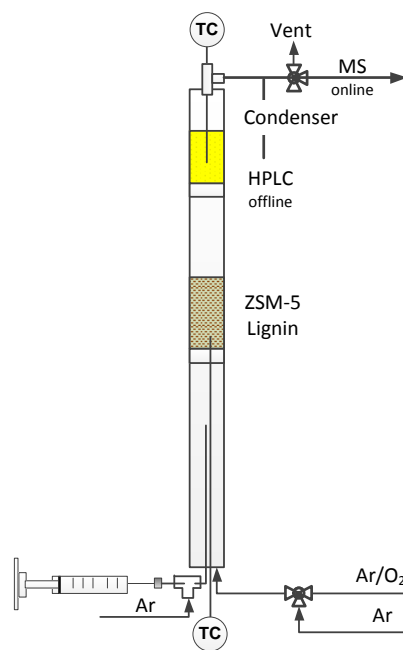
(a) Reactor configuration i



(b) Reactor configuration ii



(c) Reactor configuration iii



(d) Reactor configuration iv

Figure 6.1 Schematic of experimental setup

Table 6.1 Selectivity vs. reactor configuration

Name	Config. i	Config. ii	Config. iii	Config. iv
Carbon balance, (%)				
Liquid	19	23	24	13
Solid	46	4	5	6
Gas	35	73	71	81
Liquid selectivity, (%)				
Aromatic	6	36	31	16
Maleic/Fumaric acid	84	36.5	48	48
Butyric acid	-	-	-	10
Malonic acid	3.5	6	2.7	12
Formic acid	1	0.5	0.65	0.5
Acetic acid	0.1	0.3	-	1
Lactic acid	0.2	0.8	0.8	-
Phthalic acid	0.01	0.3	0.1	7
Vanillin	✓	0.3	-	2.6
Gallic acid	0.7	1.5	1.2	-
Acrylic acid	2.6	3	7	-
Syringic acid	0.06	-	-	-
Unknown	0.8	13.5	7	1.5
Benzoquinone	0.2	1	1.2	0.6
H <sub>2</sub> , %	0.6	0.2	1.3	0.7

methoxyl groups, respectively. The bands in the range  $3000\text{ cm}^{-1}$  to  $2860\text{ cm}^{-1}$  correspond to the aliphatic C-H stretching, whereas the ones above  $3000\text{ cm}^{-1}$  to the C-H aromatic stretching, which overlaps to the band of O-H. We attribute the band at  $1711\text{ cm}^{-1}$  to the carbonyl group of aldehydes. The bands at  $1520\text{ cm}^{-1}$  and  $1594\text{ cm}^{-1}$  are typical of skeletal vibrations of the aromatic ring. The higher intensity of the band at  $1520\text{ cm}^{-1}$  compared to the one at  $1594\text{ cm}^{-1}$  is typical of softwood lignin Sharma et al. (2004). C-H deformation and aromatic ring vibrations also adsorb at  $1464\text{ cm}^{-1}$  and  $1408\text{ cm}^{-1}$ . We attribute the bands at  $1268\text{ cm}^{-1}$  and  $1222\text{ cm}^{-1}$  to the C-O bonds in syringyl and guaiacyl units and the bands at  $1138\text{ cm}^{-1}$  and  $1082\text{ cm}^{-1}$  to the in-plane aromatic C-H deformation typical of the same compounds Ibrahim et al. (2006). The band at  $1036\text{ cm}^{-1}$  refers to the C-O stretch of the O-CH<sub>3</sub> and C-OH. The bands at  $868\text{ cm}^{-1}$  and  $822\text{ cm}^{-1}$ , respectively, may correspond to lone aryl CH wag and two-adjacent aryl CH wag, respectively. The band at  $626\text{ cm}^{-1}$  may represent the out of plane O-H band.

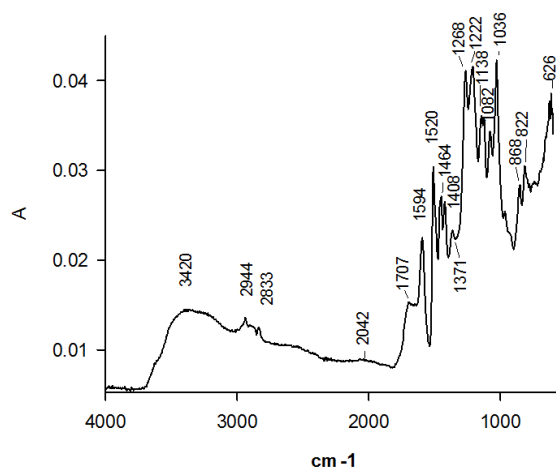
In upward shift of the FTIR spectrum baseline for most of the peaks of char remaining on the lower distributor for configuration may relate to the large carbonized compared to lignin. Many absorption peaks typical of lignin disappear, in particular, the signals of the aliphatic groups. The OH-stretching band at  $3390\text{ cm}^{-1}$  represent phenolic hydroxyl group Sharma et al. (2004). C-O in carbonyl group or in carbonyl compounds conjugated with aromatic ring ( $1714\text{ cm}^{-1}$ ) and aromatic ring ( $1590\text{ cm}^{-1}$ ) are still present. The bands at  $1160\text{ cm}^{-1}$  and  $1088\text{ cm}^{-1}$  are typical of the in-plane aromatic C-H deformation of aromatic syringyl and guaiacyl units Ibrahim et al. (2006).

The FTIR spectrum of coke on V-Mo/HZSM-5 after the lignin degradation in reactor configuration iv has a typical band at  $\sim 1580\text{ cm}^{-1}$  (Figure 6.2c). This band belongs to the highly unsaturated carbonaceous deposit called "hard coke". The bands at  $1087\text{ cm}^{-1}$  and  $870\text{ cm}^{-1}$  typical of the in-plane aromatic C-H deformation of aromatic syringyl and guaiacyl units persist Ibrahim et al. (2006).

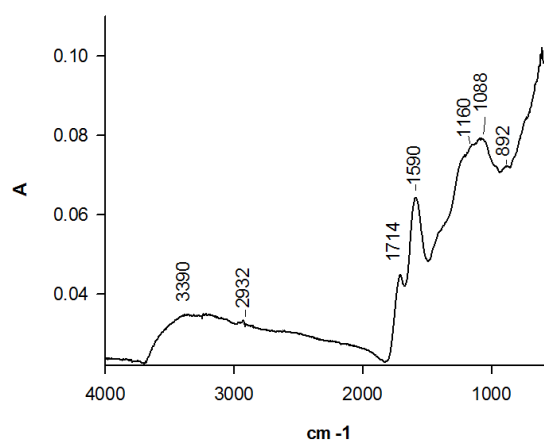
### 6.5.2 Thermo-oxidative steam cracking : catalytic activity

Besides VPP, we tested 8 other catalysts to identify the most selective towards carboxylic acids (Table 6.2). Metal oxides of group V and VI, like vanadium, molybdenum, and tungsten are common catalyst to partially oxidize hydrocarbons, particularly vanadium Neto et al.; Heidemann et al. (2003). Phosphoric, arsenic and boric acids control the activity of V, Mo and W in the gas phase oxidation of hydrocarbons Lloyd (2011).

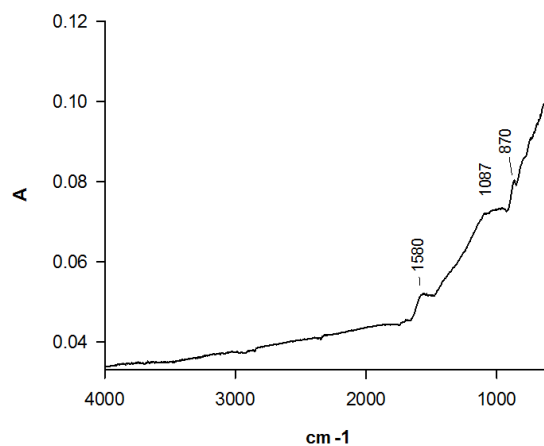
Neto et al. designed a multi-metal oxide catalyst containing ( $\text{Ag}_{a-c} \text{ Q}_b \text{ M}_c \text{ V}_2\text{O}_d \text{ eH}_2\text{O}$ ) to partially oxidize aromatic hydrocarbons in the gas phase to produce aldehydes, and carboxylic



(a) Lignin



(b) Char



(c) Coke formed during oxidation (Reaction configuration ii)

Figure 6.2 FTIR spectrum

acids or anhydrides in fixed bed reactors.

Vanadium included in polyoxometalates catalysts degraded lignin to monomeric compounds. The catalysts comprised anionic clusters of  $d^0$  metal cations, mostly,  $W^{VI}$ ,  $W^{VI}Mo^{VI}$ ,  $V^V$ ,  $Nb^V$  and oxygen anions arranged in  $Mo_6$  octahedral units. Polymetalates cleave  $\beta$ -O-4 and C-C linkages of lignin and directly produce low molecular weight phenolic compounds in different oxidative environments and liquid solutions. As much as 90 % of the lignin model compounds reacted Ma et al. (2015a). The reduction of vanadium changes with the supports and decreases as follows :  $\gamma-Al_2O_3 > SiO_2-Al_2O_3 > SiO_2 > \alpha-Al_2O_3$  (Kwan, 1985).

The properties of the support oxide affect the activity and the selectivity of the supported metal significantly (Weckhuysen and Keller, 2003). Choosing a support is as important as the choosing the oxidation catalyst.

*C1 : (V-Mo/ $Al_2O_3$ )*

The V-Mo/ $Al_2O_3$  catalyst partially oxidized lignin solutions ( $y_{O_2} = 4\%$ ) to lactic acid (S=6 %) Lotfi et al. (2015). Other co-products were formic acid (S=6 %), acetic acid, maleic anhydride, acrylic acid and phthalic anhydride. 17 % of the total carbon converted into carboxylic acids. The product distribution (Table 6.2) changes significantly with respect to our previous data, even if the catalyst is the same Lotfi et al. (2015). There are 4 main differences with our previous reactor configuration in the work described herein : i) the lignin vaporized from a solid bed instead of being injected in a liquid solution into the hot catalyst ii) the catalyst does not contact pure lignin iii) the  $O_2$  concentration is 11 % vs. 4 % iv) The T increased from 50 °C to  $\sim 500$  °C whereas in the previous experiments it was constant at 370 °C.

Here, V-Mo/  $Al_2O_3$  converted 23 % of the lignin carbon to liquids (6.2). The main products in the liquid were  $C_5$ - $C_8$  aromatic compounds (S=64 %).

The second most abundant product in the quench was maleic acid (S=20 %), followed by acrylic acid (S=5.5 %), and lactic acid (S=5 %). Vanadium and VPP in particular has a unique capacity to oxidize aromatics to maleic anhydride/acid from aromatics Lotfi et al. (2015); Uraz and Atalay (2007). Jongerius report that Mo reduces catalyst deactivation and improves the cleavage of the diphenylmethane bonds Jongerius (2013). While the bonds involving monophenolic units split at temperatures up to 450 °C, both with and without oxygen, Mo has a role in cracking biphenyl bonds and yield phenol and benzene Koyama (1993). V-Mo based catalysts oxidize o-xylene and benzene and olefins to anhydrides Lovell (1981). Mo reduces the catalyst deactivation rate and increases cleavage of 4-hydroxydiphenyl ether, diphenyl ether, and diphenylmethane bonds Jongerius (2013). Fumagalli reports that



V–Mo catalysts have a high oxygen insertion capacity that oxidize the intermediates involved in the process o-xylene to phthalic anhydride (Fumagalli et al., 1994).

We attribute the higher selectivity to maleic acid compared to lactic acid to the higher oxygen concentration with respect to our previous data 11 % vs. 4 % in Lotfi et al. (2015). Products such as formic, acetic and lactic acid form from the  $\beta$ -O-4 bonds cleavage at temperatures higher than 200 °C, depending on the reactivity of the substituents of the aromatic ring. The catalyst in the second stage may completely oxidize some of these acids to CO<sub>2</sub> and H<sub>2</sub>O. We were unable to quantify how much H<sub>2</sub>O the reaction produced because of the large excess of steam we co-fed with the O<sub>2</sub>

*C2 : (V–Mo/TiO<sub>2</sub>) and C7 : (V–Mo/HZSM-5)*

We loaded the same active components of catalyst C1 on different supports TiO<sub>2</sub> (C2) and HZSM-5 (C7). TiO<sub>2</sub> has both Lewis acid sites and basic sites that interact with high valence metal cations Ramis et al. (1992). TiO<sub>2</sub> has a promoting effect as a support for vanadium oxide; in fact most commercial catalysts for o-xylene oxidation to phthalic anhydride comprise V<sub>2</sub>O<sub>5</sub>/TiO<sub>2</sub> Centi (1996). MoO<sub>2</sub> improves the catalytic activity of V<sub>2</sub>O<sub>5</sub>/TiO<sub>2</sub> in the oxidation of 1,2-dichlorobenzene (Bagheri et al., 2014).

In our case, replacing  $\gamma$ -Al<sub>2</sub>O<sub>3</sub> with TiO<sub>2</sub> as a support decreased the yield of liquid to 15.5 %, but increased the selectivity to maleic acid (45 %). Other products were : aromatics (42 %), succinic acid (7.5 %), phthalic acid (7.5 %), formic and acetic acid and vanillin.

Surprisingly, HZSM-5 as a support for V and Mo gave the highest selectivity to liquid products not only among the V-Mo based samples, but among all the catalysts tested. HZSM-5 zeolite is a commercial catalyst for the FCC of lineal olefins and alkanes hydrocracking (Corma and Sauvanaud, 2013). HZSM-5 is a strong Brønsted acid, which is desirable for the conversion of benzene to ethylbenzene, pyrolysis biomass to liquid (Fan et al., 2013; Misono, 1984).

An hypothesis that explains the high yield of liquids relates to the very narrow pores of HZSM-5, which might be too small to host the sterically-hindered intermediates of the lignin steam cracking deriving from the first stage. The narrow pores prevent the production of those reaction intermediates that are the precursors of coke (Misono, 1984). Nevertheless, the selectivity to aromatics is lower (19 %) compared to C1 and C2 and maleic acid (+ fumaric acid) and butyric acid accounts for almost 40 % of the selectivity to liquids. Other products are benzoic acid (8 %), vanillin and phthalic acid.

*C3 : (V<sub>2</sub>O<sub>5</sub>/MnO<sub>2</sub>)*

We tested MnO<sub>2</sub> as a new support for vanadium. V<sub>2</sub>O<sub>5</sub> selectively oxidizes o-xylene to phthalic anhydride Akbari and Alavi (2015). MnO<sub>2</sub> is a promoter to partially oxidize me-

thanol to formaldehyde Chen et al. (1996) and is a support for Au in the oxidation of 5-(hydroxymethyl)furfural Zhu et al. (2015).  $V_2O_5/MnO_2$  yields 16.5 % liquid products of which the most part were aromatic compounds (36 %), followed by maleic acid (18 %) and butyric acid (16 %). Other products were succinic and phthalic acid. The  $V_2O_5$  most likely cracked many of the products and for this reason the selectivity towards liquids was low Dias et al. (2014).

#### *C4 : (MgO)*

MgO is a basic catalyst with activity towards decarbonylation and cracking Yigezu and Muthukumar (2015); Boffito et al. (2014). The oxidative steam cracking of lignin monomers over MgO produced 8.5 % of liquids from lignin and more than 80 % of gases. The main products were butyric acid (11 %), vanillin (11 %), phthalic acid (7 %) and aromatics (7 %). MgO may also adsorb hydrocarbons and retain them Chakravarthi (2009). The selectivity to the solid residue was in fact the highest among all of the catalysts.

*C5 : (Commercial Mg-K-Si-Al catalyst)* We tested a commercial catalyst that converts benzene to maleic anhydride by Chemical Packing Co. Ltd, (China). The catalyst included Mg, Al, Si, and K (SEM-EDX analyses). The main compounds in the quench were  $C_5$ - $C_8$  aromatics (33 %) followed by , butyric acid (33.5 %), phthalic acid (7.5 %), benzoic acid (15 %), maleic acid, vanillin and muconic acid.

#### *C6 : ( $WO_3/TiO_2$ )*

$WO_3/TiO_2$  dehydrates glycerol to acrolein Dalil et al. (2015).  $WO_3$  is active towards C-C bonds cleavage (Bjorgen (2013)) and W is itself more active towards oxidation than V Jongerius (2013). Moreover, W catalyzes wood hydrocracking Jongerius (2013).  $WO_3/TiO_2$  converted lignin mostly to  $C_4$  acids, including maleic acid (9 %), butyric acid (64 %), phthalic acid (5 %). Other products are aromatics (11 %), vanillin and benzoic acid.

$WO_3$  has strong Lewis acid sites ( $W^{6+}$ ) Alexandre et al. (1998); Ramis et al. (1992) that can activate the intermediates deriving from the lignin degradation of the first reaction stage (see the next section of reaction pathways).

#### *C8 : (V-W/HZSM-5)*

Since W catalyzes the hydrocracking of wood (Jongerius (2013)), we replaced molybdenum with tungsten from C7 to C8. The selectivity to liquid products decreased (21 % vs. 25 %), but the selectivity to maleic anhydride increased from 21 % to 56 %. Other products were butyric acid (14 %), succinic acid (8.5 %), aromatics (9.5 %), formic acid, acetic acid, phthalic

acid and aromatics (10 %).

### Catalyst characterization

The surface area of the V–Mo/Al<sub>2</sub>O<sub>3</sub> was the highest at 115 m<sup>2</sup> g<sup>−1</sup> and the lowest was VPP at 41 m<sup>2</sup> g<sup>−1</sup> (Table 6.3). The pore volume of the V–Mo/Al<sub>2</sub>O<sub>3</sub> was also highest at 41 cm<sup>3</sup> g<sup>−1</sup>.

The diffractogram of V–Mo/Al<sub>2</sub>O<sub>3</sub> was typical of an amorphous material. The XRD pattern of V–Mo/Al<sub>2</sub>O<sub>3</sub> and V–Mo/TiO<sub>2</sub> (Figure 6.3) resemble the data of Shishido et al. (Shishido et al.) Orthorhombic Mo<sub>4</sub>O<sub>11</sub> crystallites and V<sub>2</sub>O<sub>3</sub> form on TiO<sub>2</sub> Shishido et al.; Kondratenko et al. (2006). Peaks at  $2\theta = 24, 27, 33, 36, 37, 55$  and  $57$  relates to V<sub>2</sub>O<sub>3</sub> phase and peaks at  $2\theta = 21.8, 26$ , and  $33.4$  belongs to Mo<sub>4</sub>O<sub>11</sub> (JCPDS 13-042).

Triclinic aluminum vanadium oxide (AlVO<sub>4</sub>), tetragonal vanadyl molybdenum oxide (VOMoO<sub>4</sub>), and monoclinic molybdenum vanadium oxide (Mo<sub>0.67</sub>V<sub>0.33</sub>O<sub>2</sub>) forms on Al<sub>2</sub>O<sub>3</sub> (Figure 6.3) Shishido et al..

(VO)<sub>2</sub>P<sub>2</sub>O<sub>12</sub>, (VO)<sub>2</sub>P<sub>2</sub>O<sub>7</sub>, VO(PO<sub>3</sub>)<sub>2</sub> and VOHPO<sub>4</sub>·0.5H<sub>2</sub> phases constitute VPP (Figure 6.4) Lotfi et al. (2015).

V<sub>2</sub>O<sub>5</sub> ( $2\theta = 20, 22, 26, 31, 32, 33, 34, 39.5, 48, 52, 55, 58$ ) and MoO<sub>3</sub> ( $2\theta = 24, 26, 27, 34, 38$  and  $39$ ) phases forms on HZSM–5 Teimouri et al. (2014); Chagas et al. (2012); Kondratenko et al. (2006). XRD detected VMoO<sub>8</sub> and V<sub>0.07</sub>Mo<sub>0.93</sub> on HZSM-5 (Figure 6.5).

After the reaction, the phases detected in V-Mo/TiO<sub>2</sub> and V-No/ZSM–5 were the same as for the fresh catalyst Wilson et al. (2011). In VPP, the intensity of the peaks around 30 and at 42 reduced.

### 6.5.3 Discussion

#### Reactions pathways

Oxidative steam-cracking lignin followed by catalytic conversion of the volatile compounds produces up to 25 % liquids that includes carboxylic acids and aromatics (Table 6.2). Lignin begins to decompose at 200 °C and produces gases and liquids (Figures 6.6), which agrees with literature data Brebu and Vasile (2010). Maleic acid and butyric acid are among the most abundant compounds, which are easily detected by electrical conductivity Lorences et al. (2003).

#### *Aromatic compounds*

Steam and oxygen crack the lignin in the above the lower distributor. We hypothesize that

Table 6.2 Product selectivity vs. catalyst

Name Catalyst	C1 V-Mo/Al <sub>2</sub> O <sub>3</sub>	C2 V-Mo/TiO <sub>2</sub>	C3 V <sub>2</sub> O <sub>5</sub> /MnO <sub>2</sub>	C4 MgO	C5 Mg-Si-Al-K cat.	C6 WO <sub>3</sub> /TiO <sub>2</sub>	C7 V-Mo/HZSM-5	C8 V-W/HZSM-5
EC ( $\mu$ S/cm)	-	103	107	12	118	174	155	130
Carbon Balance (%)								
Liquid	23	15.5	16.5	8.5	19.5	20	25	21
Solid	6.5	4.5	3.5	11	6	4	4	7.5
Gas	70.5	80	80	80.5	74.5	76	71	71.5
Liquid selectivity (%)								
Aromatic	64	42	36	7	33.2	11	19	9.5
Maleic/Fumaric acid	20.5	45	18.5	1	1.5	9	26	56
Butyric acid	0.6	0.5	16	11	32.5	64	17	14
Malonic acid	-	-	-	-	✓	0.4	-	-
Formic acid	1	0.7	-	-	0.06	✓	-	0.1
Acetic acid	0.2	0.6	-	-	0.2	0.1	-	0.1
Lactic acid	5	-	-	-	-	-	-	-
Muconic acid			-	-	1.5	-	-	-
Succinic acid	0.8	7.5	3	-	-	-	1	8.5
Phthalic acid	0.3	2	2.5	7	7.5	5	0.5	1
Vanillin	✓	0.5	0.3	11	1.5	1.5	5	-
Benzoic acid	-	-	0.1	2.5	15	1.5	8	-
Gallic acid	0.3	-	0.15	-	✓	✓	-	0.3
Acrylic acid	5.5	-	1	-	-	-	-	-
Syringic acid	0.6	-	-	-	-	-	-	-
Unknown	0.7	0.7	20	59.5	8	7	23.1	10.2
Benzoquinone	0.6	-	0.2	1	-	-	0.3	0.2
H <sub>2</sub> , %	2	-	7	-	3.3	4	5.5	6

Table 6.3 Surface area and pore size of fresh catalysts

Catalyst	A m <sup>2</sup> g <sup>-1</sup>	Pore volume cm <sup>3</sup> g <sup>-1</sup>
V-Mo/Al <sub>2</sub> O <sub>3</sub>	115	0.25
V-Mo/TiO <sub>2</sub>	53	-
VPP	41	0.074
V-Mo/ZSM-5	46	0.095
V-W/ZSM-5	50.7	0.124

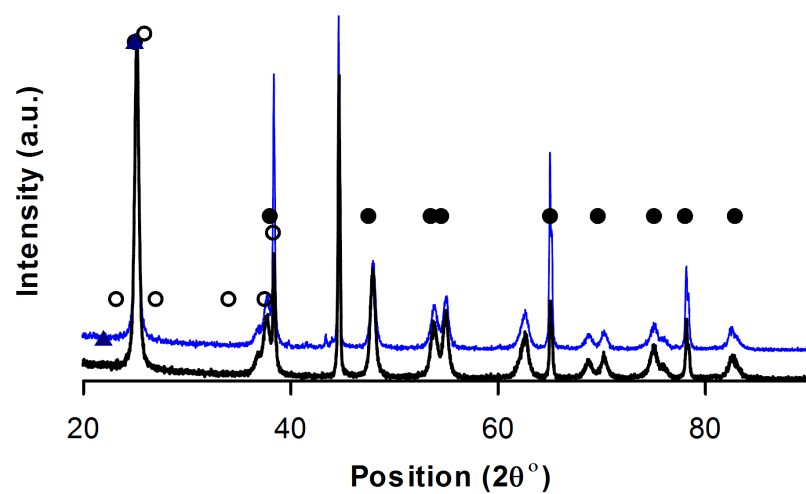


Figure 6.3 XRD–V–Mo/TiO<sub>2</sub>, ● anatase TiO<sub>2</sub>, ○ MoO<sub>3</sub>, △ Mo<sub>4</sub>V<sub>6</sub>O<sub>25</sub>, black = before reaction – Blue = after reaction.

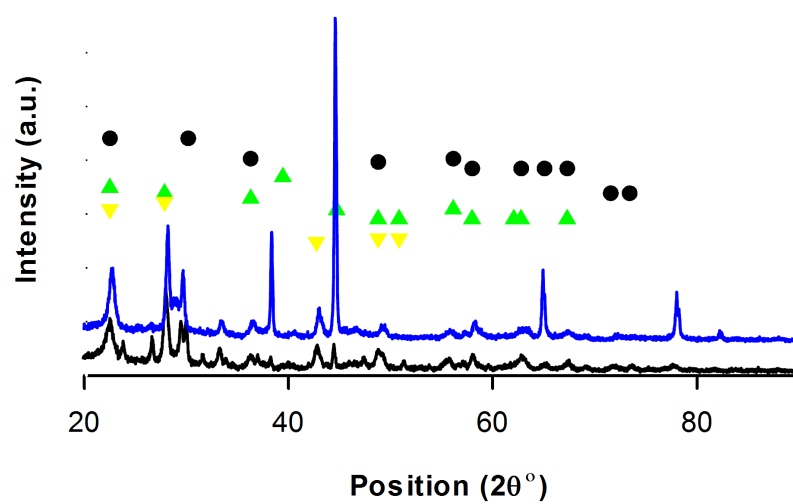


Figure 6.4 XRD–VPP, ● (VO)<sub>2</sub>P<sub>2</sub>O<sub>7</sub>Bordes (1987), ▲ VO(PO<sub>3</sub>)<sub>2</sub>, ▼ VOHPO<sub>4</sub>·0.5H<sub>2</sub>O, black = before reaction- Blue = after reaction.

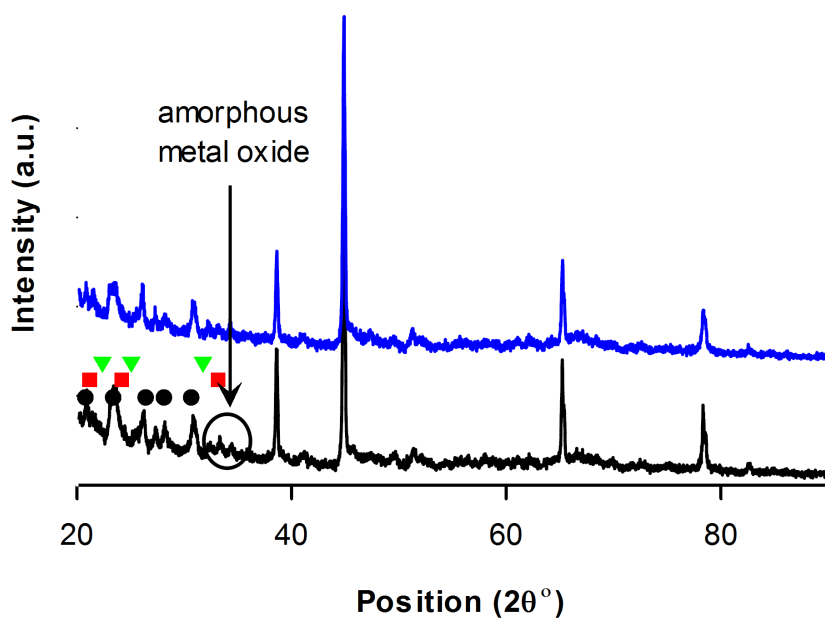
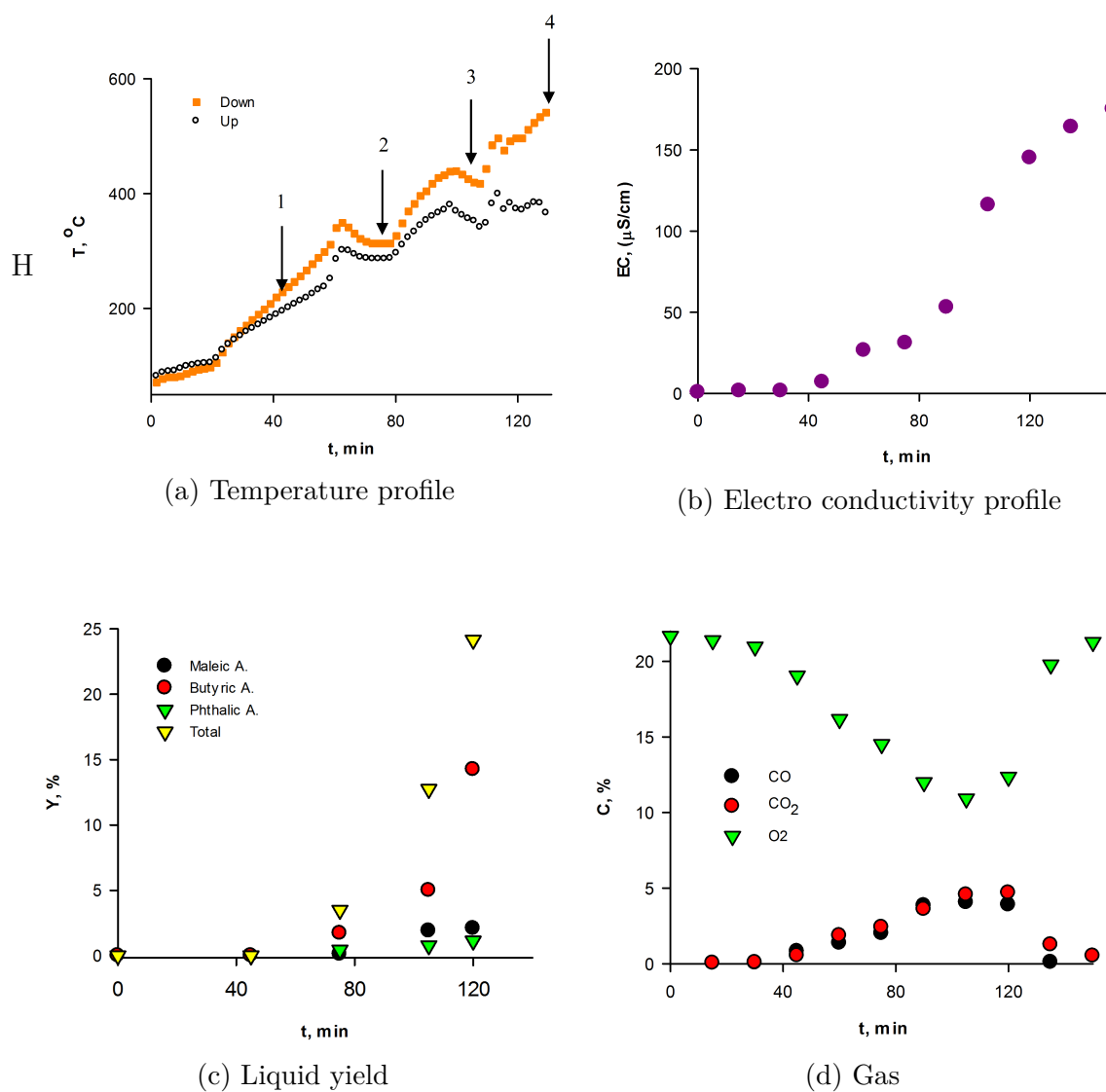


Figure 6.5 XRD–V–Mo/ZSM-5, • HZSM-5 Liu et al. (2015), ■ VMoO<sub>8</sub>, ▼ (V<sub>0</sub> · 07 Mo<sub>0</sub> · 93)<sub>5</sub>O<sub>14</sub>, black = before reaction- Blue = after reaction Bhattacharyya and Talukdar (2005).

Figure 6.6  $\text{WO}_3/\text{TiO}_2$

in this first step the  $\beta$ -O-4 bonds cleave and release the aromatic phenolic units that constitute the monomers of lignin. These units pass through the bed above the lignin or react with the catalyst to form carboxylic acids (6.2). The reactivity of the monomeric aromatic units depends on the type of substituents carrying oxygen functionalities (Brebou and Vasile, 2010). A GC-MS detected aromatic compounds for all the catalysts tested, in particular for the samples C1, C2, C3, C5. 1-ethyl-3-methyl cyclopentane, cyclopentane 1-ethyl-1-methyl, cyclohexane-1,4 dimethyl, ethyl benzene, benzene, 1,3-dimethyl, cyclohexane methyl, and others formed the aromatics.

#### *Maleic and fumaric acid*

We have recently reported the mechanism of formation of maleic anhydride, lactic acid, acetic acid and formic acid (and phthalic anhydride) from pure lignin (Lotfi et al., 2015). Vanadium has a unique capacity to produce maleic anhydride/acid.  $V^{5+}$  activates the aromatic rings of the monomeric units increasing their electrophilicity, thus exposing them to the attack of 2 molecules of  $O_2$ . After the attack of 2  $O_2$  the ring opens and re-arranges to maleic anhydride. Maleic anhydride hydrates to maleic acid and its isomer fumaric acid.

#### *Butyric acid*

Here for the first time we report a mechanism to account for the high concentration of butyric acid (Figure 6.7). We took as a representative catalyst  $WO_3/TiO_2$ . We hypothesize that butyric acid (and crotonic acid) form from lignin in 3 steps. Step 1 includes the oxidative steam cracking of the lignin. At temperatures above 200 °C the  $\beta$ -O-4 bonds cleave and release the aromatic phenolic units in the reactor space above the lignin bed below the upper distributor. This rupture generates either an anion (phenolate) or a phenol radical. The negative charge or the radical will most likely displace to carbon atoms of the ring that carry an oxygen functionality to give the chetonic form Gierer et al. (1994). In this form the carbon of the carbonyl group is strongly electrophilic and will undergo nucleophilic attack by water (steam cracking). In the attempt to recover its aromaticity, the rings open. Gierer et al. observed the same type of aromatic ring cleavage in liquid phase and presence of ( $H_2O_2$ ) under both alkaline and acid conditions Gierer et al. (1994). During step 1,  $O_2$  might oxidize the constituents of the aromatic rings, producing carboxylic acids Lotfi et al. (2015).

Step 2 includes the activation of the intermediates formed by ring cleavage onto the catalyst. We hypothesize that the acid sites on the catalyst, either of Brønsted or Lewis type, are the active species involved in this step.  $WO_3$  carries both strong Brønsted and Lewis acid sites. Lewis acid sites are  $W_6^{+}$  Alexandre et al. (1998); Ramis et al. (1992).  $V^{5+}$  is a Lewis acid strong enough to activate the reaction intermediate formed during step 1. In the activation mechanism the positive charge of tungsten displaces the  $p$  electrons of the open aromatic ring,



similarly as  $V^{5+}$  activates the aromatic ring after  $\beta$ -O-4 bonds cleavage Lotfi et al. (2015).  $O_2$  adds to the intermediates giving hydroxyls. The intermediate cleaves when an excess of electrons accumulate around an electrophilic carbon.

Step 3 involves hydrogen. We hypothesize that the intermediate formed during step 2 remains anchored to tungsten until hydrogen adds to it. Until the intermediate is absorbed on W it can be oxidized up to carboxylic acid, but only  $H_2$  can displace it from the metal. Butyric acid forms after dehydration followed by hydrogenation of the crotonic acid.

Karlsson et al. ((Karlsson et al., 1999, 2000)) report butyric acid derivates from the ozonolysis of lignin-carbohydrate complex model compound, i.e. in strong oxidant conditions. Ozonolysis of  $\beta$ -O-4 structures produces erythronic and threonic acids ((Akiyama et al., 2002)), which are precursors of the butanoic acid. Shao et al. report that GC-MS analyses detected butanoic acid both in a untreated lignosulfonate sample and after oxidation above  $Ti/SbASnO_2$  and  $Ti/PbO_2$  electrodes (Shao et al., 2014).

We hypothesized that butyric acid could form from the condensation of two molecules of acetaldehyde followed the dehydration over  $WO_3/TiO_2$  and successive oxidation to the acid. We tested this hypothesis and fed acetaldehyde over the catalyst under the same conditions but only detected acetic acid in the quench.

#### *Lactic and malonic acids*

Acrylic acid hydrates to form lactic acid Lotfi et al. (2015). However, another possible mechanism to account for lactic acid as well as malonic acid involves cleaving propylic chains of monomeric units such as syringyl and guaiacyl (Figure 6.8).

#### *Formic and acetic acid*

The cleavage of methyl and ethyl constituents followed by oxidation produces formic and acetic acids Lotfi et al. (2015).

#### *Acrylic acid*

Acrylic acid may form from the scission of a phenolic unit and one of the terminal aldehydes as a consequence of the dehydration followed by oxidation Lotfi et al. (2015). At high temperatures, lactic acid may dehydrate to acrylic acid.

#### *Muconic acid*

Muconic acid is a  $C_6$  carboxylic acid that can form from the aromatic ring opening, followed by oxidation and dehydration Hamzeh et al. (2006).

#### *Succinic acid*

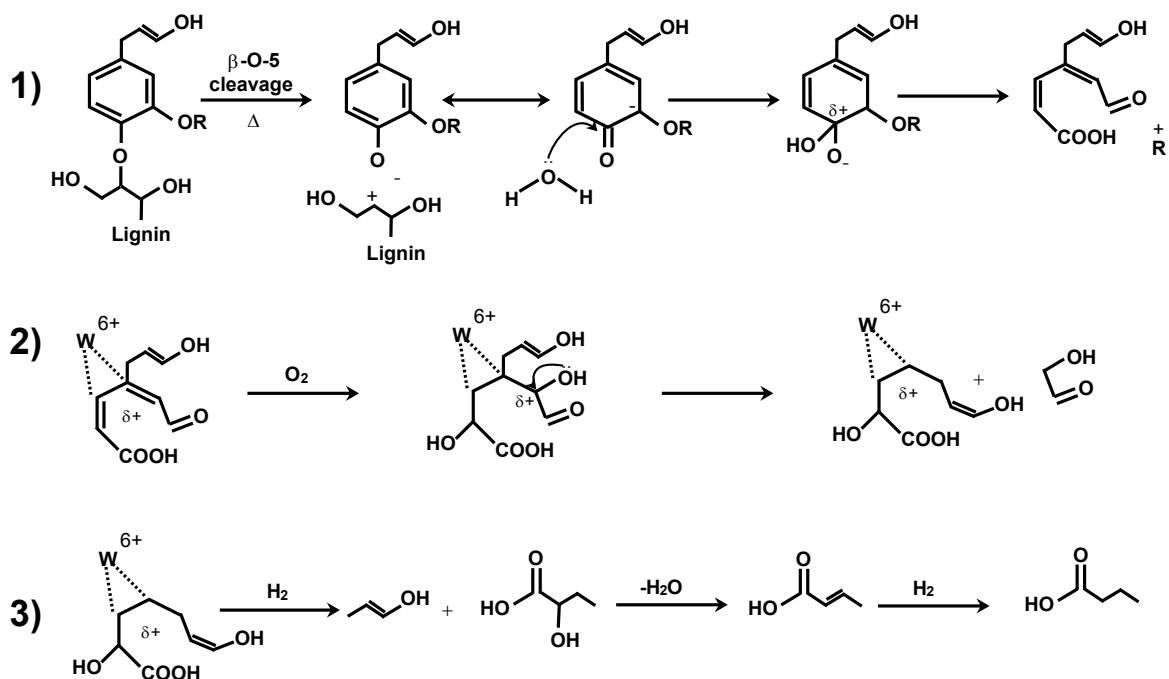


Figure 6.7 Proposed Mechanism of formation of butyric acid in 3 steps.

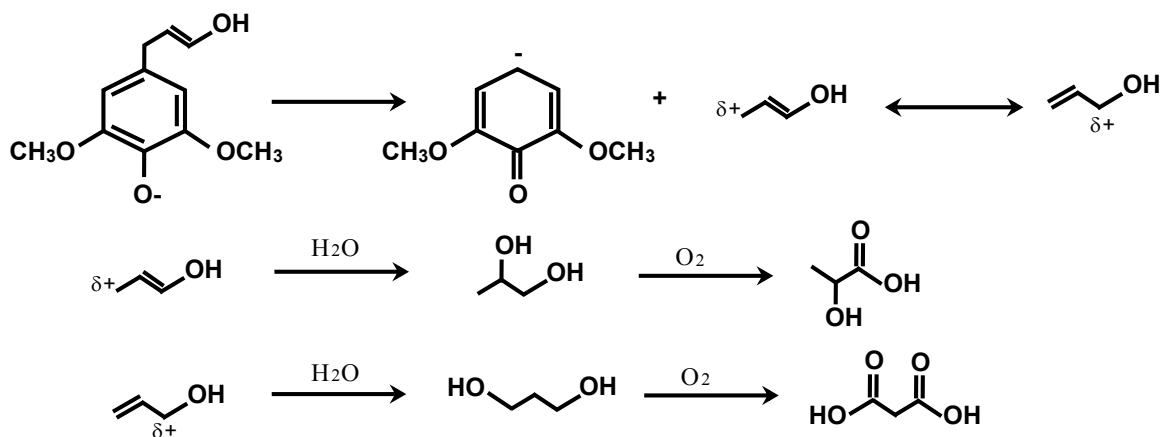


Figure 6.8 Proposed mechanism of formation of lactic and malonic acids from syringyl alcohol.

The MS detected  $H_2$  in the gas phase which could hydrogenate maleic and fumaric acids to succinic acid. The hydrogen may form either from the gasification of lignin, which decomposes into elements ( $H_2$  and C forming coke on the catalyst) Lotfi et al. (2015); Furusawaa et al. (2007) or from steam reforming of the biomass into syngas ( $H_2 + CO$ ). The concentration of succinic acid follows the same trend as that for maleic acid for the eight catalysts (Table 6.2) : V–Mo /  $TiO_2$  and V–W / HZSM-5 both produce the most maleic and succinic acids whereas the MgO and MgSiAlK make little maleic and no succinic acid.

## 6.6 Conclusions

Lignin is an inert macromolecule and because of its heterogeneity remains underexploited commercially. Activating it with high temperatures (as in pyrolysis), oxygen and/or water vapour produces phenolic compounds and bio-oils. Catalysts can improve the selectivity to target compounds and effectively decreases the required operating temperature. Pre-mixing the lignin with catalyst increases the cracking rate but it produces more coke, char and gas. Moreover, the catalyst deactivates more rapidly. We demonstrated a two-step process in which lignin is thermo-oxidatively steam cracked in the first step to volatile compounds which contact a catalyst bed in the second step. Little coke formed on the catalyst ( less than 5 % of the total C in lignin) and the catalyst did not agglomerate.

V-Mo/ $Al_2O_3$  and V-Mo/HZSM-5 converted 23 % and 25 % of the lignin into liquid products, respectively. The selectivity to maleic acid was 20 % in both cases. Replacing  $Al_2O_3$  and HZSM-5 with  $TiO_2$  reduced the liquid yield (15.5 %) but increased maleic acid selectivity (45 %). Replacing molybdenum with tungsten in V–Mo/HZSM-5 produced, butyric acid and succinic acid together with maleic acid.

## CHAPTER 7    ARTICLE 4 - KINETIC MODELLING OF LIGNIN OXIDATION OVER TITANIA/TUNGSTEN (VI) OXIDE

**Samira Lotfi and Gregory S. Patience\***

*Department of Chemical Engineering, Ecole Polytechnique de Montreal, Montreal, Quebec, Canada*

Corresponding author : Tel. : +1-514-340-4711 X 3439 ; fax : +1-514-340-4159.

E-mail address : gregory-s.patience@polymtl.ca

(Submitted to Green Chemistry)

### 7.1 abstract

Although lignin constitutes 40 % by mass of lignocellulose, it remains an uncommon feedstock for fuels or chemicals compared to cellulose and hemicellulose. Bio-refinery economics would become attractive if lignin could be de-constructed to phenolic compounds, propyl groups or carboxylic acids selectively. Activating the molecule while maintaining selectively remains a challenge. Here report that  $\text{WO}_3/\text{TiO}_2$  with water vapour and oxygen catalyses decompose lignin to low molecular weight compounds including  $\text{C}_4$  acids. In particular, butyric acid yield reached  $\sim 20$  % at a selectivity of 77 % (with respect to the total liquid product) at a contact time of 0.3 s.

### 7.2 Introduction

Lignin is the only source of aromatics from plants and it is a potential alternative to petroleum to produce phenolic compounds. Lignin represents 15 % to 40 % dry weight of lignocellulose but the heterogeneity of its structure renders it inert (versus cellulose and hemicellulose) and thus few processes rely on it as a primary feedstock (Zakzeski et al., 2012; Ragauskas et al., 2014; Azarpira et al., 2014). Developing technology to produce chemicals from lignin selectively would improve the economic viability of bio-refineries. Pyrolysis, gasification, catalytic hydrogenation, aqueous reforming, oxidation, hydrolysis, and enzymatic conversion ((Zakzeski et al., 2012; Fan et al., 2013; Ma et al., 2015a; Thielemans et al., 2002; Liu et al., 2015)) are among the technologies tested to convert lignin to carbon fibre, polymeric foams, thermoplastic elastomers and fuels. Because of lignin's heterogeneity, a broad range of phenolic compounds, carboxylic acids and quinones form when lignin reacts and purifying this product stream represents a substantial economic penalty (Ma et al., 2015a; Vardon et al., 2015).

Product yields vary with type of lignin, moisture content, pre-treatment method, reaction temperature, catalyst and heat and mass transfer rates Brebu and Vasile (2010); Jankovic (2013); Beis et al. (2010). In pyrolysis, high heating rates produce more tars (Beis et al. (2010)) whose main constituents are phenolics such as guaiacol and syringol. Cracking these tars gives lower molecular weight compounds, gases, coke and re-polymerization products.

Catalysts can selectively upgrade the primary tar compounds to monomers, fuels and carboxylic acids Ledesma et al. (2014). A catalyst can improve selectivity and decrease char and gases, but many deactivate due to polymeric type carbon species that blind active species or block pores (Fan et al., 2013).

Hydrolysing lignin in the presence of oxygen produces carboxylic acids — formic, acetic, lactic and oxalic acids, for example Fargues et al. (1996); Sales et al. (2007). Wet oxidation of lignin can also form aldehydes or aromatic carboxylic acids Lalitendu et al. (2012); Sales et al. (2007); Fargues et al. (1996). However, the wet oxidation reaction mechanism is not well developed because the intermediates of the reaction are largely unknown Fargues et al. (1996); Sales et al. (2007); Kindsigo et al. (2010). Even for pure compounds, such as phenol, many intermediates form that complicate developing reaction kinetics Zhang and Chuang (1999). Micro-kinetic models consider hundreds of reaction rates and components but are unrealistic for organic substrates Roohollahi et al. (2012). Accordingly, lumped models are more suitable to approximate lignin degradation rates Zhang and Chuang (1999). These models consider both parallel and series reaction pathways to the final products : lignin partially oxidizes to aldehydes which then combust to CO, CO<sub>2</sub> , for example.

Farag et al. (2014a) pyrolysed lignin with microwaves and analysed the gas phase and liquid phase composition with time and temperature. They derived first order rate constants for the solids fraction, gas fraction, water soluble fraction and oil fraction (Figure 7.1a). Sales et al. (2007) proposed a pseudo-first-order kinetic model for the wet oxidation of lignin to vanillin, syringaldehyde and p-hydroxybenzaldehyde by Pd- $\gamma$ -alumina. They considered a parallel series network where the lignin would form CO, CO<sub>2</sub> and acids directly or in series with aldehydes as intermediates (Figure 7.1b). Kindsigo et al. (2010) considered series and parallel reactions with two lumps : compounds that resist biological oxidation and those that are susceptible to biologic oxidation (Figure 7.1c). Both Araujo et al. (2009) and Fargues et al. (1996) simulated the oxidation of lignin to vanillin in a packed bed and bubble column reactor. The experimental design considered liquid feed flow rate, gas feed flow rate, bath temperature, and oxygen partial pressure. They found that lignin ( $LOH$ ) first depolymerizes in alkaline solutions to polyphenolate anions ( $LO^-$ ) the react with oxygen to radicals ( $LO\dot{O}$ ). The radicals then form syringaldehyde and vanillin, which are unstable and oxidize further

to low molecular weight acids or CO and CO<sub>2</sub>. Nie et al. (2014) developed a second order reaction model for the oxidation of 1-(3,4- Dimethoxyphenyl) ethanol (MVA) as a lignin model compound in a wide acidic pH range with chlorine dioxide (Table 7.1). Oxidizing softwood kraft lignin produces C<sub>4</sub> and C<sub>3</sub> acids such as lactic acid, maleic acid, butyric acid. Butyric acid is a monomer for fibres (cellulose acetate butyric plastics), a fibre additive to resist heat and sunlight as well as in the food and pharmaceutical industry Zhang and Chuang (1999); Dwidar et al. (2012). Propylene and butter are the two primary feeds stocks for butyric acid Dwidar et al. (2012).

Lotfi et al. (2015); Lotfi and Patience (2015) tested micro-fluidized beds to oxidize softwood kraft lignin. In commercial reactors, gas pass through orifices at velocities up to 100 m s<sup>-1</sup> to fluidized the catalyst powder. The optimum particle size lies between 20 µm to 200 µm. Lignin can be fed to the fluidized bed as a powder or sprayed into the bed through nozzles. Because the heat and mass transfer rates are high, both water and volatile fraction of lignin evaporates. If the feed rate of the lignin solution is too high, catalyst agglomerates and the bed will slump (collapse). Here we report for the first time that WO<sub>3</sub>/TiO<sub>2</sub> catalyses the oxidative degradation of lignin to mainly butyric acid. We followed a statistical experimental design with oxygen concentration (C<sub>O<sub>2</sub></sub>), water concentration (ω) and residence time (τ) as the factors and derived a kinetic model based on the data.

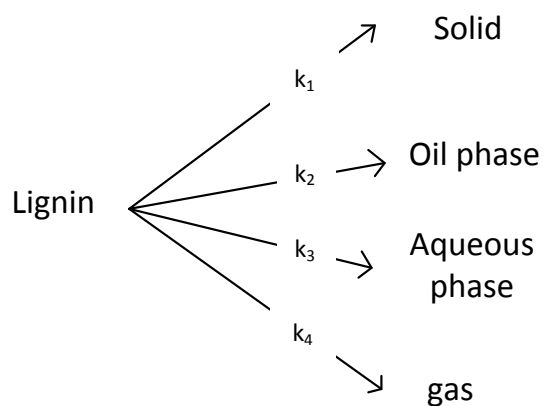
Table 7.1 Kinetic model of lignin oxidation.

Process	Catalyst	T °C	O <sub>2</sub> %	P bar	Kinetic expression	Ref.
Catalytic wet oxidation	Pd-γ-alumina	100–140	10–50	20	$r_L = k_L[C_L]$ $r_A = k_A[C_A]$	Sales et al. (2007)
Kraft lignin to vanillin	-	130	33	9	$r_C = k_{NC}[O_2]^{1.75}[L]$ pH > 11.5 : $-r_C = k_{CI}[O_2][L]$ pH < 11.5 : $-r_C = Af(pH)[C]^2$	Araujo et al. (2009); Fargues et al. (1996)
Wet oxidation of treated debarking water	Pt-Co	130–200	0.3–1.5	50–120	$\frac{dC_i}{dt} = -k_i[C_L]$ $k_i = k_i^0 \exp\left(\frac{-E_{a,i}}{RT}\right) C_{O_2}^{n_i}$	Kindsigo et al. (2010)
Pyrolysis	–	250–700	–	1	$\frac{dC_i}{dt} = -k_i[C_L]$ $k_i = k_i^0 \exp\left(\frac{-E_{a,i}}{RT}\right)$	Farag et al. (2014a)

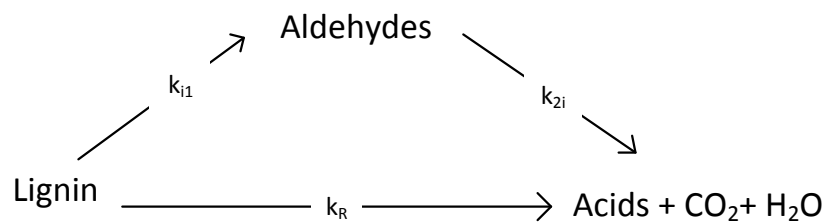
## 7.3 Experimental

### 7.3.1 Materials

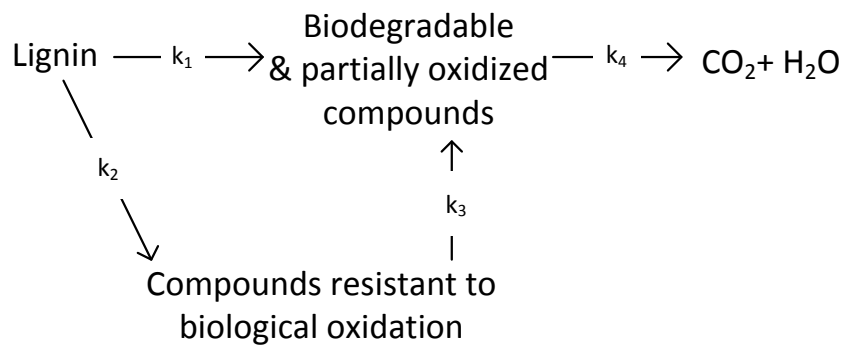
FPIInnovations (Quebec, Canada) supplied the softwood kraft lignin (elemental characterization described in Lotfi et al. (2015) (Kouisni et al., 2012; Kouisni and Paleologou)). The catalyst was WO<sub>3</sub>/TiO<sub>2</sub> (Dubois et al.; Dalil et al., 2015).



(a) Pyrolysis of lignin



(b) Wet oxidation of lignin to aldehydes



(c) Wet oxidation of lignin to biodegradable chemicals

Figure 7.1 scheme of mechanism-

### 7.3.2 Partial oxidation tests

The reactor was an 8 mm ID quartz tube (Figure 7.2) (Lotfib and Patience, 2015). We loaded lignin to the middle of the tube and oxidatively steam-cracked while ramping the temperature from ambient to 550 °C at a heating rate ( $\gamma$ ) of 5 °C min<sup>-1</sup>. The vapours passed through a distributor then contacted the WO<sub>3</sub>/TiO<sub>2</sub> catalyst. The effluent from the catalyst bed condensed in a flask immersed in an ice bath. A Hanna electrical conductivity meter monitored the concentration of ionizable solutes throughout the test and a Pfeiffer mass spectrometer monitored the permanent gases on-line at 3 Hz. Every 30 min we sampled the liquid in the flask and a Varian HPLC (Metacarb 87H column) measured the solute concentration. After the reaction, a Thermo-Gravimetric Analyser (TGA)(TA-Q50) was used to measure the coke formation on the catalyst. We followed a partial factorial experimental design and repeated some tests two or three times. The main factors in the design were residence time and oxygen and water mole fractions.

### 7.4 Mechanism and kinetic modeling

At high temperatures, lignin can react homogeneously in the gas phase to produce products (A<sub>s</sub>) (I) or their vapours can react with catalyst heterogeneously (A<sub>g</sub>) (II) (Figure 7.3) Lotfic and Patience (2015). In this paper, we first steam crack lignin in the presence of oxygen and pass the vapours from this reaction over a catalyst in a second step.

We consider the heterogeneous reaction of the second step (II) where the vapours contact catalyst (Equations 7.1-7.2), while  $k_{L,ad}$ ,  $k_{L,-ad}$ ,  $k_{A,ad}$  and  $k_{A,-ad}$  represent kinetic parameters of gas-solid adsorption and desorption steps, respectively. We assume adsorption equilibrium and steady-state conditions for the adsorbed compounds ( $\frac{dC_{Ls}}{dt} = \frac{dC_{Ais}}{dt} \approx 0$ ), the rate equation of lignin consumption ( $r_L = \bar{k}_i C_L$ ), acids and gas production ( $r_{A_i} = k'_i C_L$ ), where  $\bar{k}_i$  and  $k'_i$  are the pseudo-first-order kinetic constants (Equations 7.1-7.2).  $k''_{mi} = k_{mi} C_{O_2}^m C_w^n$ , m=I, II are the oxidation rate constant of the reaction in steps I and II.  $K_A$  are their adsorption equilibrium constants and index  $i$  represents the product.

For the consumption of lignin to product acids we have :

$$\bar{k}_i = [K_L(\frac{1}{k_{Li}} + \frac{1}{k_{-Lad}})^{-1}] + k_{Ii} \quad (7.1)$$

Acid and gas production on the surface of the catalyst can be formulated as follows :



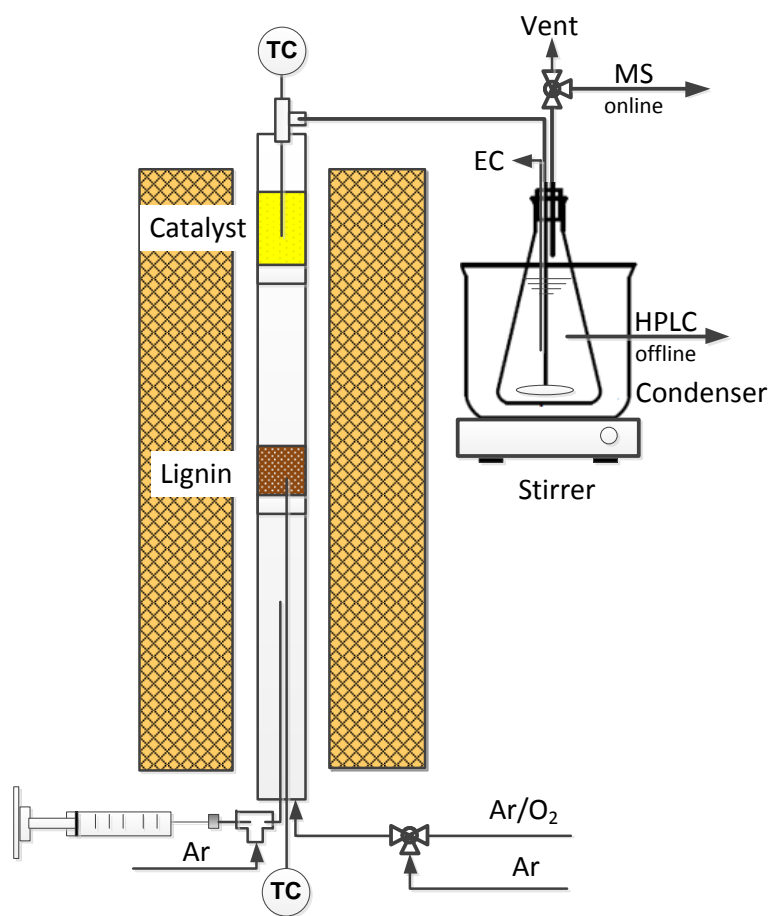


Figure 7.2 Schematic diagram of the 8 mm quartz reactor, manifold and quench

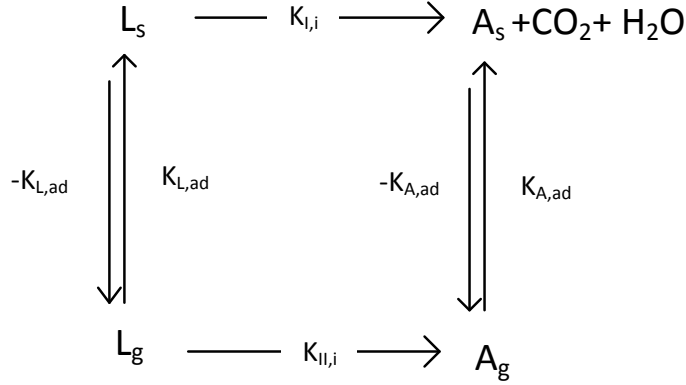


Figure 7.3 Scheme 1 – Lignin catalytic oxidation via homogeneous and heterogeneous steps

$$k'_i = \bar{k}_{\Pi,i} + \left[ \frac{\bar{k}_i k_{ad}}{K_A (1 + k'_{\Pi,i})} \left( \frac{k'_i}{k_{Lad}} + \frac{1}{K_L} \right)^{-1} \right] \quad (7.2)$$

The experimental kinetic data obtained by mass balance of the components (Equations 7.3 ,7.4 ,7.5 ,7.6)

$$\begin{aligned} \frac{dL}{dt} &= k'_{o,L} \exp \left[ -\frac{E_L}{R} \left( \frac{1}{T} - \frac{1}{T_o} \right) \right] C_L \\ &= -k'_{o,B} \exp \left[ -\frac{E_B}{R} \left( \frac{1}{T} - \frac{1}{T_o} \right) \right] C_L - k'_{o,MA} \exp \left[ -\frac{E_{MA}}{R} \left( \frac{1}{T} - \frac{1}{T_o} \right) \right] C_L \\ &\quad - k'_{o,CO_x} \exp \left[ -\frac{E_{CO_x}}{R} \left( \frac{1}{T} - \frac{1}{T_o} \right) \right] C_L - k'_{o,R} \exp \left[ -\frac{E_R}{R} \left( \frac{1}{T} - \frac{1}{T_o} \right) \right] C_L \end{aligned} \quad (7.3)$$

$$\frac{dB}{dt} = k'_{o,B} \exp \left[ -\frac{E_B}{R} \left( \frac{1}{T} - \frac{1}{T_o} \right) \right] C_L \quad (7.4)$$

$$\frac{dMA}{dt} = k'_{o,MA} \exp \left[ -\frac{E_{MA}}{R} \left( \frac{1}{T} - \frac{1}{T_o} \right) \right] C_L \quad (7.5)$$

$$\frac{dCO_x}{dt} = k'_{o,CO_x} \exp \left[ -\frac{E_{CO_x}}{R} \left( \frac{1}{T} - \frac{1}{T_o} \right) \right] C_L \quad (7.6)$$

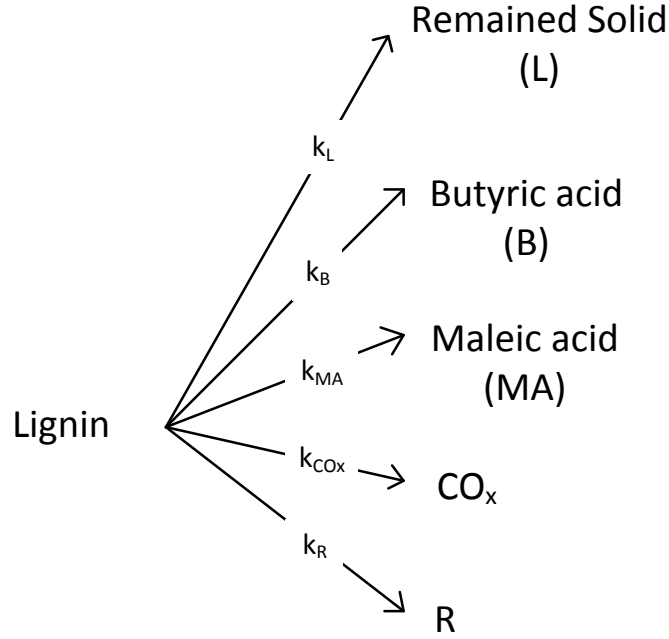


Figure 7.4 Scheme 2 – Lignin vapours catalytic oxidation

where  $k'_{o,i} = k_{o,i} C_{O_2}^m C_{\omega}^n \tau^p$  and  $\tau = \frac{V_{cat}}{Q_{gas}}$ .  $k_{o,i}$  is the pre-exponential factor,  $E_a$  is the apparent activation energy  $J mol^{-1} K^{-1}$ ,  $T$  is the reaction temperature (K) and  $R$  (gas constant) equals  $8.314 J K^{-1} mol^{-1}$ .

Since the temperature ramped from ambient to  $550^\circ C$ , we divided equations 7.3, 7.4, 7.5, 7.6 by  $\gamma$  (the heating rate). So, our equations were based on temperature rather than time  $k''_{o,i} = \frac{k'_{o,i}}{\gamma}$ .

At  $t=0$  that  $T=150^\circ C$ , the concentration of butyric acid, maleic acid,  $CO_x$  and  $R$  equal to 0 and  $C_L=C_{Lo}$ .

We estimated the kinetic parameters with a fourth-order Runge-kutta interaction method on the basis of minimizing the square difference between the model result and the experimental data ( $y_{cal}$  and  $y_{exp}$ ) (Equation 7.7).

$$RSS = \sum (y_{exp} - y_{cal})^2 = \min \quad (7.7)$$

## 7.5 Results and discussions

### 7.5.1 Reaction conditions

WO<sub>3</sub>/TiO<sub>2</sub> oxidizes the lignin vapours mainly to butyric acids. At low oxygen concentration (5 %), lignin reaction rate is low and tends to remain as a solid rather than conversion to gas or liquid. Consequently, the acid yield was low (Table 7.2–R7–R8–R9) — only 5 % of the carbon made up the liquid phase. Increasing the temperature beyond 550 °C would pyrolyse much of the remaining lignin (since oxygen conversion was 100 %. At C<sub>O<sub>2</sub></sub>=10 % yield of liquid was ~ 16 % (Table 7.2–R4–R5–R6). Increasing oxygen to 19 % improved liquid yield to ~ 21 % (Table 7.2–R1–R2–R3). Oxygen breaks down the lignin polymer (Fargues et al. (1996)) and produces lower molecular weight compounds compared to pyrolysis. Catalysts convert these compounds to fine chemicals more easily than pyrolysis oils that have a higher molecular weight.

Table 7.2 Product selectivity vs. reaction condition, cat. WO<sub>3</sub>/TiO<sub>2</sub>

	R1	R2	R3	R4	R5	R6	R7	R8	R9	R10
O <sub>2</sub> (%)	0.21	0.21	0.21	0.1	0.1	0.1	0.05	0.05	0.05	0.21
$\omega$ (mL min <sup>-1</sup> )	0	0.02	0.05	0	0.05	0.02	0	0.02	0.05	0.05
$\tau$ (s)	0.2	0.1	0.3	0.2	0.2	0.2	0.3	0.1	0.1	0.3
EC ( $\mu$ S/cm)	154	202	218	184	195	206	162	197	160	178
Carbon balance (%)										
Liquid	19	19	18.5	16.5	13	16.5	4	3	4.5	18.5
Solid	2	2	4	19.5	30.5	17.5	64	71.5	63.5	2
Gas	79	79	77.5	64	56.5	66	32	25.5	32	79.5
Liquid selectivity (%)										
Aromatic	0.7	41	15	1.5	2.5	8	50	14	13	12
Maleic/fumaric acid	17	15.5	5	16	10	17.5	5.5	9	9.	6
Butyric acid	75	38	77	78	84	61	41	76	73	80
Formic acid	✓	-	✓	-	-	✓	✓	-	-	✓
Acetic acid	✓	0.2	0.4	0.3	0.4	1.2	0.2	0.3	0.3	0.3
Succinic acid	0.5	2	1	4	2	7	1	-	3	0.6
Phthalic acid	✓	0.11	-	0.2	-	0.6	0.1	-	-	-
Benzoic acid	✓	0.4	-	-	-	1	-	-	0.3	0.45
Syringic acid	-	1.5	-	-	-	1	0.9	-	-	-
Unknown	1	0.4	0.4	0.3	0.5	1.5	0.5	0.3	1	0.3
H <sub>2</sub> , %	3.5	6	2.5	3.5	3	7	4.5	5	3.5	2

At  $C_{O_2}=5\%$  most produced vapours don't react even at the higher contact time (R7) because the catalyst requires oxygen. Adding water (at this low oxygen concentration) decreased the yield of aromatics but increased that of butyric acid and maleic acid (R8–R9). Water facilitates the oxygen-promoted decomposition of lignin Brebu and Vasile (2010).

At  $C_{O_2}=10\%$ , adding water (0.02 ml/min) improved yield of MA (R4–R6). Adding water diluted the  $O_2$  concentration and as a result more solids remained (R6). Increasing the water flow rate further reduced the  $O_2$  concentration and even less lignin reacted; however, butyric acid selectivity increased (R5).

At  $C_{O_2}=21\%$  adding water had no effect on the distribution of the carbon in the liquid, solid and gas phases (R1–R3). Butyric acid selectivity was high, as in most other experiments, but it was uncharacteristically low in R2 (and coincidentally high for the same experiment). Lignin formed more phenolic compounds, rather than char and tar, while co-feeding  $O_2$  during the thermal treatment. In addition,  $O_2$  depolymerized more lignin through a free radical mechanism while water facilitated the oxygen-promoted decomposition Brebu and Vasile (2010).

In almost every reactions acetic acid was traced. This acid was produced in the first step; so the, catalyst did not affect its yield.

## 7.5.2 Mechanism and modeling

### Estimate of kinetic parameters

We considered a pseudo-first-order reaction kinetic model for the oxidation of lignin to various compounds (Equations 7.3, 7.4, 7.5, 7.6). We obtained kinetic parameters using a fourth order Runge-kutta method (Table 7.3). The calculated data were comparable with the experimental results (Figure 7.7)

Table 7.3 Estimated kinetic parameters-  $k'_{o,i}$ .

Name	$O_{2real}$	$\omega_{real}$	$\tau$ s	$-k'_{o,L}$ $s^{-1} \times 10^7$	Lignin $E_L$ $kJ\ mol^{-1}$	$R^2$	$k'_{o,B}$ $s^{-1} \times 10^3$	Butyric acid $E_B$ $kJ\ mol^{-1}$	$R^2$	$k'_{o,MA}$ $s^{-1} \times 10^5$	Maleic acid $E_{MA}$ $kJ\ mol^{-1}$	$R^2$	$k'_{o,CO_x}$ $s^{-1} \times 10^4$	COx $E_{CO_x}$ $kJ\ mol^{-1}$	$R^2$
R1	0.21	0	0.2	50		0.99	20.0		0.82	-		-	12.5		0.83
R2	0.17	0.2	0.1	25		1	8.0		0.99	12.0		1	6.8		1
R3	0.16	0.22	0.3	17.5		0.95	15.5		0.95	4.0		0.95	2.7		0.7
R10	0.11	0.5	0.3	15	44	0.99	23.0	31	0.9	7.5	44	0.95	1.0	31	0.7
R5	0.05	0.5	0.2	15		0.99	14.0		0.88	7.0		0.92	2.1		0.93
R6	0.08	0.2	0.2	10		0.99	6.5		0.96	13.0		0.97	2.3		0.85
R8	0.04	0.2	0.1	7.5		1	2.5		0.97	1.0		0.95	1.6		0.95
R9	0.024	0.2	0.1	9.5		0.99	3.0		0.99	1.5		0.98	2.3		0.98

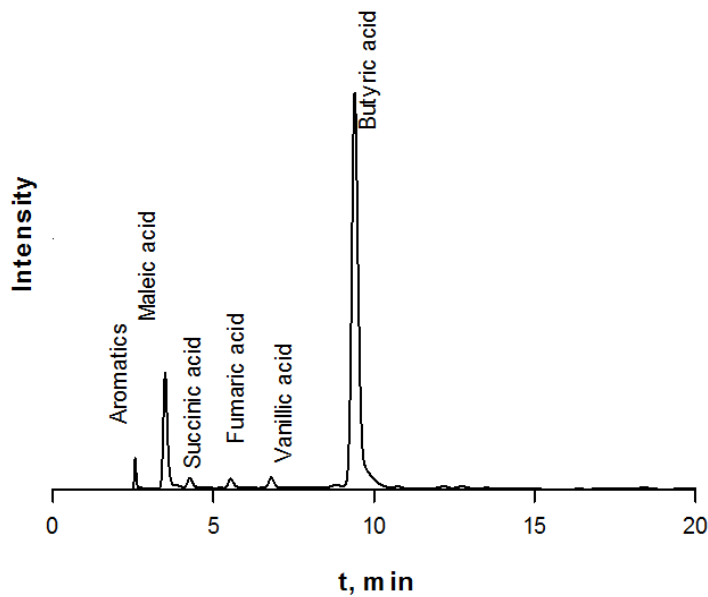


Figure 7.5 HPLC trace of test R1

### Regression model

We developed a non-linear regression model to calculate the reaction order for each of the factors — oxygen concentration, water concentration and residence time. The reaction orders and rate constants were optimized by minimizing the sum of the squares of the error for the liquid yield and butyric acid yield (Table 7.5).

$$\ln k'_{o,i} = \beta_o + \beta_1 * \ln C_{O_2} + \beta_2 * \ln C_w + \beta_3 * \ln \tau \quad (7.8)$$

$$\sigma^2 = \frac{S^2}{N - K} = \sum_{i=1}^N \frac{(k_{\text{cal}} - k_{\text{model}})^2}{N - K} \quad (7.9)$$

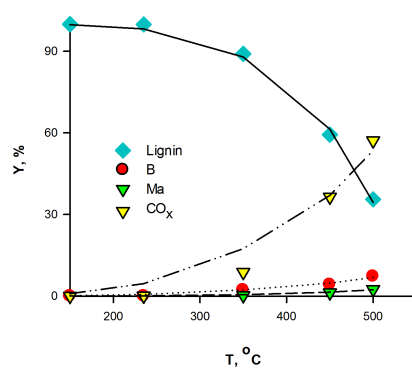
Where

N = number of experiments

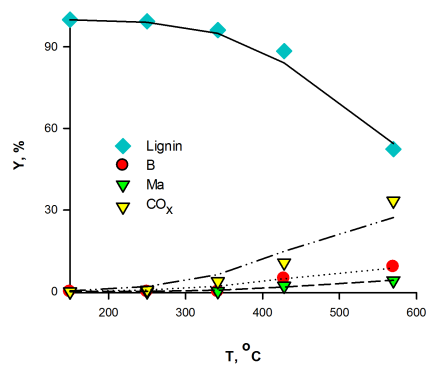
K = number of determined parameters

$k_{\text{cal}}$  = measured yield

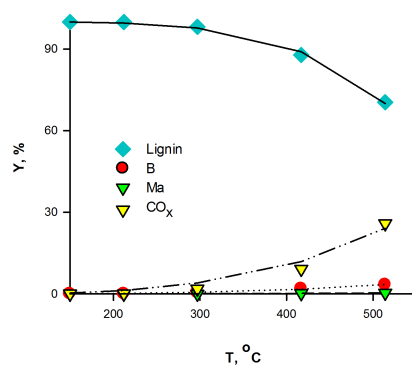
$k_{\text{model}}$  = calculated yield



(a) R2



(b) R6



(c) R9

Figure 7.6 Experimental (scatter) vs. model calculated (line)

$$\tau = \frac{V_{\text{cat}}}{Q_{\text{gas}}}$$

Table 7.4 Kinetic parameters–literatures.

Process		$k_{o,l}$	$E_l$ kJ mol <sup>-1</sup>	$k_{o,a}$	$E_a$ kJ mol <sup>-1</sup>	$k_{o,acid}$	$E_{acid}$ kJ mol <sup>-1</sup>	Ref.
Catalytic wet oxidation of lignin to aromatics		0.3–1.4 10 <sup>6</sup> s <sup>-1</sup>	43	0.03–0.9 10 <sup>6</sup> s <sup>-1</sup>	~ 65	0.2–1.9 10 <sup>6</sup> s <sup>-1</sup>	10–43	Sales et al. (2007)
Kraft lignin to vanillin	$pH > 11.5$	$0.6 \times 10^2 \text{ L mol}^{-1} \text{ s}^{-1}$	29	$2.3 \times 10^5 (\text{L/mol})^{1.75} \text{ s}^{-1}$	46	–	–	Fargues et al. (1996)
	$pH < 11.5$	$1.5 \times 10^{11} \text{ L mol}^{-1} \text{ s}^{-1}$		$0.7 \times 10^5 (\text{L/mol})^{1.75} \text{ s}^{-1}$		–	–	
Wet oxidation of treated debarking water*		$1.38 \times 10^3$ – $2.9 \times 10^9 \text{ s}^{-1}$	3–74	–	–	$2.3$ – $59.5 \times 10^4 \text{ s}^{-1}$	10–35	Kindsigo et al. (2010)
Pyrolysis		remained solid $0.4 \times 10^2 \text{ s}^{-1}$	19	liquids $0.1 \times 10^4 \text{ s}^{-1}$	29	gases $0.4 \times 10^3 \text{ s}^{-1}$	22	Farag et al. (2014a)

\* pH extremely affects kinetic parameters

Table 7.5 Estimated kinetic parameters–  $k_{o,i}$ .

Name	$k_{o,i}$		$\beta_1$	$\beta_2$	$\beta_3$	$R^2$
L	$-5.6 \times 10^7$	$\text{mol}^{-0.56} \text{ s}^{-1}$	0.6	-0.06	0	0.99
B	$6.4 \times 10^5$	$\text{mol}^{-1} \text{ s}^{-2}$	0.45	0.55	1	0.93
CO <sub>x</sub>	$2 \times 10^4$	$\text{mol}^{-0.4} \text{ s}^{-1}$	0.6	-0.2	-0.8	0.99

The obtained results by lumped kinetic models was almost at the same magnitude with the literature (Table 7.4).

## Optimization

The three considered parameters include oxygen concentration, water concentration and residence time affect butyric acid yield (Table 7.5). Oxygen had the almost same effect on degradation of lignin and gas formation. Increase of oxygen concentration increase lignin degradation and gas yield. While, water had a negative effect on gas formation and lignin degradation. Water mainly increases acid selectivity. Also, higher contact time between vapours and catalyst increases yield of butyric acid (Table 7.5). To introduce the limitations, we considered the ratio of  $\frac{k_B}{k_L}$  (Equation 7.10) and  $\frac{k_B}{k_{\text{CO}_x}}$  (Equation 7.11).

$$\frac{k_B}{k_L} = 5.2 \times 10^{-3} C_{\text{O}_2}^{-0.2} C_{\omega}^{0.66} \tau^1 \quad (7.10)$$

$$\frac{k_B}{k_{\text{CO}_x}} = 14.6 C_{\text{O}_2}^{-0.17} C_{\omega}^{0.8} \tau^{1.78} \quad (7.11)$$

The maximum amount of butyric acid concentration to total conversion of lignin will occur at low oxygen concentration ( $\sim 2\%$ ) and water concentration higher than  $5\%$  (Figure 7.7).



However, low oxygen concentration will decrease lignin degradation. Or to increase the butyric acid formation to gas, we need a residence time  $> 0.55$  s while oxygen level is less than 6 % (Equation 7.11). Consequently, the major effect of water is on acid selectivity and the main effect of oxygen is on lignin conversion.

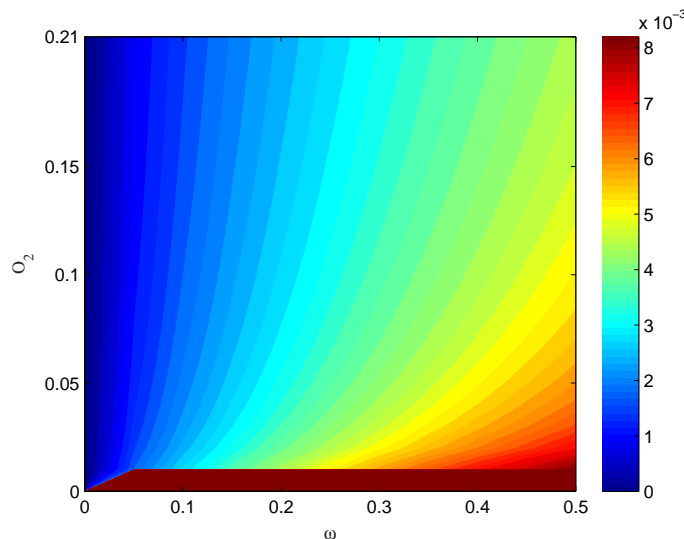


Figure 7.7  $O_2$  vs.  $\omega - k_{o,B}/k_{o,L}$  – Equation 7.10

## 7.6 Conclusions

Lignin is the main waste product of the pulp and paper and bio-refinery industries. Conversion of this lignin into valuable material and chemicals instead of burning it as a low value fuel is a promising way for bio-refineries to enhance their economic viability. On the other hand, the high demand of butyric acid has attracted attention as a sustainable alternative to petroleum-based sources. However, bio-resource methods are expensive. The oxidation of lignin in the presence of  $WO_3/TiO_2$  yields  $C_4$  acids, butyric acid in particular. The selectivity of butyric acid reached 80 %. Water concentration, oxygen concentration and gas contact time affects the yields of liquid and butyric acid. Higher oxygen concentration increases the lignin degradation ( $>10$  %), and water open aromatic rings and increase acid selectivity. Increase of butyric acid selectivity versus lignin conversion occurs at  $C_{O_2} < 5$  % when water concentration is higher than 5 %. In addition, an increase in residence time improves butyric acid selectivity. As these parameters somewhat conflict with each other, further study is required to increase the total yield. Heating rate and temperature are other two parameters that affect yield of liquid and ultimately, the total yield of carboxylic acids. This reaction occurred in two steps, and the optimization of each step will improve the targeted products.

## 7.7 Nomenclature

$K$  = adsorption equilibrium constant

$k$  = kinetic constant

$C$  = concentration

$E$  = activation energy

*Greek Letters*

$\omega$  = water

$\tau$  = residence time

## 7.8 Acknowledgements

The authors would like to acknowledge FPInnovation for supplying lignin and analytical assistance. In addition, we offer a special thanks to the NSERC Biomaterials, Chemicals Strategic Network ([www.lignowork.ca](http://www.lignowork.ca)) and FIBRE Network ([www.fibrenetwork.org](http://www.fibrenetwork.org)) for all their supports.

## CHAPTER 8 GENERAL DISCUSSION

The depletion of fossil fuels, due to their consumption as a source of fuel, chemicals and energy, is expected to increase in the foreseeable future. Evidence of an increase in greenhouse gas concentration adds urgency to the need to develop sustainable bio-refineries. Modifying biomass conversion methods and agricultural technologies caused bio-fuels meets the nation's need. However, on the industrial scale, there are still struggles with economic challenges to developing sustainable bio-refineries. For high energy impact, and out of economic necessity, a bio-refinery should be able to valorize all the compounds of lignocellulosic biomass including hemicellulose, cellulose and lignin. After cellulose, lignin is the second-most abundant agricultural polymer, and is a ubiquitous component of almost all plant biomasses. The ability of the bio-refinery process of effective convert of enormous volumes of lignin remains into valuable chemicals will guarantee its economic viability. Annually, the pulp and paper industry produces huge amounts of lignin waste, and this amount is much higher than it's need to be when used as a source of energy in the same industry.

The process of converting lignin to valuable chemicals includes thermochemical treatment, homogeneous and heterogeneous catalysis and biological de-polymerization. At harsh reaction conditions, hydrolysis and hydro-deoxydation upgrade lignin to gasoline range aromatics. The oxidation process targets mostly the production of aromatics and aldehydes, which have a limited market value. The enzyme process yields low molecular weight aromatics. All these methods are hindered by a lack of suitable technology. For example, the complexity of lignin's structure cause low selectivity and requires improvement in product separation and conversion technology. Introducing a process that converts lignin to high selective products is challenging. The conversion of lignin to biomaterial such as carbon fiber composite materials, fibers and, polyurethane is promising. However, not all lignin left-over from bio-refineries or the pulp and paper industry can be used in a bio-material application valuable for conversion to fuels and chemicals. This paper focuses on the upgrading of lignin to ring-opened carboxylic acids, which have a higher market value, but have attracted less attention.

In order to accomplish this, we first investigated a gas-solid system in which a sparger atomizes the lignin solution directly into a micro-fluidized bed.

Lignin was soluble in NaOH, KOH and aqueous ammonia solutions at ambient temperatures, but the ammonia solution had high volatility and evaporated in the line upstream of the nozzle tip and blocked the injector. To model black liquor, we dissolved lignin in a basic solution. At lignin and NaOH concentrations of  $30 \text{ g L}^{-1}$  and  $70 \text{ g L}^{-1}$ , respectively, the injector remained

clear for several hours of operation. At a liquid flow rate lower than  $125 \mu\text{L min}^{-1}$ , the injection line blocked in less than 5 min after the experiments start. Droplet formation and line blockage are more probable in a downward facing injector orientation, while the upward orientation of the injector in the bed could cause the catalyst to agglomerate at the tip of the injector or cause fine particles to go to the injector and block the line.

We tested VPP, that is an active catalyst to partially oxidize n-butane and saturated aliphatic hydrocarbons to maleic acid and Al-V-Mo catalyst.  $\text{Al}_2\text{O}_3$  and molybdenum were able to cleave lignin bonds and vanadium, which is widely used in oxidation reactions. Lignin vaporize and react with solid catalysts.

Lignin injected continuously from the top of the reactor at  $375^\circ\text{C}$  and  $\text{C}:\text{O}_2$  equals 0.7 ; 1.4 % malonic acid , 0.7 % maleic anhydride, 0.1 % acrylic acid, acetic acid, fumaric acid and vanillic acid formed in the presence of VPP. Catalysis of lignin with Al-V-Mo yielded predominantly lactic acid (6 %) and several compounds such as acetic acid 0.2 %, acrylic acid (0.4 %), maleic anhydride (0.6 %), fumaric and phthalic acid. At higher and lower temperatures, organic acid yield was less than 1 %.

In this condition, lots of coke formed, the catalyst deactivated rapidly and the fluidized-bed slumped after 16 min. Lower mechanical stresses and higher liquid bridging of micro-fluidized bed reactors accelerated agglomeration and the catalyst deactivation rate in comparison to larger scale.

To address catalyst deactivation, we intermittently fed the lignin solution (45 s), purged the sparger line with water for 45 s, then stopped liquid injection and regenerated the catalyst with a higher oxygen concentration. This sequence helped keep the line clear and allowed us to operate for several hours uninterrupted. As a result, the mass conversion of the lignin approached 25 %, and 17 % of the carbon gave carboxylic acids.

At  $y_{\text{O}_2} = 4\%$  and  $T = 600\text{ K}$  with Al-V-Mo the maximum yield of lactic acid was 7 % and MA 1 % while 7 % formic acid, 3 % acetic acid, 1 % acrylic acid and 4 % phthalic acid was formed.

Ma et al. (2014) achieved a 14 % yield for a diluted-acid corn stover lignin and a 11 % yield for steam-exploded spruce lignin Lochar and Smolakova (2009). The selectivity to dicarboxylic acids after 5 h at 333 K was 95 % while in comparison, the yield of carboxylic acids in the fluidized bed was almost twice as high.

The NMR test showed carbon in lignin remained in the reactor, either as coke or aromatic compounds. However, forced cycling (switching between air and lignin solution) reduced coke formation and catalyst deactivation, while direct contact of lignin with the catalyst

increased its deactivation rate. To deter catalyst deactivation, a two-step reaction system of thermo-oxidative cracking of lignin followed by catalytic oxidation of volatile to acids was introduced. Lignin degrades gradually through an increase in temperature. The aromatic vapours produced pass through the catalyst bed for selective partial oxidation.

However, prior to the NMR test we characterized lignin stability and product distribution (Chapter 4). We monitored product selectivity versus temperature in an 8 mm ID quartz micro-fluidized-bed while heating lignin at  $5 \text{ K min}^{-1}$  under argon, and 21 % oxygen under argon. The liquid product yield (predominantly aromatics) was  $\sim 20 \%$  for both cases. The aromatics include o-guaiacol, creosol, oxime, vanillin, and apocynin. In air, oxygen reacted with lignin to form  $\text{CO}$ ,  $\text{CO}_2$  and  $\text{CH}_4$  while in nitrogen char was the principal product. Lignin degraded in the wide range of  $150^\circ\text{C}$  to  $600^\circ\text{C}$  and pyrolysis occurred over a wider range of temperature. Heat and mass transfer limited the reaction rate in thermo-oxidative decomposition. 0.3 %, 3 %, 27 % and 37 % solids remained at 550 K by heating rates of 5, 10, 20, 30, and  $100 \text{ K min}^{-1}$ , respectively. A two-step model allowed us to predict the lignin degradation rate properly.

In the two-step reactor (Chapter 5), lignin degraded gradually versus temperature. This semi-continuous reactor, in which a mixture of oxygen, argon and steam were passed through a bed of lignin, removed the aromatic compounds rapidly and catalyst selectively oxidized them to desirable product, and avoided the undesirable secondary reaction like re-polymerization or gasification. We tested various catalysts while the lignin degraded gradually at a heating rate of  $10^\circ\text{C min}^{-1}$  up to  $550^\circ\text{C}$ . Oxygen concentration was 21 %,  $\omega = 0.05 \text{ mL min}^{-1}$ , and  $\tau$  was equal to 0.2 s. A vanadium catalyst was able to cleave lignin bonds, open aromatic rings and oxidize lignin to carboxylic acid and especially maleic acid. Alumina has a higher surface area, causing high activity but poor selectivity, while supports with lower surface areas of open porosity can yield more desired products with less over-oxidation. The Al-V-Mo catalyst yielded liquid at 23 % but had a lower selectivity to maleic acid (20 %). Replacement of  $\text{Al}_2\text{O}_3$  with  $\text{TiO}_2$  reduced liquid yield (15.5 %) but maleic acid (45 %) selectivity increased. HZSM-5 led to more liquid (25 %) and less maleic acid (21 %). Replacing molybdenum with tungsten in HZSM-5-V-Mo produced, in addition to MA, butyric acid and succinic acid as well.  $\text{WO}_3\text{-TiO}_2$  yielded butyric acid rather than maleic acid. Basic catalyst are not as active as acidic catalysts in degradation of lignin and in the opening of aromatic rings. As such, major components in the presence of basic components were aromatic compounds. The two-step partial oxidation of unwashed lignin yielded 19 %, which was almost the same as pure lignin, and MA had a higher selectivity to MA 65 %. In this method, the coke formation reduced to  $\sim 5 \%$ .

$\text{WO}_3\text{--TiO}_2$  was able to convert lignin to  $\text{C}_4$  acids, and butyric acid in particular. We screened the effects of  $\text{O}_2$ , water concentration and  $\tau$  on the yields of liquid, gas and product selectivity and modeled the lignin decomposition, and the acid and gas formation through the use of the lumped model (Chapter 6). For complex reactions such as the oxidation of lignin where a lot of intermediates enter, the reaction lumped model allowed us to predict the reaction rate with appropriate accuracy. We considered a pseudo-first order reaction and calculated the effects of various parameters in the selectivity of various products. A higher oxygen concentration increased the liquid to gas ratio ( $>10\%$ ), and oxygen degraded lignin to smaller aromatic compounds. To convert this liquid to butyric acid  $<10\%$ , oxygen is required when  $\omega$  is higher than  $25\%$ . In addition, an increase in residence time improved butyric acid selectivity.

## CHAPTER 9 CONCLUSION

### 9.1 Conclusion

The main objective of this work was the partial oxidation of lignin in a gas-solid fluidized bed reactor in the presence of heterogeneous catalyst.

Our first target was to synthesize, or introduce, an active catalyst that breaks lignin linkages, opens aromatic rings and selectively yields carboxylic acids. The heterogeneity of lignin structure yields heterogeneous liquid mixtures and is a barrier to the conversion of lignin to chemicals. For the first time, we tested transition metal oxides including vanadium, molybdenum, and tungsten while using  $\text{TiO}_2$ ,  $\text{Al}_2\text{O}_3$  and HZSM-5 as supports in oxidation of lignin to carboxylic acids. Product selectivity and yield depended upon the support and the catalyst. The catalysts used were able to open aromatic rings of lignin and yields mainly  $\text{C}_4$  acids including maleic acid, butanoic acid, succinic acid or  $\text{C}_3$  acids like lactic acid. Vanadium and molybdenum catalyst showed a good activity in oxidation of lignin to maleic acid while tungsten yielded mainly butanoic acid.

In parallel, we explored a gas-solid fluidized bed that reduces issues of catalytic degradation of lignin, more specifically fast catalyst deactivation and agglomeration. First, we studied a gas-solid reactor with a lignin solution sprayed on the surface of the bed. Direct contact between the huge molecules of lignin and catalyst, with the basic solution used to dissolve lignin, accelerated the catalyst deactivation rate. This problem was reduced considerably through intermittent feeding of the lignin solution, purged the sparger line with water, and regenerating of catalyst with higher oxygen concentration once liquid injection stopped. This sequence helped keep the line clear, which was another issue in the initial setup. This system increased the yield of carboxylic acids up to 25 % in the presence of Al-V-Mo.

To reduce catalyst deactivation we introduced a gas-solid system that lignin degraded gradually versus temperature in the presence of water and oxygen and produced vapours. produced vapours passed through the catalyst for selective oxidation and prevented unselective products like repolymerization. Lignin completely converted to liquid and gas at 10 % oxygen and water mole fraction at 50 %. Less coke formed in the gas-solid system compared to the gas-solid-liquid system.

To improve catalyst performance we tested different reaction conditions in each system. The first setup was very sensitive to reaction conditions. Higher yields were obtained at an oxygen concentration of  $\sim 4\%$  and temperature equal to  $370^\circ\text{C}$ . At higher and lower temperatures

acid yields were reduced considerably. Our results showed, water concentration and oxygen concentration affected lignin conversion and residence time,  $C_{O_2}$ , and  $C_w$  affected butyric acid and gas formation.

A lumped kinetic model can properly predict partial oxidation of lignin in the presence of  $WO_3$ - $TiO_2$ . We considered a pseudo-first order reaction.

In this study, we found that the introduce gas-solid system in able to oxidize lignin to carboxylic acid in a micro-fluidized bed reactor in the presence of vanadium, molybdenum and tungsten heterogeneous catalysts. Using heterogeneous catalysts has advantageous such as easy separation, and less catalyst consumption and coke removal is easier in the fluidized-bed reactors. It should be noted that, the test occurred at a medium temperature, and atmospheric pressure and reaction rate was fast.

For the first time, we introduced a gas-solid system for fast oxidation of lignin while we targeted carboxylic acids production. According to the higher selectivity to carboxylic acids specially maleic acid that reduce separation cost, this work has a real potential to be considered to oxidation of lignin to carboxylic acids.

## 9.2 Limitations of the solution proposed

For the gas-solid system, solid injection for a continuous system could be a barrier. Recently, however, solutions for biomass injection in pyrolysis systems have been presented.

## 9.3 Recommendations for future research

Gas-solid oxidation of lignin was presented for the first time as a possibility in the conversion of lignin to fine chemicals, especially, carboxylic acids. A new way of valorizing lignin was introduced, however, despite the method increasing the yield of carboxylic acid up to two times, the findings still needs more study.

A vanadium oxide catalyst demonstrated suitable activity in breaking lignin linkages, opening aromatic rings and converting lignin to carboxylic acids. Supports and addition of other transition metal oxides, such as molybdenum and tungsten, changed lignin selectivity. Still, there remain a lot of transition metal oxides to study for their role in oxidation of lignin and their selectivity in producing a special carboxylic acid. The precise design and synthesis of the catalyst should be investigated in the future.

In the first system, a syringe pump injected dissolved lignin in an alkaline solution to the reactor bed, and this system proved useful for black liquor as well. In lignin gasification,



unwashed lignin rather than pure lignin, was used as the feed. Our primary test demonstrated that unwashed lignin can be used as the feedstock in this process. Using unwashed lignin as the feedstock removed the cost of lignin purification. On the other hand, factors such as the type of plant and pretreatment methods for removing lignin, change the lignin structure and its behaviour in the reaction accordingly. Partial oxidation of various kinds of lignin in these systems will make this method more globally efficient.

All experiments were run in a micro-fluidized bed reactor. The agglomeration of powders is problematic in small reactor systems, and injecting liquid solution adds a level of complexity to this system. Also, small reactors limit the gas flow rate of the injector to spray the solution. The ability to run a series of experiments in a large-scale reactor will be a big step in scaling up.

In the two step gas-solid reactor, we ran the two-steps in the same reactor, but the optimization of each step would improve the final product yield and selectivity. In the degradation of lignin, oxygen and steam concentration affect degradation yield and product distribution. On the other hand, the heating rate has a considerable effect in the yield of lignin evaporates, for example, the yield of liquid increase with flash pyrolysis. The optimization of each step includes the heating rate, temperature and residence time and many other parameters, while a new design could control product composition.

Conversion of system from semi-batch into continuous would be very interesting.

Moreover, process integration would give higher yields and enhance the economy of the process. In the process presented, we targeted the conversion of the monomers to carboxylic acid and aromatics. However, gases such as CO, CO<sub>2</sub>, H<sub>2</sub> and CH<sub>4</sub> formed, as well as char. The syngas formed has the possibility to be converted to chemicals and bio-fuels and the solid lignin, mainly char, could be used as a source of fuel. The quality of the parameters listed above, and the economic evaluation of this process, should be studied in the future.

## LIST OF REFERENCES

- A. Akbari et S. M. Alavi, "The effect of cesium and antimony promoters on the performance of ti phosphate supported vanadium v oxide catalysts in selective oxidation of o xylene to phthalic anhydride", *Chemical Engineering Research and Design*, no. 102, pp. 286–296, 2015.
- T. Akiyama, T. Sugimoto, Y. Matsumoto, et G. Meshitsuka, "Erythrothreo ratio of bo4 structures as an important structural characteristic of lignin i improvement of ozonation method for the quantitative analysis of lignin side chain structure", *Journal of Wood Science*, vol. 48, pp. 210–215, 2002.
- A. G. Alejandre, J. Ramirez, et G. Busca, "A vibrational and spectroscopic study of wo3 tio2 al2o3 catalyst precursors", *Langmuir*, vol. 14, pp. 630–639, 1998.
- G. Almendros, A. T. Martinez, A. E. Gonziilez, F. J. GonzalezVila, R. Frund, et H. Ludemann, "Cpmas 13c nmr study of lignin preparations from wheat straw transformed by five lignocellulose degrading fungi", *Journal of Agricultural and Food Chemistry*, vol. 40, no. 40, pp. 1297–1302, 1992.
- J. Araujo, C. Grande, et A. Rodrigues, "Vanillin production from lignin oxidation in a batch reactor", *Chemical Engineering Research and Design*, vol. 88, no. 8, pp. 1024–1032, 2010.
- J. D. Araujo, C. A. Grande, et A. E. Rodrigues, "Structured packed bubble column reactor for continuous production of vanillin from kraft lignin oxidation", *Catalysis Today*, vol. 147, pp. 330–335, 2009.
- F. W. Atadana, "Catalytic pyrolysis of cellulose hemicellulose and lignin model compounds", 2010.
- P. Azadi, O. R. Inderwildi, R. Farnood, et D. A. King, "Liquid fuels hydrogen and chemicals from lignin a critical review", *Renewable and Sustainable Energy Reviews*, vol. 21, pp. 506–523, 2013.
- A. Azarpira, J. Ralph, et F. Lu, "Catalyticalkaline oxidation of lignin and its model compounds : a pathway to aromatic biochemicals", *BioEnergy Research*, vol. 7, no. 1, pp. 78–86, 2014.

- S. Bagheri, N. M. Julkapli, et S. B. A. Hamid, "Titanium dioxide as a catalyst support in heterogeneous catalysis", *The Scientific World Journal*, vol. 2014, p. 727496, 2014.
- R. S. Barker, "Method of oxidizing benzene to maleic anhydride using a vanadium, molybdenum, boron containing catalyst", 1975.
- M. Bartels, W. Lin, J. Nijenhuis, F. Kapteijn, et R. van Ommen, "Agglomeration in fluidized beds at high temperatures mechanisms detection and prevention", *Progress in Energy and Combustion Science*, vol. 34, no. 5, pp. 633–666, 2008.
- J. Bayne, I. R. King, et J. R. Morey, "Vapour phase oxidation of benzene to maleic anhydride using an aluminum phosphate supported catalyst", 1972.
- S. Beis, S. Mukkamala, N. Hill, J. Clayton, B. Frederick, A. Heiningen, A. Berg, et W. J. DeSisto, "Fast pyrolysis of lignins", pp. 1408–1424, 2010.
- R. I. Bergman et N. W. Frisch, "Production of maleic anhydride by oxidation of n-butane", 1966.
- F. M. Berruti, L. Ferrante, C. L. Briens, et F. Berruti, "Pyrolysis of cohesive meat and bone meal in a bubbling fluidized bed with an intermittent solid slug feeder", *Journal of Analytical and Applied Pyrolysis*, vol. 94, pp. 153–162, 2012.
- K. G. Bhattacharyya et A. K. Talukdar, *Catalysis in petroleum and petrochemical industries*. Narosa Publishing House, 2005.
- A. Bielanski et M. Najbar, "V<sub>2</sub>O<sub>5</sub> / MoO<sub>3</sub> catalysts for benzene oxidation", *Applied Catalysis A General*, vol. 157, no. 1–2, pp. 223–261, 1997.
- J. B. Binder, M. J. Gray, J. F. White, Z. Zhang, et J. E. Holladay, "Reactions of lignin model compounds in ionic liquids", *Biomass and Bioenergy*, vol. 33, pp. 1122–1130, 2009.
- C. Bjorgen, "One pot conversion of biomass to ethylene glycol, propylene glycol and other polyols over carbon supported tungsten catalysts", 2013.
- D. C. Boffito, C. Neagoe, M. Edake, B. Pastor-Ramirez, et G. Patience, "Biofuel synthesis in a capillary fluidized bed", *Catalysis Today*, no. 237, pp. 13–17, 2014.
- E. Bordes, "Crystallochemistry of vpo phases and application to catalysis", *Catalysis Today*, vol. 1, no. 5, pp. 499–526, 1987.

- M. Brebu et C. Vasile, "Thermal degradation of lignin a review", *Cellulose Chemistry and Technology*, vol. 44, no. 9, pp. 353–363, 2010.
- M. Brown, M. Maciejewski, S. Vyazovkin, R. Nomen, J. Sempere, A. Burnham, J. Opfermann, R. Strey, H. Anderson, A. Kemmler, R. Keuleers, J. Janssens, H. Desseyn, C.-R. Li, T. B. Tang, B. Roduit, J. Malek, et T. Mitsunashi, "Computational aspects of kinetic analysis part a the ictac kinetics project data, methods and results", *Thermochimica Acta*, vol. 355, no. 1–2, pp. 125–143, 2000.
- S. Bruhns et J. Werther, "An investigation of the mechanism of liquid injection into fluidized beds", *AIChE Journal*, pp. 766–775, 2005.
- T. D. H. Bugg, M. Ahmad, E. M. Hardiman, et R. Singh, "The emerging role for bacteria in lignin degradation and bio-product formation", *Current opinion in biotechnology*, vol. 22, no. 3, pp. 394–400, 2011.
- M. Cardona, D. C. Boffito, et G. S. Patience, "Thermogravimetric heat and mass transfer modeling of bitumen pyrolysis", *Fuel*, vol. 143, pp. 253–261, 2015.
- G. Centi, "Nature of active layer in vanadium oxide supported on titanium oxide and control of its reactivity in the selective oxidation and ammoxidation of alkylaromatics", *Applied Catalysis A*, no. 147, pp. 267–298, 1996.
- C. A. Chagas, L. C. Dieguez, et M. Schmal, "Investigation of the stability of  $\text{CeO}_2$ ,  $\text{V}_2\text{O}_5$  and  $\text{CeV}$  mixed oxide on the partial oxidation of propane", *Catalysis Letters*, vol. 142, no. 6, pp. 753–762, 2012.
- K. Chakravarthi, "A solid catalyst method for biodiesel production", Thèse de doctorat, 2009.
- E. Chan, B. A. Knapper, E. Mueller, J. Mcmillan, J. Tyler, et R. P. Davuluri, "Fluid injection nozzle for fluid bed reactors", 2013.
- H. Chen, N. Liu, et W. Fan, "Two step consecutive reaction model of biomass thermal decomposition by dsc", *Acta Physico Chimica Sinica*, vol. 22, no. 7, pp. 786–790, 2006.
- H. Chen, M. Tang, Z. Rui, et H. Ji, "Nature of active layer in vanadium oxide supported on titanium oxide and control of its reactivity in the selective oxidation and ammoxidation of alkylaromatics", *Industrial and Engineering Chemistry Research*, no. 147, pp. 267–298, 1996.

- L. Chen, E. G. Derouane, et J. C. Vedrine, “High throughput preparation and testing of monobasic mixed oxide catalysts for direct oxidation of propane to acrylic and acetic acids”, *Applied Catalysis A General*, vol. 270, no. 1–2, pp. 157–163, 2004.
- T. Chen, J. Wu, J. Zhang, J. Wu, et L. Sun, “Gasification kinetic analysis of the three pseudocomponents of biomass cellulose semicellulose and lignin”, *Bioresource Technology*, vol. 153, pp. 223–229, 2014.
- H. S. Choi et D. Meier, “Fast pyrolysis of kraft lignin vapor cracking over various fixed-bed catalysts”, *Journal of Analytical and Applied Pyrolysis*, vol. 100, pp. 207–212, 2013.
- A. Corma et L. Sauvanaud, “Fcc testing at bench scale new units new processes new feeds”, *Catalysis Today*, vol. 218–219, pp. 107–114, 2013.
- C. Couhert, J.-M. Commandre, et S. Salvador, “Is it possible to predict gas yields of any biomass after rapid pyrolysis at high temperature from its composition in cellulose hemicellulose and lignin”, *Fuel*, vol. 88, no. 3, pp. 408–417, 2009.
- C. Crestini, P. Pro, V. Neri, et R. Saladino, “Methyltrioxorhenium : a new catalyst for the activation of hydrogen peroxide to the oxidation of lignin and lignin model compounds”, *Bioorganic and Medicinal Chemistry*, vol. 13, no. 7, pp. 2569 – 2578, 2005.
- C. Crestini, M. C. Caponi, D. S. Argyropoulos, et R. Saladino, “Immobilized methyltrioxorhenium into  $\text{H}_2\text{O}_2$  systems for the oxidation of lignin and lignin model compounds”, *Bioorganic and Medicinal Chemistry*, vol. 14, no. 15, pp. 5292–5302, 2006.
- C. Crestini, M. Crucianelli, M. Orlandi, et R. Saladino, “Oxidative strategies in lignin chemistry a new environmental friendly approach for the functionalisation of lignin and lignocellulosic fibers”, *Catalysis Today*, vol. 156, no. 1–2, pp. 8–22, 2010.
- M. Dalil, D. Carnevali, J.-L. Dubois, et G. S. Patience, “Transient acrolein selectivity and carbon deposition study of glycerol dehydration over  $\text{WO}_3/\text{TiO}_2$  catalyst”, *Chemical Engineering Journal*, vol. 270, pp. 557–563, 2015.
- S. V. den Bosch, W. Schutyser, R. Vanholme, T. Driessen, S. Koelewijn, T. Renders, B. Meester, W. Huijgen, W. Dehaen, C. Courtin, B. Lagrain, W. Boerjan, et B. Sels, “Reductive lignocellulose fractionation into soluble lignin-derived phenolic monomers and dimers and processable carbohydrate pulps”, *Energy Environ. Sci.*, vol. 8, pp. 1748–1763, 2015.
- H. Deng, L. Lin, Y. Sun, C. Pang, J. Zhuang, P. Ouyang, J. Li, et S. Liu, “Activity and

stability of perovskite-type oxide  $\text{LaCoO}_3$  catalyst in lignin catalytic wet oxidation to aromatic aldehydes process”, *Energy and Fuels*, vol. 23, pp. 19–24, 2009.

H. P. Dias, G. R. Goncalves, J. C. Freitas, A. O. Gomes, E. V. R. D. Castro, B. G. Vaz, G. M. F. V. Aquije, et W. Romao, “Catalytic decarboxylation of naphthenic acids in crude oils”, *Energy Conversion and Management*, no. 84, pp. 326–333, 2014.

J. Diedenhoven, A. Reitzmann, G. Mestl, et T. Turek, “A model for the phosphorus dynamics of vpo catalysts during the selective oxidation of nbutane to maleic anhydride in a tubular reactor”, *Chemie Ingenieur Technik*, vol. 84, no. 4, pp. 517–523, 2012.

W. Dong, J. K. Bartley, F. Girgsdies, R. Schlögl, et G. J. Hutchings, “The hydration and transformation of vanadyl pyrophosphate”, *Journal of Material and Chemistry*, vol. 15, pp. 4147–4153, 2005.

J. Dubois, C. Duquenne, et W. Hoelderlich, “Process for dehydrating glycerol to acrolein”.

M. Dwidar, J. Park, R. J. Mitchell, et B. I. Sang, “The future of butyric acid in industry”, *The Scientific World Journal*, vol. 2012, p. 471417, 2012.

P. Dwivedi, J. R. Alavalapati, et P. Lal, “Cellulosic ethanol production in the united states conversion technologies, current production status, economics, and emerging developments”, *Energy for Sustainable Development*, vol. 13, no. 3, pp. 174–182, 2009.

T. Elder, “Bond dissociation enthalpies of a pinoresinol lignin model compound”, *Energy and Fuels*, vol. 28, pp. 1175–1182, 2014.

P. Emmett, *Oxidation hydration dehydration and cracking catalysts*. Chapman and Hall, 1960.

M. Fan, P. Jiang, P. Bi, S. Deng, L. Yan, Q. Zhai, T. Wang, et Q. Li, “Directional synthesis of ethylbenzene through catalytic transformation of lignin”, *Bioresource Technology*, vol. 143, pp. 59–67, 2013.

S. Farag, “Production of chemicals by microwave thermal treatment of lignin”, Thèse de doctorat, Ecole polytechnique de Montreal, Déc. 2013.

S. Farag, D. Fu, P. G. Jessop, et J. Chaouki, “Detailed compositional analysis and structural investigation of a bio-oil from microwave pyrolysis of kraft lignin”, *Journal of Analytical and Applied Pyrolysis*, vol. 109, pp. 249–257, 2014.

- S. Farag, L. Kouisni, et J. Chaouki, “Lumped approach in kinetic modeling of microwave pyrolysis of kraft lignin”, *Energy and Fuels*, vol. 28, no. 2, pp. 1406–1417, 2014.
- T. Faravelli, A. Frassoldati, G. Migliavacca, et E. Ranzi, “Detailed kinetic modeling of the thermal degradation of lignins”, *Biomass and Bioenergy*, vol. 34, no. 3, pp. 290–301, 2010.
- C. Fargues, A. Mathias, et A. Rodrigues, “Kinetics of vanillin production from kraft lignin oxidation”, *Industrial and Engineering Chemistry Research*, vol. 35, no. 1, pp. 28–36, 1996.
- I. Fechete, Y. Wang, et J. C. Vedrine, “The past, present and future of heterogeneous catalysis”, *Catalysis Today*, vol. 189, no. 1, pp. 2–27, 2012.
- E. Feghali, G. Carrot, P. Thuery, C. Genre, et T. Cantat, “Convergent reductive depolymerization of wood lignin to isolated phenol derivatives by metal-free catalytic hydrosilylation”, *Energy Environ. Sci.*, vol. 8, p. 2734, 2015.
- D. Ferdous, A. K. Dalai, S. K. Bej, et R. W. Thring, “Pyrolysis of lignins : experimental and kinetics studies”, *Energy and Fuels*, vol. 16, pp. 1405–1412, 2002.
- A. Ferraz, C. Parra, J. Freer, J. Baeza, et J. Rodriguez, “Occurrence of iron-reducing compounds in biodelignified palo podrido wood samples”, *International Biodeterioration and Biodegradation*, vol. 47, no. 4, pp. 203–208, 2001.
- J. Filley et C. Roth, “Vanadium catalyzed guaiacol deoxygenation”, *Journal of Molecular Catalysis A Chemical*, vol. 139, no. 2–3, pp. 245–252, 1999.
- P. D. Fletcher, S. J. Haswell, E. P. Villar, et B. H. Warrington, “Micro reactors principles and applications in organic synthesis”, *Tetrahedron*, vol. 58, no. 24, pp. 4735–4757, 2002.
- F. C. Flores et J. Dobado, “Lignin as renewable raw material”, *ChemSusChem*, vol. 3, no. 11, pp. 1227–35, 2010.
- C. Fumagalli, G. Golinelli, G. Mazzoni, M. Messori, G. Stefani, et F. Trifiro, dans *Production of maleic and phthalic anhydrides by selective vapor phase oxidation with vanadium oxide based catalysts*, V. C. Corberan et S. V. Bellon, eds., 1994, vol. 82, pp. 221–231.
- T. Furusawaa, T. Satoa, M. Saitoa, Y. Ishiyamaa, M. Satob, N. Itoha, et N. Suzuki, “The evaluation of the stability of ni mgo catalysts for the gasification of lignin in supercritical water”, *Applied Catalysis A*, vol. 327, pp. 300–310, 2007.

- T. Ghaznavi, C. Neagoe, et G. Patience, "Partial oxidation of dxylose to maleic anhydride and acrylic acid over vanadyl pyrophosphate", *Biomass and Bioenergy*, vol. 71, pp. 285–293, 2014.
- J. Gierer, E. Yang, et T. Reitberger, "On the significance of the superoxide radical  $O_2^{\cdot -}$  in oxidative delignification, studied with 4 t butylsyringol and 4 t butylguaiacol", *Holzfor-schung*, vol. 48, pp. 405–413, 1994.
- J. Gierer, T. Reitberger, E. Yang, et B. H. Yoon, "Formation and involvement of radicals in oxygen delignification studied by the autoxidation of lignin and carbohydrate model compounds", *Journal of Wood Chemistry and Technology*, vol. 21, no. 4, pp. 313–341, 2001.
- A. Gomez-Barea, B. Leckner, D. Santana, et P. Ollero, "Gas–solid conversion in fluidised bed reactors", *Chemical Engineering Journal*, vol. 141, no. 1–3, pp. 151–168, 2008.
- R. Guettel et T. Turek, "Assessment of micro-structured fixed-bed reactors for highly exo-thermic gas phase reactions", *Chemical Engineering Science*, vol. 65, no. 5, pp. 1644–1654, 2010.
- C. Haggstrom, O. Ibhrman, A. A. Rownaghi, J. Hedlund, et R. Gebart, "Catalytic methanol synthesis via black liquor gasification", *Fuel Processing Technology*, vol. 94, no. 1, pp. 10–15, 2012.
- Y. Hamzeh, G. Mortha, D. Lachenal, J. C. Hostachy, et C. Calais, "Comparative studies of chlorine dioxide reactions with muconic acid derivatives and lignin model compounds", *Journal of Wood Chemistry and Technology*, vol. 2, no. 26, pp. 153–164, 2006.
- T. Hara et N. Nakamura, "Gas phase oxidization process and process for the preparation of phthalic anhydride", 2002.
- I. Hasegawa, Y. Inoue, Y. Muranaka, T. Yasukawa, et K. Mae, "Selective production of organic acids and depolymerization of lignin by hydrothermal oxidation with diluted hydrogen peroxyde", *Energy and Fuels*, vol. 25, pp. 791–796, 2011.
- J. I. Hedges et J. R. Ertel, "Characterization of lignin by gas capillary chromatography of cupric oxide oxidation products", *Analytical Chemistry*, vol. 54, no. 2, pp. 174–178, 1982.
- T. Heidemann, F. Rosowski, G. Linden, M. Seufert, G. Hefele, et P. M. Lorz, "Method for producing shell catalysts for the catalytic vapor phase oxidation of aromatic hydrocarbons and catalysts obtained in such a manner", 2003.



- G. J. Hutchings, “Heterogeneous catalysts discovery and design”, *Journal of Material and Chemistry*, vol. 19, pp. 1222–1235, 2009.
- A. B. Ibanez et S. Bauer, “Analytical method for the determination of organic acids in dilute acid pretreated biomass hydrolysate by liquid chromatography time of flight mass spectrometry”, *Biotechnology for biofuels*, vol. 7, no. 1, p. 145, 2014.
- M. M. Ibrahim, M. N. Nadiyah, et H. Azian, “Comparison studies between soda lignin and soda-anthraquinone lignin in terms of physico chemical properties and structural features”, *Journal of Applied Sciences*, vol. 6, no. 2, pp. 292–296, 2006.
- B. Jankovic, “Thermal characterization and detailed kinetic analysis of cassava starch thermo oxidative degradation”, *Carbohydrate polymers*, vol. 95, no. 2, pp. 621–9, 2013.
- S. Jia, B. J. Cox, X. Guo, Z. C. Zhang, et J. G. Ekerdt, “Hydrolytic cleavage of  $\beta$  o 4 ether bonds of lignin model compounds in an ionic liquid with metal chlorides”, dans *Industrial and Engineering Chemistry Research*, vol. 50, no. 2, 2011, pp. 849–855.
- Y. Jie-wang, F. Guizhen, et J. Chunde, “Hydrogenation of alkali lignin catalyzed by  $\text{Pd/C}$ ”, *APCBEE Procedia*, vol. 3, pp. 53–59, 2012.
- M. Jiliang, C. Xiaoping, et L. Daoyin, “Minimum fluidization velocity of particles with wide size distribution at high temperatures”, *Powder Technology*, vol. 235, pp. 271–278, 2013.
- P. E. Jimenez, L. A. Maqueda, A. Perejon, et J. M. Criado, “Clarifications regarding the use of model-fitting methods of kinetic analysis for determining the activation energy from a single non-isothermal curve”, *Chemistry Central journal*, vol. 7, no. 1, p. 25, 2013.
- B. Joffres, D. Laurenti, A. D. Nadege Charon, A. Quignard, et C. Geante, “Thermochemical conversion of lignin for fuels and chemicals a review”, *Industrial and Engineering Chemistry Research*, vol. 68, pp. 753–763, 2013.
- R. Johannes et A. Gosselink, “Lignin as a renewable aromatic resource for the chemical industry”, 2011, PhD thesis Wageningen University.
- A. Jongerius, “Catalytic conversion of lignin for the production of aromatics”, 2013.
- K. Kadowaki, K. Sarumaru, et T. Shibano, “Production of acrylic acid”.
- O. Karlsson, T. Ikeda, T. Kishimoto, K. Magara, et Y. Matsumoto, “Ozonation of lignin-carbohydrate complex model compound of the benzyl ether type”, *International symposium*

*of wood and pulp conference Yokohama*, vol. 1, pp. 178–181, 1999.

O. Karlsson, T. Ikeda, T. K. K. Magara, Y. Matsumoto, et S. Hosoya, “Ozonation of a lignin carbohydrate complex model compound of the benzylether type”, *Journal of Wood Science*, vol. 46, pp. 263–265, 2000.

M. Kindsigo, M. Hautaniemia, et J. Kallasa, “Kinetic modelling of wet oxidation treated debarking water”, *Chemistry*, vol. 59, no. 3, pp. 233–242, 2010.

M. T. Klein et P. S. Virk, “Modeling of lignin thermolysis”, *Energy and Fuels*, vol. 22, pp. 2175–2182, 2008.

E. V. Kondratenko, N. Steinfeldt, et M. Baerns, “Transient and steady state investigation of selective and non-selective reaction pathways in the oxidative dehydrogenation of propane over supported vanadia catalysts”, *Physical chemistry chemical physics PCCP*, vol. 8, no. 13, pp. 1624–33, 2006.

L. Kouisni et M. Paleologou, “Method for separating lignin from black liquor”.

L. Kouisni, P. Hindle, K. Maki, et M. Paleologou, “The lignoforce system tm a new process for the production of high-quality lignin from black liquor”, *Science and Technology for Forest Products and Processes*, vol. 2, no. 4, pp. 6–10, 2012.

M. Koyama, “Hydrocracking of lignin related model dimers”, *Bioresource Technology*, vol. 44, no. 3, pp. 209–215, 1993.

P. Kumar, D. M. Barrett, M. J. Delwiche, et P. Stroeve, “Methods for pretreatment of lignocellulosic biomass for efficient hydrolysis and biofuel production”, *Industrial and Engineering Chemistry Research*, vol. 48, no. 8, pp. 3713–3729, 2009.

D. Kunii et O. Levenspiel, *Fluidization Engineering*, M. I. o. T. Howard Brenner, éd. Elsevier, 1991.

B. Kurek et F. Gaudard, “Oxidation of spruce wood sawdust by mno<sub>2</sub> plus oxalate : a biochemical investigation”, *Journal of Agricultural and Food Chemistry*, vol. 48, no. 7, pp. 3058–3062, 2000.

M. Kwan, N. Cant, D. Trimm, et M. Wainwright, “Modified alumina supports for catalytic oxidation of benzene to maleic anhydride over vanadia”.

Y. Kwan, “The influence of support in the vanadia catalyzed oxidation of benzene unsaturated”, Thèse de doctorat, University of New South Wales, 1985.

D. Lalitendu, K. Praveen, et S. Ratna, “Heterogeneous catalytic oxidation of lignin into value added chemicals”, *Biofuels*, vol. 3, no. 2, pp. 155–166, 2012.

H. Lange, S. Decina, et C. Crestini, “Oxidative upgrade of lignin recent routes reviewed”, *European Polymer Journal*, vol. 49, pp. 1151–1173, 2013.

O. Lanzalunga et M. Bietti, “Photo and radiation chemical induced degradation of lignin model compounds”, *Journal of Photochemistry and Photobiology B Biology*, vol. 56, no. 2–3, 2000.

M. Latifi, F. Berruti, et C. Briens, “Non catalytic and catalytic steam reforming of a bio oil model compound in a novel jiggle bed reactor”, *Fuel*, vol. 129, pp. 278–291, 2014.

E. B. Ledesma, J. N. Hoang, A. J. Solon, M. M. H. Tran, M. P. Nguyen, H. D. Nguyen, T. Hendrix-Doucette, J. V. Vu, C. K. Fortune, , et S. Batamo, “Vapor-phase cracking of 4 vinylguaiacol in a laminar flow reactor kinetics and effect of temperature on product composition”, *Industrial and Engineering Chemistry Research*, vol. 53, no. 31, pp. 12 527–12 536, 2014.

C. Lequart, B. Kurek, P. Debeire, et B. Monties, “MnO<sub>2</sub> and oxalate an abiotic route for the oxidation of aromatic components in wheat straw”, *Journal of Agricultural and Food Chemistry*, vol. 46, no. 9, pp. 3868–3874, 1998.

L. Lloyd, *Handbook of industrial catalysts*, M. Twigg et M. Spencer, éd. CSpringer, 2011.

B. Liu, F. Liam, W. Chen, J. Zheng, K. Vladimir, H. A. Megren, M. AlKinany, S. A. Aldrees, T. Xiao, et P. P. Edwards, “Methanol to hydrocarbons conversion over MoO<sub>3</sub>/HZSM-5 catalysts prepared via lower temperature calcination : a route to tailor the distribution and evolution of promoter Mo species, and their corresponding catalytic properties”, *Chemical Science*, vol. 6, no. 9, pp. 5152–5163, 2015.

X. Liu, G. Xu, et S. Gao, “Micro fluidized beds : Wall effect and operability”, *Chemical Engineering Journal*, vol. 137, no. 2, pp. 302–307, 2008.

V. Locher et L. Smolakova, “Selective oxidation of crotyl alcohol and crotonaldehyde on V<sub>2</sub>O<sub>5</sub>/MgO FTIR study”, *Reaction Kinetics and Catalysis Letters*, vol. 96, no. 1, pp. 117–123, 2009.

- M. J. Lorences, G. S. Patience, F. V. Diez, et J. Coca, "Butane oxidation to maleic anhydride kinetic modeling and byproducts", *Industrial and Engineering Chemistry Research*, vol. 42, pp. 6730–6742, 2003.
- S. Lotfi, D. C. Boffito, et G. S. Patience, "Gas-phase partial oxidation of lignin to carboxylic acids over vanadium pyrophosphate and aluminum–vanadium–molybdenum", *ChemSusChem*, vol. 8, no. 2, pp. 3424–3432, 2015.
- S. Lotfi et G. S. Patience, "Kinetic study of lignin thermal and thermo oxidative degradation", *Unpublished results of the authors*, 2015.
- S. Lotfi et G. S. Patience, "Gas-solid conversion of lignin to carboxylic acids", *Unpublished results of the authors*, 2015.
- R. Lou et S. Wu, "Products properties from fast pyrolysis of enzymatic mild acidolysis lignin", *Applied Energy*, vol. 88, no. 1, pp. 316–322, 2011.
- P. F. Lovell, "Heterogeneous catalysis in practice", *AIChE Journal*, vol. 27, no. 2, pp. 316–316, 1981.
- D. Lv, M. Xu, X. Liu, Z. Zhan, Z. Li, et H. Yao, "Effect of cellulose lignin alkali and alkaline earth metallic species on biomass pyrolysis and gasification", *Fuel Processing Technology*, vol. 91, no. 8, pp. 903–909, 2010.
- R. Ma, M. Guo, et X. Zhang, "Selective conversion of biorefinery lignin into dicarboxylic acids", *ChemSusChem*, vol. 7, no. 2, pp. 412–5, 2014.
- R. Ma, Y. Xu, et X. Zhang, "Catalytic oxidation of biorefinery lignin to value-added chemicals to support sustainable biofuel production", *ChemSusChem*, vol. 8, no. 1, pp. 24–51, 2015.
- Y. Ma, Z. Du, J. Liu, F. Xiaab, et J. Xu, "Selective oxidative c c bond cleavage of a lignin model compound in the presence of acetic acid with a vanadium catalyst", *Green Chemistry*, vol. 17, pp. 4968–4973, 2015.
- Y. Matsumura, M. Sasaki, K. Okuda, S. Takami, S. Ohara, M. Umetsu, et T. Adschiri, "Supercritical water treatment of biomass for energy and material recovery", *Combustion Science and Technology*, vol. 178, no. 1–3, pp. 509–536, 2006.
- D. Meier, J. Berns, C. Grunwald, et O. Faix, "Analytical pyrolysis and semicontinuous catalytic hydrolysis of organocell lignin", *Journal of Analytical and Applied Pyrolysis*,

vol. 25, pp. 335–347, 1993.

M. Misono, *Catalysis on the Energy Scene*. Elsevier, 1984, vol. 19.

W. Mu, H. Ben, A. Ragauskas, et Y. Deng, “Lignin pyrolysis components and upgrading technology review”, *BioEnergy Research*, vol. 6, no. 4, pp. 1183–1204, 2013.

R. Munirathinam, J. Huskens, et W. Verboom, “Supported catalysis in continuous flow microreactors”, *Advanced Synthesis and Catalysis*, vol. 357, no. 6, pp. 1093–1123, 2015.

Z. Mycroft, M. Gomis, P. Mines, P. Law, et T. D. Bugg, “Biocatalytic conversion of lignin to aromatic dicarboxylic acids in *rhodococcus jostii* rha1 by re-routing aromatic degradation pathways”, *Green Chemistry*, 2015.

N. N. Nassar, A. Hassan, et G. Vitale, “Comparing kinetics and mechanism of adsorption and thermo oxidative decomposition of athabasca asphaltenes onto tio<sub>2</sub>, zro<sub>2</sub>, and ceo<sub>2</sub> nanoparticles”, *Applied Catalysis A General*, vol. 484, pp. 161–171, 2014.

E. B. Nauman, *Chemical reactor design optimization and scaleup*. McGraw Hill Professional, 2002.

S. Neto, H. Hibst, F. Rosowski, et S. Storck, “Multimetal oxide containing silver, vanadium and a promoter metal and use thereof”.

S. Nie, X. Liu, Z. Wu, L. Zhan, G. Yin, S. Yao, H. Song, et S. Wang, “Kinetics study of oxidation of the lignin model compounds by chlorine dioxide”, *Chemical Engineering Journal*, vol. 241, pp. 410–417, 2014.

J. Nikiema, F. Rivard, et M. Heitz, “Lignin oxidation to generate vanillin an integrated learning project for chemical engineering students”, *Education for Chemical Engineers*, vol. 4, no. 4, pp. 68–73, 2009.

S. Nishimura, “Handbook of heterogeneous catalytic hydrogenation for organic synthesis”, 2001.

L. M. Nollet et F. Toldra, *Food Analysis by HPLC, Third Edition*. CRC Press, 2012, vol. 16.

R. N. Olcese, G. Lardier, M. Bettahar, J. Ghanbaja, S. Fontana, V. Carre, F. Aubriet, D. Petitjean, et A. Dufour, “Aromatic chemicals by iron-catalyzed hydrotreatment of lignin pyrolysis vapor”, *ChemSusChem*, vol. 6, no. 8, pp. 1490–1499, 2013.

- A. Otto et M. J. Simpson, "Evaluation of cuo oxidation parameters for determining the source and stage of lignin degradation in soil", *Biogeochemistry*, vol. 80, no. 2, pp. 121–142.
- A. Pandey, T. Bhaskar, M. Stocker, et R. K. Sukumaran, éd., *Recent advances in thermochemical conversion of biomass*. Elsevier, 2015.
- M. P. Pandey et C. S. Kim, "Lignin depolymerization and conversion a review of thermochemical methods", *Chemical Engineering and Technology*, vol. 34, no. 1, pp. 29–41, 2011.
- S. G. Paradis, D. M. Marquis, et K. R. Bakshi, "Maleic anhydride production".
- W. Partenheimer, "The aerobic oxidative cleavage of lignin to produce hydroxyaromatic benzaldehydes and carboxylic acids via metal bromide catalysts in acetic acid water mixtures", *Advanced Synthesis and Catalysis*, vol. 351, no. 3, pp. 456–466, 2009.
- V. Pasangulapati, A. Kumar, C. L. Jones, et R. L. Huhnke, "Characterization of switchgrass cellulose hemicellulose and lignin for thermochemical conversions", *Journal of Biobased Materials and Bioenergy*, vol. 6, no. 3, pp. 249–258, 2012.
- V. Pasangulapati, K. D. Ramachandriya, A. Kumar, M. R. Wilkins, C. L. Jones, et R. L. Huhnke, "Effects of cellulose, hemicellulose and lignin on thermochemical conversion characteristics of the selected biomass", *Bioresource technology*, vol. 114, pp. 663–9, 2012.
- G. S. Patience et R. E. Bockrath, "Butane oxidation process development in a circulating fluidized bed", *Applied Catalysis A General*, vol. 376, pp. 4–12, 2010.
- G. Patience et P. Mills, *Studies in Surface Science and Catalysis*. Elsevier, 1994, vol. 82.
- P. R. Pinto, E. A. B. da Silva, et E. Rodrigues, "Insights into oxidative conversion of lignin to high added value phenolic aldehydes", *Industrial and engineering chemistry research*, vol. 50, pp. 741–748, 2011.
- M. Poletto, A. J. Zattera, et R. M. Santana, "Thermal decomposition of wood kinetics and degradation mechanisms", *Bioresource Technology*, vol. 126, pp. 7–12, 2012.
- J. A. Raffensberger, B. J. Glasser, et J. G. Khinast, "Analysis of heterogeneously catalyzed reactions close to bubbles", *AIChE Journal*, vol. 51, no. 5, pp. 1482–1496, 2005.
- A. J. Ragauskas, G. T. Beckham, M. J. Bidy, R. Chandra, F. Chen, M. F. Davis, B. H. Davison, R. A. Dixon, P. Gilna, M. Keller, P. Langan, A. K. Naskar, J. N. Saddler, T. J.

- Tschaplinski, G. A. Tuskan, et C. E. Wyman, "Lignin valorization : improving lignin processing in the biorefinery", *Science*, vol. 344, no. 6185, p. 1246843, 2014.
- A. Rahimi, A. Ulbrich, J. J. Coon, et S. S. Stahl, "Formic-acid-induced depolymerization of oxidized lignin to aromatics", *Nature*, vol. 515, no. 7526, pp. 249–252, 2014.
- G. Ramis, G. Busca, C. Cristiani, L. Lietti, P. Forzatti, et F. Bregani, "Characterization of tungsta-titania catalysts", *Langmuir*, vol. 8, pp. 1744–1749, 1992.
- T. Ren, L. Yan, X. Zhang, et J. Suo, "Selective oxidation of benzene to phenol with n<sub>2</sub>o by unsupported and supported fepo<sub>4</sub> catalysts", *Applied Catalysis A General*, vol. 244, no. 1, pp. 11–17, 2003.
- L. Rihko-Struckmann, Y. Ye, L. Chalakov, Y. Suchorski, H. Wei, et K. Sundmacher, "Bulk and surface properties of a vpo catalyst used in an electrochemical membrane reactor conductivity xrd tpo and xps study", *Catalysis Letters*, vol. 109, no. 1–2, pp. 89–96, 2006.
- W. D. Robinson, "Catalytic production of maleic and phthalic anhydride us patent 310656", 1963.
- G. Roohollahi, M. Kazemeini, A. Mohammadrezaee, et R. Golhoseini, "Application of a simple lumped kinetic model for the catalytic cracking reaction of nbutane over the hzsm5 zeolite", *Procedia Engineering*, vol. 42, pp. 140–147, 2012.
- A. A. Rownaghi, Y. H. Taufiq-Yap, et F. Rezaei, "Innovative process for the synthesis of vanadyl pyrophosphate as a highly selective catalyst for n-butane oxidation", *Chemical Engineering Journal*, vol. 165, no. 1, pp. 328–335, 2010.
- F. G. Sales, C. Abreu, et J. Pereira, "Catalytic wet air oxidation of lignin in a three phase reactor with aromatic aldehyde production", *Brazilian Journal of Chemical Engineering*, vol. 21, pp. 211–218, 2004.
- F. G. Sales, L. C. Maranhao, N. M. L. Filho, et C. A. Abreu, "Experimental evaluation and continuous catalytic process for fine aldehyde production from lignin", *Chemical Engineering Science*, vol. 62, no. 18–20, pp. 5386–5391, 2007.
- H. G. Sanjay et A. R. Tarrer, "Reactor system development to reduce coal liquefaction severity", *Energy and Fuels*, vol. 8, no. 2, pp. 324–329, 1994.
- J. Shabanian et J. Chaouki, "Performance of a catalytic gas–solid fluidized bed reactor in the presence of interparticle forces", *International Journal of Chemical Reactor Engineering*,

2015.

D. Shao, J. Liang, X. Cui, H. Xu, et W. Yan, "Electrochemical oxidation of lignin by two typical electrodes  $\text{Ti/SnO}_2$  and  $\text{Ti/PbO}_2$ ", *Chemical Engineering Journal*, vol. 244, pp. 288–295, 2014.

R. K. Sharma, J. B. Wooten, V. L. Baliga, X. Lin, W. G. Chan, et M. R. Hajaligol, "Characterization of chars from pyrolysis of lignin", *Fuel*, vol. 83, no. 11–12, pp. 1469–1482, 2004.

A. Shekari, "Butane partial oxidation to maleic anhydride experimental and kinetic studies under transient conditions", 2011.

A. Shekari et G. S. Patience, "Maleic anhydride yield during cyclic nbutane oxygen operation", *Catalysis Today*, vol. 157, no. 1–4, pp. 334–338, 2010.

D. Shen, S. Gu, K. Luo, A. Bridgwater, et M. Fang, "Kinetic study on thermal decomposition of woods in oxidative environment", *Fuel*, vol. 88, no. 6, pp. 1024–1030, 2009.

T. Shishido, A. Inoue, T. Konishi, I. Matsuura, et K. Takehira, "Oxidation of isobutane over  $\text{MoVSB}$  mixed oxide catalyst", *Catalysis Letters*, vol. 68, no. 3–4.

Q. Song, W. ang, J. Cai, Y. Wang, J. Zhang, W. Yu, et J. Xu, "Lignin depolymerization (ldp) in alcohol over nickel based catalysts via a fragmentation-hydrogenolysis process", *Energy Environmental Science*, vol. 6, pp. 994–1007, 2013.

H. Suzuki, J. Cao, F. Jin, A. Kishita, H. Enomoto, et T. Moriya, "Wet oxidation of lignin model compounds and acetic acid production", *Journal of Materials Science*, vol. 41, no. 5, pp. 1591–1597, 2006.

H. Taheri, C. D. Dickinson, et P. A. Jacobson, "Flow reactors for chemical conversions with heterogeneous catalysts", 2012.

A. Teimouri, B. Najari, A. Najafi, H. Salavati, et M. F. Najafabadi, "Characterization and catalytic properties of molybdenum oxide catalysts supported on  $\text{ZrO}_2/\text{Al}_2\text{O}_3$  for ammoxidation of toluene", *RSC Adv*, vol. 4, pp. 37 679–37 686, 2014.

W. Thielemans, E. Can, S. S. Morye, et R. P. Wool, "Novel applications of lignin in composite materials", *Journal of Applied Polymer Science*, vol. 83, no. 2, pp. 323–331, 2002.



- I. S. Tomskii, M. V. Vishnetskaya, et A. I. Kokorin, "The partial catalytic oxidation of toluene on vanadium and molybdenum oxides", *Russian Journal of Physical Chemistry B*, vol. 2, no. 4, pp. 562–567, 2008.
- T. Umezawa et T. Higuchi, "Mechanism of aromatic ring cleavage b o 4 lignin substructure models by lignin peroxidase", *FEBS letters*, vol. 218, no. 2, pp. 255–260, 1987.
- C. Uraz et S. Atalay, "Supported catalysis in continuous flow microreactors", *Chemical Engineering Technology*, vol. 12, pp. 1708–1715, 2007.
- D. R. Vardon, M. A. Franden, C. W. Johnson, E. M. Karp, M. T. Guarnieri, J. G. Linger, M. J. Salm, T. J. Strathmannb, et G. T. Beckham, "Adipic acid production from lignin", *Energy Environtal Science*, vol. 8, pp. 617–628, 2015.
- S. Vyazovkin, A. K. Burnham, J. M. Criado, L. A. Perez-Maqueda, C. Popescu, et N. Sbirrazzuoli, "Ictac kinetics committee recommendations for performing kinetic computations on thermal analysis data", *Thermochimica Acta*, vol. 520, no. 1–2, pp. 1–19, 2011.
- Y. Wang, J. Wang, W. Cheng, Z. Zhao, et J. Cao, "Hplc method for the simultaneous quantification of the major organic acids in angeleno plum fruit", *IOP Conference Series Materials Science and Engineering*, vol. 62, no. 1, pp. 120–135, 2014.
- B. M. Weckhuysen et D. E. Keller, "Chemistry, spectroscopy and the role of supported vanadium oxides in heterogeneous catalysis", *Catalysis Today*, vol. 78, no. 1–4, pp. 25–46, 2003.
- S. Wilson, W. Abraham, F. R. Carl, Z. Jin, et Z. Yiping, "Quasi core shell tio2 wo3 and wo3 tio2 nanorod arrays fabricated by glancing angle deposition for solar water splitting", *J. Mater. Chem.*, vol. 21, pp. 10 792–10 800, 2011.
- A. Witsuthammakul et T. Sooknoi, "Direct conversion of glycerol to acrylic acid via integrated dehydration oxidation bed system", *Applied Catalysis A General*, vol. 413-414, pp. 109–116, 2012.
- G. Wu, M. Heitz, et E. Chornet, "Improved alkaline oxidation process for the production of aldehydes vanillin and syringaldehyde from steam explosion hardwood lignin", *Industrial and Engineering Chemistry Research*, vol. 33, no. 3, pp. 718–723, 1994.
- R. Xing, W. Qia, et G. W. Huber, "Production of furfural and carboxylic acids from waste aqueous hemicellulose solutions from the pulp and paper and cellulosic ethanol industries", *Energy Environtal Science*, vol. 4, pp. 2193–2205, 2011.

- X. Xu, J. Lin, et P. Cen, "Advances in the research and development of acrylic acid production from biomass", *Chinese Journal of Chemical Engineering*, vol. 14, no. 4, pp. 419–427, 2006.
- B. R. Yadav et A. Garg, "Catalytic wet oxidation of ferulic acid a lignin model compound in the presence of non noble metal based catalysts at mild conditions", *Chemical Engineering Journal*, vol. 252, pp. 185–193, 2014.
- C. C. Yang, *Handbook of fluidization and fluid particle systems*. CRC Press, 2003.
- Z. D. Yigezu et K. Muthukumar, "Catalytic cracking of vegetable oil with metal oxides for biofuel production", *Fuel*, no. 158, pp. 113–121, 2015.
- J. Yu, C. Yao, X. Zeng, S. Geng, L. Dong, Y. Wang, S. Gao, et G. Xu, "Biomass pyrolysis in a micro fluidized bed reactor characterization and kinetics", *Chemical Engineering Journal*, vol. 168, no. 2, pp. 839–847, 2011.
- J. Zakzeski, P. C. Bruijninx, A. L. Jongerius, et B. M. Weckhuysen, "The catalytic valorization of lignin for the production of renewable chemicals", *Chemical reviews*, vol. 110, no. 6, pp. 3552–99, 2010.
- J. Zakzeski, A. L. Jongerius, P. C. A. Bruijninx, et B. M. Weckhuysen, "Catalytic lignin valorization process for the production of aromatic chemicals and hydrogen", *ChemSusChem*, vol. 5, no. 8, pp. 1602–1609, 2012.
- X. Zeng, G. Yao, Y. Wang, et F. Jin, *Application of Hydrothermal Reactions to Biomass Conversion*. Springer Science and Business Media, 2014.
- Q. Zhang et K. Chuang, "Lumped kinetic model for catalytic wet oxidation of organic compounds in industrial wastewater", *AIChE Journal*, vol. 45, no. 1, pp. 145–150, 1999.
- Y. Zhu, M. Shen, Y. Xia, et M. Lu, "Au mno<sub>2</sub> nanostructured catalysts and their catalytic performance for the oxidation of 5 hydroxymethyl furfural", *Catalysis Communication*, no. 64, pp. 37–43, 2015.